

GENETIC DISSECTION OF SYNAPTIC VESICLE ENDOCYTOSIS

APPROVED BY SUPERVISORY COMMITTEE

Committee Chairperson's Name _____
Jon Terman, PhD

Committee Member's Name _____
Sandra Schmid, PhD

Committee Member's Name _____
Lisa Monteggia, PhD

Committee Member's Name _____
Helmut Kramer, PhD

Supervising Professor's Name _____
Ege Kavalali, PhD

DEDICATION

I would like to thank the members of my Graduate Committee, my wife, my family, my friends, my fellow labmates, and most importantly, my mentor.

GENETIC DISSECTION OF SYNAPTIC VESICLE ENDOCYTOSIS

by

Olusoji Adeyemi Taofeek Afuwape

DISSERTATION

Presented to the Faculty of the Graduate School of Biomedical Sciences
The University of Texas Southwestern Medical Center
In Partial Fulfillment of the Requirements
For the Degree of

DOCTOR OF PHILOSOPHY

The University of Texas Southwestern Medical Center
Dallas, TX
May, 2019

Copyright

by

Olusoji Adeyemi Taofeek Afuwape, 2019
All Rights Reserved

GENETIC DISSECTION OF SYNAPTIC VESICLE ENDOCYTOSIS

Publication No. _____

Olusoji Adeyemi Taofeek Afuwape

The University of Texas Southwestern Medical Center, 2013

Supervising Professor: Ege T. Kavalali, Ph.D.

Synaptic transmission is mediated by the quantal release of neurotransmitters through the fusion of discrete synaptic vesicles with the presynaptic membrane. To maintain reliable transmission, synaptic vesicles and proteins must be recycled after release of neurotransmitters. A key protein in this recycling process is dynamin. Dynamin is a GTPase that catalyzes the scission of a budding endosome off its parent membrane. The mammalian brain expresses three isoforms of dynamin. Using genetically modified mouse hippocampal neurons, I analyzed the functional significance of dynamin in synaptic vesicle endocytosis. Specifically, I assessed dynamin 2 function in synaptic vesicle recycling and neurotransmission and investigated the role of dynamin independent endocytosis at the synapse. My data demonstrates that synaptic transmission after post-natal knockout of dynamin 2 remains intact and synaptic vesicle endocytosis, assessed by the trafficking of vesicular glutamate transporter fused to pHluorin, is unperturbed. Synaptic vesicle endocytosis in the absence of dynamin 2 was assessed at both room temperature and 32 °C. At both temperatures, my results reveal that synaptic vesicle recycling functions independent of dynamin 2 but also, the kinetics of single vesicle recycling is unaffected by changes in temperature suggesting that a single, temperature insensitive (within the limits of testing) form of endocytosis mediates single synaptic vesicle endocytosis. Further experiments reveal that the retrieval of single synaptic vesicles persists after the knockout of all dynamin isoforms. However, after multivesicular release, my results show an overall decrease in synaptic vesicle pool size and a retardation of subsequent vesicle endocytosis in neurons lacking all dynamin isoforms suggesting dynamin

function at the synapse is activity dependent. This finding is consistent with prior reports showing dynamin function at the synapse is dependent on its dephosphorylation by the Ca^{2+} -dependent phosphatase, calcineurin. My results also demonstrate a dichotomy in the dependence of dynamin for synaptic neurotransmission. Whereas I observe a decrease in evoked amplitude, release probability and frequency of spontaneously released events in glutamatergic synapses, I observe no discernable defects in GABAergic neurotransmission. This result suggests inhibitory synapses are better equipped with compensatory mechanisms to deal with the loss of dynamins 1,2 and 3. Overall, my data demonstrate that dynamin is crucial but not essential for synaptic vesicle endocytosis. Dynamin is an activity dependent GTPase that is required for synaptic vesicle recycling after exocytosis of multiple vesicles. However, the underlying mechanism of single synaptic vesicle endocytosis is both dynamin and temperature independent.

TABLE OF CONTENTS

DEDICATION.....	ii
ABSTRACT.....	v
TABLE OF CONTENTS.....	vii
PRIOR PUBLICATIONS	x
LIST OF FIGURES.....	xi
LIST OF DEFINITIONS.....	xiii
CHAPTER ONE: GENERAL INTRODUCTION.....	1
Overview of Synaptic Vesicle Cycle.....	1
Forms of Endocytosis.....	1
Clathrin Mediated Endocytosis.....	1
Kiss and Run.....	2
Activity Dependent Bulk Endocytosis.....	2
Ultrafast Endocytosis.....	3
Overview of Dynamin.....	3
Basic Structure of Dynamin.....	4
Dynamin in other Forms of Endocytosis.....	5
Dynamin Function in Actin Networks.....	5
Distinct Functions of Dynamin Isoforms.....	6
Dynamin I.....	6
Dynamin II.....	7
Dynamin III.....	8
Techniques to Study Endocytosis.....	9
Electron Microscopy.....	9
Fluorescent Dyes.....	9
PHluorin.....	10

CHAPTER TWO: ACUTE MANIPULATION OF SYNAPTOTAGMIN-1 AND ITS EFFECTS ON SYNAPTIC VESICLE TRAFFICKING.....	13
BACKGROUND.....	13
METHODS.....	14
RESULTS.....	17
DISCUSSION.....	23
CHAPTER THREE: DYNAMIN 2 IS NOT REQUIRED FOR SYNAPTIC VESICLE RECYCLING AND NEUROTRANSMISSION.....	25
BACKGROUND.....	25
METHODS.....	26
RESULTS.....	28
DISCUSSION.....	35
CHAPTER FOUR: LOSS OF DYNAMIN AFFECTS SYNAPTIC VESICLE EXOCYTOSIS-ENDOCYTOSIS COUPLING AFTER STRONG STIMULATION.....	36
BACKGROUND.....	36
METHODS.....	37
RESULTS.....	39
DISCUSSION.....	48
CHAPTER FIVE: THE RECYCLING OF A SINGLE SYNAPTIC VESICLE IS DYNAMIN INDEPENDENT.....	50
BACKGROUND.....	50
METHODS.....	51
RESULTS.....	53
DISCUSSION.....	57

CHAPTER SIX: CONCLUSIONS AND FUTURE WORK.....58

BIBLIOGRAPHY.....62

PRIOR PUBLICATIONS

Afuwape OA, Wasser CR, Schikorski T, Kavalali ET. Synaptic vesicle pool-specific modification of neurotransmitter release by intravesicular free radical generation. (2017) *J Physiol* 595(4):1223-1238.

Afuwape OA, Kavalali ET. Imaging synaptic vesicle exocytosis-endocytosis with pH-sensitive fluorescent proteins. (2016) *Methods Mol Biol* 1474:187-200

McMahon DB, Bondar IV, Afuwape OA, Ide DC, Leopold DA. One month in the life of a neuron: longitudinal single-unit electrophysiology in the monkey visual system. (2014) *J Neurophysiol* 112(7):1748-1762.

LIST OF FIGURES

FIGURE 1.1. FORMS OF ENDOCYTOSIS: CLATHRIN-MEDIATED ENDOCYTOSIS, KISS AND RUN, BULK ENDOCYTOSIS.....	3
FIGURE 1.2. FORMS OF ENDOCYTOSIS: ULTRAFAST ENDOCYTOSIS.....	3
FIGURE 1.3. STRUCTURAL DOMAINS OF DYNAMIN.....	5
FIGURE 2.1. ACUTE CHEMOGENETIC IMPAIRMENT OF SYNAPTOTAGMIN-1.....	19
FIGURE 2.2. SYNAPTOTAGMIN-1 LUMINAL ANTIBODY ACUTELY DISRUPTS SYNAPTOTAGMIN-1 FUNCTION.....	22
FIGURE 3.1. WESTERN BLOT ANALYSIS OF DYNAMIN 2 KO.....	28
FIGURE 3.2. EXCITATORY NEUROTRANSMISSION IN DYNAMIN 2 KO NEURON.....	29
FIGURE 3.3. SYNAPTIC VESICLE RETRIEVAL IN THE ABSENCE OF DYNAMIN 2.....	31
FIGURE 3.4. RECYCLING OF SINGLE SYNAPTIC VESICLE IN THE ABSENCE OF DYNAMIN 2 AT ROOM TEMPERATURE	33
FIGURE 3.5. KINETICS OF SINGLE VESICLE RECYCLING IN THE ABSENCE OF DYNAMIN 2 AT 32 °C.....	34
FIGURE 4.1. BY 17 DIV, DYNAMIN IS EFFECTIVELY KNOCKED OUT IN DYNAMIN TKO NEURONAL CULTURES.....	40
FIGURE 4.2. BOTH DYNAMINS 1 AND 2 ARE CLEARED FROM SYNAPSES BY 17 DIV IN DYNAMIN TKO NEURONS.....	41
FIGURE 4.3. SYNAPTIC STRUCTUE OF DYNAMIN TKO NEURONS.....	41
FIGURE 4.4. DECREASE IN RELEASE PROBABILITY IN EXCITATORY.....	43
NEUROTRANSMISSION IN DYNAMIN TRIPLE KNOCKOUT NEURONS.....	45
FIGURE 4.5. INHIBITORY NEUROTRANSMISSION REMAINS IN-TACT IN DYNAMIN TKO NEURONS.....	46
FIGURE 4.6. DYNAMIN IS KNOCKED OUT BOTH GLUTAMATERGIC AND GABAERGIC SYNAPSES IN DYNAMIN TKO SYNAPSES.....	48
FIGURE 5.1. SINGLE VESICLE RECYCLING IS DYNAMIN INDEPENDENT.....	54

FIGURE 5.2.SINGLE VESICLE RECYCLING IN 8 mM EXTRACELLULAR Ca ²⁺ IN DYNAMIN TKO NEURONS.....	55
FIGURE 5.3. SPONTANEOUS NEUROTRANSMISSION IN DYNAMIN TKO NEURONS AFTER TREATMENT WITH MDIVI1, CK-666 AND LATRUNCULIN.....	56

LIST OF DEFINITIONS

Ab - Antibody

AMPA – alpha amino-3-hydroxy-5-methyl-4-isoxazolepropionic acid

AP – action potential

AP5 – 2-amino-5-phosphonopentanoic acid

BAR – Bin Amphiphysin Rvs

BSA – bovine serum albumin

CME – clathrin-mediated endocytosis

CNQX – 6-cyano-7-nitroquinoxaline-2,3-dione

DIV – days in vitro

DKO – double knockout

Dnm – dynamin

eHRP – enhanced horse radish peroxidase

EM – electron microscopy

EPSC – excitatory postsynaptic current

FEME – fast endophilin mediated endocytosis

GABA – gamma-Aminobutyric acid

GFP – green fluorescent protein

f/f – floxed/floxed

HZ - hertz

IPSC – inhibitory postsynaptic current

KO – knockout

mEPSC – miniature excitatory postsynaptic current

mIPSC – miniature inhibitory postsynaptic current

NMDA – N-methyl-D-aspartate

NMDAR – N-methyl-D-aspartate receptor

PRD – proline rich domain

PH – pleckstrin homology

PTX – picrotoxin

SEM – standard error of the mean

SH3 – SRC homology 3

SV – synaptic vesicle

Syt1 – synaptotagmin-1

TKO – triple knockout

TTX – tetrodotoxin

VGAT – vesicular GABA transporter

VGLUT– vesicular glutamate transporter

WT – wild type

CHAPTER 1 GENERAL INTRODUCTION

Overview of SV Cycle

To maintain the reliability and fidelity of synaptic neurotransmission, neurons recycle synaptic vesicle and proteins in a tightly coupled exocytosis-endocytosis loop. Upon the stimulation of an axon and propagation of an action potential down the terminal and into the presynaptic terminal, voltage gated Ca^{2+} channels open and the influx of Ca^{2+} binds synaptotagmin-1 that facilitates the synchronous release of synaptic vesicles.

Neurotransmitters diffuse across the synaptic cleft and bind receptors on the postsynaptic neuron continuing the propagation of signal. Meanwhile, in the presynaptic terminal, the synaptic vesicle is retrieved from the presynaptic terminal membrane at the periaxial zone, reacidified and refilled with neurotransmitter and trafficked to be used again. This process is tightly coupled and regulated to sustain the reliability and fidelity of neurotransmission.

Whereas the mechanics for synaptic vesicle exocytosis have been elucidated and identified, the specifics of synaptic vesicle endocytosis remain elusive. My dissertation investigates the limits and changes in synaptic vesicle endocytosis in small central synapses after genetic modifications.

Forms of endocytosis

Clathrin mediated endocytosis

At restrictive temperature, depletion of Shibire mutant synaptic vesicles resulted in an accumulation of arrested coated pits (Koenig & Ikeda, 1989). These coated pits were revealed to be clathrin. Clathrin-mediated endocytosis is a well-characterized form of vesicle retrieval that occurs in five steps: initiation, cargo selection, coat formation, scission and uncoating. In synapses, stonin 2 recruits synaptotagmin-1 that recruits the adaptor protein, AP-2 that recruits the clathrin triskelion, which bind around the budding endosome (McMahon & Boucrot, 2011) however, see Li *et al.* (2017). Dynamin is recruited for scission and uncoating of clathrin is achieved through heat shock proteins (McMahon & Boucrot, 2011). This is the accepted form of endocytosis for the retrieval of a single synaptic vesicle (Granseth, Odermatt, Royle, & Lagnado, 2006).

Kiss and run

Kiss and run involves the formation of a transient fusion for exocytosis and subsequent endocytosis without a full collapse of vesicle into the membrane. Kiss and run was proposed as a mechanism for endocytosis after EM observations of an Ω profile at the neuromuscular junction (Ceccarelli, Hurlbut, & Mauro, 1973). Capacitance measurements from secretory cells provided further evidence for the plausibility of kiss and run endocytosis (Chow, von Ruden, & Neher, 1992). Further electrophysiological measurements in mast cells confirmed the release of neurotransmitter from the formation of a transient fusion pore (Alvarez de Toledo, Fernandez-Chacon, & Fernandez, 1993). Kiss and run has been shown to exist in small central synapses using quantum dots and pHluorin techniques (Zhang, Li, & Tsien, 2009). A role for dynamin in kiss and run was reported in chromaffin cells. Dynamin was demonstrated to be required to modulate fusion pore expansion during kiss and run events (Jackson et al., 2015). However, the extent of kiss and run endocytosis at different synapses remains to be determined.

Activity-dependent bulk endocytosis

After intense stimulation and massive synaptic vesicle exocytosis, activity dependent bulk endocytosis (ADBE) is triggered. The presence of ADBE at the synapse was discovered using electron microscopy and confirmed with cell attached capacitance measurements at the calyx of Held (de Lange, de Roos, & Borst, 2003; Heuser & Reese, 1973; Koenig & Ikeda, 1996). ADBE is dependent on both membrane expansion and Ca^{2+} influx (Morton, Marland, & Cousin, 2015). The increase in Ca^{2+} activates calcineurin, which dephosphorylates dynamin and other proteins like syndapin-1 (Cousin & Robinson, 2001). However, ADBE persists in dynamin 1, 3 DKO suggesting that dynamin is not necessary for scission in ADBE (Y. Wu et al., 2014). This is corroborated with a report that showed the acute inactivation of dynamin at the synapse induced bulk endosome formation (Kasprowicz, Kuenen, Swerts, Miskiewicz, & Verstreken, 2014). In contrast, dynamin is reported to control actin rings in conjunction with myosin II to mediate fission during ADBE in neurosecretory cells (Gormal, Nguyen, Martin, Papadopoulos, & Meunier, 2015). One key protein retrieved

by ADBE at the synapse is VAMP4 (Nicholson-Fish, Kokotos, Gillingwater, Smillie, & Cousin, 2015).

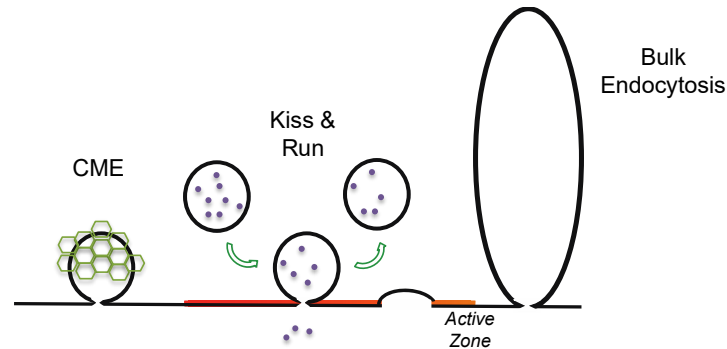


Figure 1.1. Forms of endocytosis: Clathrin-mediated endocytosis, Kiss and Run, Bulk Endocytosis

Ultrafast endocytosis

Until recently, CME was believed to be the dominant form of endocytosis for the retrieval of a single synaptic vesicle. However, with the advent of new techniques, Watanabe *et al.* (2013) discovered another form of endocytosis they termed ultrafast endocytosis.

Ultrafast endocytosis dictates that synaptic vesicles are retrieved from the periaxial zone within 100 ms of release. The retrieved vesicle is further broken down into synaptic vesicles using CME. This form of endocytosis is temperature, actin and dynamin dependent. Whereas Ca^{2+} influx into the nerve terminal is required, it is not sufficient to trigger ultrafast endocytosis.

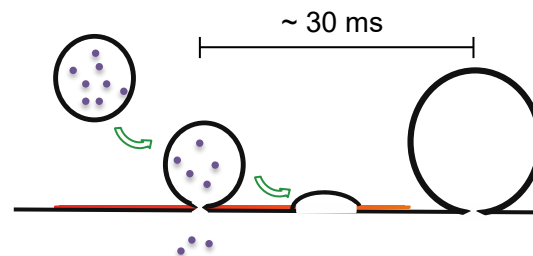


Figure 1.2. Forms of endocytosis: Ultrafast endocytosis

Overview of dynamin

One of the common proteins amongst the different forms of endocytosis is

dynamamin. Prior to its discovery as the catalyst for scission for the budding endosome off the nascent membrane, dynamamin was first discovered as a protein that co-purified with microtubules (Obar, Collins, Hammarback, Shpetner, & Vallee, 1990; Shpetner & Vallee, 1989). Dynamamin's function in endocytosis was first identified in shibire drosophila mutants that suffered from temperature dependent paralysis (Chen et al., 1991; van der Bliek & Meyerowitz, 1991). Upon further investigation into the synapses of these fly mutants, it was discovered that the synapses had been depleted of synaptic vesicles and accumulated what appeared to be arrested collared pits. Later studies further revealed that dynamamin is a GTPase and the presence of nonhydrolyzable GTP, can recapitulate the arrested collared pits phenotype in the mammalian presynaptic terminal (Takei, McPherson, Schmid, & De Camilli, 1995). Currently, we now know dynamamin is a membrane remodeling GTPase that plays a role in multiple forms of endocytosis, actin remodeling dynamics, signaling networks, microtubule dynamics and apoptosis (Cao, Chen, Awoniyi, Henley, & McNiven, 2007; Fish, Schmid, & Damke, 2000; Gold et al., 1999; Henley, Krueger, Oswald, & McNiven, 1998; Ivanov, Ronai, & Hei, 2006; Y. W. Liu, Surka, Schroeter, Lukiyanchuk, & Schmid, 2008; McNiven et al., 2000; Soulet, Schmid, & Damke, 2006; Tanabe & Takei, 2009).

Basic structure of dynamamin

The mammalian system expresses three isoforms of dynamamin (Cao, Garcia, & McNiven, 1998). The basic structure for dynamamin comprises of an N-terminal GTPase domain, a middle domain, a pleckstrin homology (PH) domain, a GTPase effector domain (GED) and a C-terminal proline-rich domain (PRD) (Faelber et al., 2011; Ford, Jenni, & Nunnari, 2011). The GTPase domain functions in conjunction with the GED domain to hydrolyze GTP (Sever, Muhlberg, & Schmid, 1999). The GTPase domain is also important for the dimerization of dynamamin molecules, which is the basic functional unit of dynamamin (Faelber et al., 2011; Ford et al., 2011). Upon GTP hydrolysis, dynamamin undergoes a conformational change that transduces through the polymer and produces the force required for fission (Morlot & Roux, 2013).

The PH domain functions to bind dynamamin to phospholipids (K. M. Ferguson, Lemmon, Schlessinger, & Sigler, 1994). Mutations in the PH domain of dynamamin exert a

dominant negative effect on endocytosis (Vallis, Wigge, Marks, Evans, & McMahon, 1999). The affinity for the PH domain for phospholipid is increased upon dynamin polymerization (Bethoney, King, Hinshaw, Ostap, & Lemmon, 2009). Dynamin PRD domain binds other proteins containing SH3 domains that help direct and coordinate dynamin function (Anggono et al., 2006; Grabs et al., 1997; Shpetner, Herskovits, & Vallee, 1996). Similar to the PH domain, the PRD domain affinity for SH3 containing proteins increases upon dynamin polymerization. The PRD domain is also a site of further regulation of dynamin activity through phosphorylation (Anggono et al., 2006; Armbruster, Messa, Ferguson, De Camilli, & Ryan, 2013).

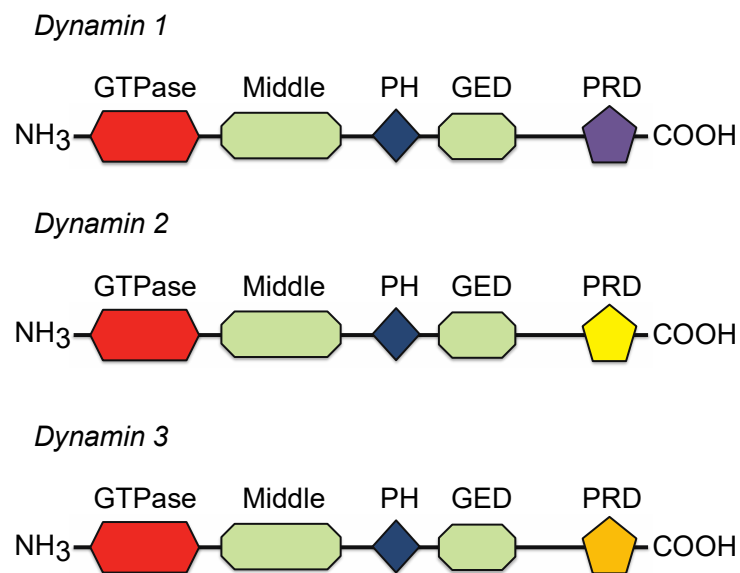


Figure 1.3. Structural domains of Dynamin

Dynamin in other forms of endocytosis

Dynamin function in endocytosis is not limited to clathrin-mediated endocytosis. Dynamin has been implicated in the internalization of caveole in caveolin dependent endocytosis (Henley et al., 1998). However, there is no buildup of caveole in the absence of dynamin similar to the accumulation of clathrin-coated pits suggesting that dynamin is not catalyzing scission of caveolin pits. In epithelial cells, dynamin was revealed to mediate fluid phase micropinocytosis (Cao et al., 2007). Dynamin has also been implicated in

PDGF-stimulated macropinocytosis (Y. W. Liu et al., 2008).

Dynamin function in actin networks

Dynamin and its functional relationship with actin has garnered more interest as of late due to multiple reports showing extensive colocalization between dynamin and actin (Collins, Warrington, Taylor, & Svitkina, 2011; S. M. Ferguson et al., 2009; Taylor, Perrais, & Merrifield, 2011). These studies identify dynamin within actin dense meshworks enucleated by Arp2/3 complex in lamellipodia, actin comets, membrane ruffles and invadopodia (Baldassarre et al., 2003; Gold et al., 1999; Lee & De Camilli, 2002; Orth, Krueger, Cao, & McNiven, 2002; Schlunck et al., 2004). Dynamin function in these complexes is yet to be determined but appears to extend beyond its function at the membrane surface. Dynamin interaction with actin is mediated through the stalk region of a dimer however dynamin can also interact with actin as a polymer through its binding partner cortactin (Gu et al., 2010; Krueger, Orth, Cao, & McNiven, 2003; Mooren, Kotova, Moore, & Schafer, 2009). The interaction between dynamin and actin also extends to sites of clathrin mediated endocytosis (Boulant, Kural, Zeeh, Ubelmann, & Kirchhausen, 2011; Yarar, Waterman-Storer, & Schmid, 2005).

Distinct functions of dynamin isoforms

Dynamin 1

Dynamin 1 is the most abundant dynamin isoform in neuronal tissue and is required for proper synapse development through its interaction with cortactin to drive growth cone and neurite formation (Cao et al., 1998; Torre, McNiven, & Urrutia, 1994; Yamada et al., 2013). At the synapse, dynamin is phosphorylated by cdk5 (Tan et al., 2003). Upon depolarization and Ca²⁺ influx, calcineurin is activated and dynamin 1 is dephosphorylated along with other endocytic proteins called ‘dephosphins’ (Cousin & Robinson, 2001; J. Xue et al., 2011). This cycle of phosphorylation is reported to be necessary for dynamin 1’s synaptic function (Armbruster et al., 2013; Raimondi et al., 2011). Loss of dynamin 1 at a large synapse, the calyx of Held reveals a stimulation dependent synaptic vesicle endocytosis defect consistent with dynamin 1’s accepted function (Lou,

Paradise, Ferguson, & De Camilli, 2008). Similarly, in superior cervical ganglion neurons, knockdown of dynamin 1 resulted in defects in vesicle recycling during and after high levels of synaptic activity (Tanifuji, Funakoshi-Tago, Ueda, Kasahara, & Mochida, 2013). However, tissue specific deletion of dynamin 1 resulted in decreased short term depression and enhanced post tetanic potentiation hinting at an increase in synaptic transmission efficiency (Mahapatra, Fan, & Lou, 2016; Mahapatra & Lou, 2017). In neuroendocrine cells, synaptotagmin-1 was reported to directly interact with dynamin 1 to modulate fission pore dynamics of fusing secretory vesicles (McAdam et al., 2015). This interaction could play a key role in the exocytosis-endocytosis coupling of vesicle release.

Dynamin 2

The complete knockout of dynamin 2 is embryonic lethal (S. M. Ferguson & De Camilli, 2012). However, conditional knockout of dynamin 2 reveals defects in clathrin-mediated endocytosis (Y. W. Liu et al., 2008). Dynamin 2 is targeted through its interaction with sorting nexin 9 (SNX9). While bound to dynamin 2 and upon phosphorylation, SNX9 targets dynamin 2 to the membrane where it interacts with $PI_{4,5}P_2$ and BAR domain proteins such as amphiphysins 1 and 2 (Lundmark & Carlsson, 2004, 2005; Zoncu et al., 2007). Dynamin 2 oligomerization is triggered and upon GTP hydrolysis, dynamin excises the budding endosome off the parent membrane. Evidence for an earlier role for dynamin 2 in clathrin mediated endocytosis is supported by reports showing dynamin recruitment to sites of clathrin mediated endocytosis prior to vesicle internalization (Grassart et al., 2014; Warnock, Baba, & Schmid, 1997). Dynamin 2 is also implicated in vesicle exocytosis. After activation, NK cells require dynamin 2 to release lytic granules during cell-mediated killing of pathogens (Arneson et al., 2008). Similarly, macrophages require dynamin 2 GTPase activity for exocytosis of secretory vesicles (Jaiswal, Rivera, & Simon, 2009).

Dynamin 2 is functionally significant for cellular migration. Dynamin 2 colocalizes with cortactin in lamellipodia where they promote actin reorganization to initiate cellular migration (Krueger et al., 2003). Mutant expression of dynamin 2 blocks the lamellipodia formation (Schlunck et al., 2004). Dynamin 2 also colocalizes with cortactin in

leading membrane ruffles in migrating fibroblasts (McNiven et al., 2000). Dynamin also regulates formation and functions locally within invadopodia and podosomes (Baldassarre et al., 2003; Ochoa et al., 2000). Additionally, mutant dynamin 2 expression leads to increased actin stress fiber formation suggesting that dynamin 2 regulates actin stress fiber formation (McNiven et al., 2000).

Dynamin 2 is located in the centrosome bound to γ -tubulin through the PRD domain (Hamao, Morita, & Hosoya, 2009; Lin, Barylko, Achiriloaie, & Albanesi, 1997; Thompson, Cao, Chen, Euteneuer, & McNiven, 2004). The knockdown of dynamin 2 leads to an increase in acetylated tubulin implicating dynamin 2 as a regulator for microtubule growth dynamics (Tanabe & Takei, 2009). Dynamin 2 functions throughout mitosis through its interaction with microtubules and the loss of dynamin 2 prolongs the separation of daughter cells (Y. W. Liu et al., 2008; Thompson, Skop, Euteneuer, Meyer, & McNiven, 2002). Dynamin 2's intimate interaction with microtubule and its growth dynamics can also serve to implicate dynamin 2 in synaptic vesicle recycling as more reports highlight microtubule function in synaptic vesicle trafficking (Eguchi et al., 2017; Guillaud, Dimitrov, & Takahashi, 2017).

In adrenal chromaffin cells, dynamin 2 is reported to regulate single vesicle release kinetics and quantal size through a Ca^{2+} dependent polymerization of the actin cytoskeleton (Gonzalez-Jamett et al., 2010; Graham, O'Callaghan, McMahon, & Burgoyne, 2002). Knockdown of dynamin 2 decreased vesicle recycling during high frequency stimulation and delayed retrieval after an action potential firing (Tanifuji et al., 2013). In the postsynapse, dynamin 2 mediated endocytosis recycles receptors through both clathrin dependent and independent endocytosis mechanisms. AMPA receptor internalization is decreased in the presence of dynamin 2 mutant K44A, suggesting that dynamin 2 regulates excitatory neurotransmission (Carroll et al., 1999). Dopamine induced D2 receptor endocytosis was retarded in the presence of dynamin 2 mutant expression (Kabbani, Jeromin, & Levenson, 2004). This finding is supported by dynamin 2's enrichment in dopaminergic synapses (Kabbani et al., 2004).

Dynamin 3

Dynamin 3 is the least characterized dynamin isoform. Initially, dynamin 3 function at the synapse was proposed to be postsynaptic due to its enrichment in the postsynaptic densities (Gray et al., 2003). Consistent with this, in the same report, dynamin 3 is shown to interact with Homer1, a post synaptic protein and metabotropic glutamate receptor mGluR5. Dynamin 3 interaction with Homer is required for proper AMPA receptor trafficking as disruption of this interaction results in defective AMPA trafficking (Lu et al., 2007). Dynamin 3 interaction with cortactin is implicated in the morphogenesis of dendritic spines and this complex is reportedly required for the development of the axonal growth cone in developing neurons (Gray, Kruchten, Chen, & McNiven, 2005). Interestingly, the loss of dynamin 3 results in no gross phenotype suggesting that these functions might not be unique to dynamin 3 (Raimondi et al., 2011). Dynamin 3 function in the synaptic vesicle recycling was uncovered when dynamin 3 was knocked out in conjunction with dynamin 1. Dynamin 1, 3 DKO neurons revealed defects in compensatory endocytosis and an accumulation of clathrin coated pits and deep invaginations of the plasma membrane (Raimondi et al., 2011). Consistent with this, knockdown of dynamin 3 in superior cervical ganglion neurons revealed dynamin 3 function in refilling the readily releasable pool (Tanifuji et al., 2013). However, new evidence demonstrates that neurons lacking dynamins 1 and 3 can still undergo bulk endocytosis at the synapse after strong stimulation (Y. Wu et al., 2014). Increasing evidence suggest dynamin 3 function at the synapse to be activity dependent (Calabrese & Halpain, 2015; Hayashida, Tanifuji, Ma, Murakami, & Mochida, 2015; Tanifuji et al., 2013).

Techniques to study endocytosis

Electron Microscopy

Electron microscopy used to be the gold standard for studying endocytosis. The study of synaptic vesicle recycling using EM involves stimulation and repeated fixing at multiple time points. Initially, Heuser and Reese used this technique to establish and confirm quantal neurotransmission by demonstrating the recycling of synaptic vesicles at the frog neuromuscular junction. Recently, this technique was optimized by Watanabe *et. al* (2013) and led to the discovery of ultrafast endocytosis proving it's worth. The advent of electron dense markers and faster and more sophisticated fixings is making EM an alluring technique.

The major drawback of electron microscopy is the loss of temporal information and as such makes this approach non-suitable for studying dynamic processes like synaptic vesicle recycling. In addition, EM only provides information on membrane recycling and nothing on protein sorting and recycling.

Fluorescent Dyes

Synaptic vesicle endocytosis is a process that occurs within live tissue. Fluorescent dyes can be used to mark recycling vesicles. FM dyes are amphipathic compounds that bound strongly to membranes leading to an increase in fluorescence (Betz & Bewick, 1992; Betz, Mao, & Bewick, 1992). This is advantageous as dye release will be accompanied with a decrease in fluorescence providing temporal information on the recycling vesicle. However, different dyes partition out of membranes at differing rates and such should be considered when designing experiments (Klingauf, Kavalali, & Tsien, 1998). Information about the form of vesicle exocytosis, either full collapse or kiss-and-run can be determined with the data provided with FM dyes (Gaffield & Betz, 2006). FM dye studies can be combined with electrophysiological recordings for a more detailed approach (Stevens & Williams, 2000). In addition, photoconversion of FM dyes can be used in conjunction with EM to gain ultrastructure information of dye location (Harata, Ryan, Smith, Buchanan, & Tsien, 2001; Henkel, Lubke, & Betz, 1996). However, this technique has major drawbacks. The loading of dye is a tedious process that requires washout and since the dye binds membrane avidly, allows for strong background staining thereby reducing the signal to noise ratio. In addition, the dynamics of dye unbinding to membrane complicates measured rates of exocytosis and amounts of dye release.

pHluorin

Prior to the advent of pHluorin, synaptic vesicle exocytosis and endocytosis was monitored using fluorescent dyes. One of the major drawbacks of this technique is the tedious nature of dye loading and washout, which may lead to non-specific labeling (Kavalali & Jorgensen, 2014). This drawback is easily mitigated with the use of pHluorin tagged synaptic vesicular proteins. pHluorin was developed by Miesenbock in 1998 by mutating

green fluorescent protein (GFP) (Miesenbock, De Angelis, & Rothman, 1998). To visualize synaptic vesicle recycling, Miesenbock developed synapto-pHluorin, a pHluorin tagged to the luminal domain of synaptobrevin2 (also called Vesicle-associated membrane protein, VAMP2) and demonstrated an increase in fluorescence with neuronal stimulation. Upon endocytosis and vesicle reacidification, fluorescence slowly decays back to baseline. This decay can be inhibited in the presence of proton pump inhibitors such as bafilomycin or folimycin suggesting that the change in fluorescence is indeed reflective of the recycling of synaptic vesicles (Granseth et al., 2006; H. Li et al., 2011; Ramirez, Khvotchev, Trauterman, & Kavalali, 2012; Voglmaier et al., 2006; Zhu, Xu, & Heinemann, 2009). Since the introduction of synapto-pHluorin, multiple pHluorin variants have been reported and tagged to other synaptic vesicular proteins. This has provided the opportunity to study the recycling of multiple proteins at once. However, the molecular specificity of this technique can also be a major drawback in the sense that it is limited to that molecule and different molecules traffic differently in the same synapse (Granseth et al., 2006; Raingo et al., 2012; Ramirez et al., 2012; Voglmaier et al., 2006; Zhu et al., 2009). A quick review of these probes and proteins is provided below:

Probes

pHluorin – There are two classes of pHluorin: ratiometric and ecliptic. Both are derived by mutating green fluorescent protein (GFP). All ratiometric pHluorins contain a S202H mutation and demonstrate a reversible excitation ratio change between pH 7.5 and 5.5 (Miesenbock et al., 1998). This pH dependent ratio can be utilized as a pH indicator as demonstrated by Miesenbock et al (Miesenbock et al., 1998). Ecliptic pHluorin exhibits a pH dependent fluorescence quench (eclipsing) in an acidic environment. The pH dependence of ecliptic pHluorin is derived from the protonation of a hydroxyl group on Tyrosine at the 66th position. When protonated, the fluorescent signal is quenched and vice versa. This feature and a pKa of 7.1 make ecliptic pHluorin an ideal marker for monitoring exo- and endocytosis (Sankaranarayanan, De Angelis, Rothman, & Ryan, 2000).

mOrange2 - This is a red shifted fluorescent protein developed objectively for photostability (Shaner et al., 2004). It is excited at 549 nm and emits at 565 nm and therefore can be used for dual imaging in combination with pHluorin. However, mOrange2

has a pKa of 6.5 which drastically reduces the signal to noise ratio as fluorescence is dependent on the deprotonated protein.

pHTomato – This is also red shifted and can be used for dual imaging with pHluorin. It is excited at 550 nm and emits at 580 nm. Unlike mOrange2, pHTomato has a pKa around 7.8 and as such displays a better signal to noise ratio. At pH 7.5, pHTomato has been reported to be as bright as enhanced Green Fluorescent Protein (EGFP) with less light scattering due to the longer wavelength required for excitation (Y. Li & Tsien, 2012).

pHuji – This is the latest red shifted fluorescent protein potentially capable of dual imaging in combination with pHluorin. It emits at 598 nm and has a pKa of 7.7. It is reported to have a 20 fold increase in fluorescence in response to a pH change from 5.5 to 7.5 (Shen, Rosendale, Campbell, & Perrais, 2014).

Synaptic Vesicle Proteins

VAMP – The first reported pHluorin labeled synaptic vesicle protein was called synapto-pHluorin, a fusion of pHluorin and the luminal domain of synaptobrevin/VAMP. This chimeric protein demonstrated the power of this technique but as most premier inventions, had major setbacks. The surface membrane expression of synapto-pHluorin proved quite excessive and in some instances required pre-quenching of the surface fluorescence prior to testing (Gandhi & Stevens, 2003). Also, upon exocytosis, synapto-pHluorin has been shown to laterally diffuse away from the site of exocytosis resulting in a decrease in measured fluorescence that can be misinterpreted as endocytosis (Granseth et al., 2006).

Synaptophysin – pHluorin fused to a singular intravesicular loop of synaptophysin (sypHy) has been shown to report synaptic vesicle recycling as well as synapto-pHluorin (Granseth et al., 2006). Unlike synapto-pHluorin, sypHy is reported to have less surface membrane expression and little lateral protein diffusion. This allows for a much higher signal to noise ratio (4).

Vesicular Glutamate Transporter 1 – Another reported synaptic vesicular protein tagged to pHluorin is the vesicular glutamate transporter 1 (vGlut1). Synaptic vesicles have been reported to have a small number of copies of vGlut1 (Takamori et al., 2006). The low vGlut1 copy number per vesicle further increases the signal to noise ratio of vGlut-phluorin

in addition to its low surface membrane expression.

The trafficking of other synaptic vesicle associated proteins has successfully been studied using pHluorin tags (Raingo et al., 2012; Ramirez et al., 2012). These studies have not only revealed differences in protein recycling but differences in synaptic vesicle labeling when co-expressed with a red shifted pHluorin (e.g. mOrange or pHTomato).

CHAPTER 2

ACUTE MANIPULATION OF SYNAPTOTAGMIN-1 AND ITS EFFECTS ON SYNAPTIC VESICLE TRAFFICKING

BACKGROUND

A majority of presynaptic nerve terminals in the central nervous system contain ~200 synaptic vesicles (Harris and Sultan, 1995). Depending on the type of presynaptic input, varying fractions, or “pools” of these vesicles participate in activity-dependent synaptic vesicle recycling and neurotransmitter release (Chamberland and Toth, 2016). Most central synapses have, a “resting pool” of vesicles, which do not respond swiftly to presynaptic action potentials (Sudhof, 2000, 2004; Harata et al., 2001a, 2001b; Marra et al., 2012) but see (Xue et al., 2013). Recent studies suggest that differences in protein components of synaptic vesicles underlie this apparent functional heterogeneity (Fredj and Burrone, 2009; Hua et al., 2011; Raingo et al., 2012; Ramirez et al., 2012; Bal et al., 2013). This molecular heterogeneity is thought to be encoded—at least in part—by differential distribution of synaptic vesicle-associated SNARE proteins and not only dictate the dichotomy between recycling and resting pools but also determine how synaptic vesicles respond to incoming action potentials or release neurotransmitter spontaneously at rest (Hua et al., 2011; Ramirez and Kavalali, 2011; Raingo et al., 2012; Ramirez et al., 2012; Kavalali, 2015).

While essential for dissecting the mechanisms underlying synaptic vesicle heterogeneity, molecular manipulations of synaptic vesicle-associated SNAREs or other key molecules typically take days to weeks to alter protein levels to enable examination of their functional consequences. This delay provides a sufficient time frame for other molecular adaptations to compensate for the functional impact of the manipulation in question. A striking example is seen in the case of voltage-gated calcium channel knockouts (e.g. Piedras-Renteria

et al., 2004). These approaches, therefore, need to be complemented with more acute manipulations to probe heterogeneity between presynaptic vesicle populations to obtain a more accurate understanding of presynaptic function and neurotransmitter release (e.g. Poskanzer et al., 2003; Snellman et al., 2011). Ideally, a manipulation that can tag recycling vesicles and modify their functional properties to alter neurotransmitter release output could be used to monitor the impact of vesicle pool dynamics on neurotransmission. To achieve this objective, we took advantage of horse radish peroxidase (HRP), a heme containing plant enzyme, that utilizes hydrogen peroxide (H_2O_2) to oxidize organic as well as inorganic targets (Veitch, 2004), which we have used previously to label endocytosed synaptic vesicles and visualized them with electron microscopy (Deak et al., 2004). The H_2O_2 passes through the membrane and reacts with HRP producing free radical molecules which reacts with 3,3'-diaminobenzidine (DAB) as a substrate to create an electron dense precipitate that can be visualized via electron microscopy. However, these free radicals are also expected to modify protein or lipid targets in their vicinity and impair their functional interactions. Using this approach, we aimed to target specific synaptic vesicles pools and found that the formation of free radicals within vesicles differentially affect synaptic neurotransmission depending on the route of HRP uptake. Upon free radical generation after strong stimulation and subsequent uptake of HRP, we observed a decrease in eEPSC amplitude and an increase in mEPSC frequency. However, upon free radical generation within synaptic vesicles after spontaneous uptake of HRP, we observed an increase in mEPSC frequency and no change to eEPSC amplitude. These results are consistent with potential inactivation of syt1, the Ca^{2+} sensor for synchronizing synaptic vesicle exocytosis upon stimulation (Geppert et al., 1994; Fernandez-Chacon et al., 2001). To probe if syt1 was a target of free radical modification, we expressed e-HRP tagged to the luminal domain of syt1 in hippocampal neurons and were able to recapitulate a syt1 loss-of-function phenotype. We corroborated these findings using a polyclonal antibody to target the luminal domain of syt1 and again detected alterations in synaptic neurotransmission depending on the route of syt1 antibody uptake. This finding suggests that syt1 function in suppression of spontaneous neurotransmission can be acutely dissociated from syt1 function to synchronize synaptic vesicle exocytosis upon stimulation.

METHODS

Lentiviral Infection

HEK293 cells (ATCC) were transfected with 3 packaging plasmids (pMDLg/pRRE, pRSV-Rev, and pCMV-VSV-G) and a pFUGW transfer vector containing a syt1-eHRP construct using the Fugene 6 transfection reagent (Promega). Cell culture supernatants containing the virus were collected 72 hours later and spun down to participate out cellular debris and other contaminants. Neurons were infected at 4 days *in vitro* (DIV) by adding 300 μ l of virus containing supernatant to the neuronal culture media. For the syt1-eHRP construct, HRP's catalytic activity was enhanced via direct evolution and was added to the luminal domain of syt1 with a short amino acid linker to make the construct syt1-eHRP.

Cell Culture

Dissociated hippocampal cultures from postnatal day 0-3 Sprague-Dawley rats were prepared as previously described (Kavalali, Klingauf, & Tsien, 1999). Neurons were infected at 4 DIV with lentivirus expressing syt1-eHRP or an empty L307 vector for control and experiments were performed at 15-21 DIV. All experiments were performed following protocols approved by the University of Texas Southwestern Institutional Animal Care and Use Committee.

Fluorescent detection of syt1-eHRP

Neuronal cultures were processed for immunocytochemistry as described in Ramirez et al. (2008) using an anti-synapsin mouse monoclonal antibody, 1:200 dilution (Synaptic Systems). Cultures were then processed for syt1-eHRP labeling using a Tyramide Signaling Amplification kit (#14, Molecular Probes, Eugene, OR) and then processed for confocal imaging.

Synaptic Localization of Syt1-eHRP: The percentage of synapses expressing syt1-eHRP was determined by randomly selecting 80-85 synapsin labeled puncta and counting the number of puncta with a syt1-eHRP signal greater than 2 times the standard deviation above the mean background.

Electrophysiology

A modified Tyrode's solution was used for all experiments (except where noted otherwise) that contained (in mM): 145 NaCl, 4 KCl, 2 MgCl₂•(6H₂O), 10 glucose, 10 HEPES, 2 CaCl₂ (pH 7.4, osmolarity 300 mOsM). Pyramidal neurons were whole-cell voltage clamped at -70 mV with borosilicate glass electrodes (3-5 MΩ) filled with a solution containing (in mM): 105 Cs-methanesulphonate, 10 CsCl, 5 NaCl, 10 HEPES, 20 TEA.Cl hydrate, 4 Mg-ATP, 0.3 GTP, 0.6 EGTA, 10 QX-314 (pH 7.3, osmolarity 290 mOsM).

Inhibitory-postsynaptic currents (IPSCs) were evoked with 0.1-ms, 10mA pulses delivered via a bipolar platinum electrode in a modified Tyrode's solution containing 6-Cyano-7-nitroquinoxaline-2-3-dione (CNQX, 10 μM) and DL-2-Amino-5-phosphonovaleric acid (APV, 50 μM, NMDA receptor blocker). Spontaneous miniature IPSCs (mIPSCs) were recorded in a modified Tyrode's solution containing TTX (1 μM), CNQX (10 μM) and APV (50 μM). Data was analyzed offline with Clampfit 9 software.

Syt1-eHRP- After establishing the whole cell recording configuration, either mIPSCs or eIPSC responses (evoked by 5 pulses at a 1 Hz frequency) were recorded. We then perfused a modified Tyrode's solution containing 0.1% or 0.2% H₂O₂ respectively for 5 minutes to generate free radicals. For washout, we perfused with H₂O₂ free Tyrode's solution for 2 minutes and then recorded corresponding mIPSC or eIPSCs.

Loading of luminal syt1 antibody- To test if synaptotagmin-1 luminal domain antibody can disrupt synaptotagmin-1 synaptic function, we treated neuronal cultures with either a 1% anti syt1 antibody (synaptic systems #105 103) or 3% BSA modified Tyrode's solution. For depolarization induced uptake of anti-syt1 antibody, cultures were incubated with either BSA or anti-syt1 lumen antibody in modified Tyrode's solution containing 47 mM K⁺ for 120 seconds. BSA or anti-syt1 lumen antibody was subsequently washed out with Tyrode's solution for 2 minutes and mIPSC or eIPSC (evoked by 5 pulses at a 1 Hz frequency) recordings were obtained. For spontaneous uptake of anti-syt1 lumen antibody, we incubated neuronal cultures in 1% anti syt1 lumen antibody or 3% BSA modified Tyrode's solution containing TTX (1 μM) for 30 minutes. Then we subsequently washed out the antibody with Tyrode's solution for 5 minutes and mIPSC or eIPSC (evoked by 5 pulses at a

1 Hz frequency) recordings were obtained.

Statistical analysis

Statistical analyses were performed with Graphpad Prism 6.07 software using one of the following tests: two-tailed Student's t-test, one-way or two-way ANOVA. All datasets were checked for normality with both the D'Agostino & Pearson omnibus and Shapiro-Wilk normality test or KS normality test (when $n < 7$ values). If data was non-normal, a non-parametric test was used to calculate significance. For pairwise comparison of two treatments, a two-tailed Student's t-test was used (no data sets were non-normal). For parametric comparisons of three or more groups, the one-way ANOVA was used (with the Sidak's *post hoc* multiple comparisons test, if significant). For non-parametric comparisons of three or more groups, the Kruskal-Wallis test was performed (Dunn's *post hoc* multiple comparisons test). For comparison of cumulative mEPSC amplitude distributions, eIPSC cumulative charge transfer or 1Hz depression of normalized EPSC amplitudes, the two-way ANOVA test was used with a Sidak's *post-hoc* multiple comparisons test to calculate exact multiplicity adjusted p-values between groups when the p-value of the treatment-interaction was significantly different ($p < 0.05$). Error bars represent the SEM.

RESULTS

Synaptotagmin-1 as a potential target for vesicular reactive oxygens.

Prior work in our lab demonstrated that the intravesicular generation of free radical oxygen species within synaptic vesicles leads to an increased mEPSC frequency and decrease in response amplitude after stimulation. These modifications of neurotransmission mimic transmission defects observed in neurons deficient of synaptotagmin (Geppert et al., 1994; Fernandez-Chacon et al., 2001; Maximov and Sudhof, 2005; Liu et al., 2014).

Synaptotagmin-1 (syt1) is a Ca^{2+} sensor that synchronizes synaptic vesicle release after stimulation. To test whether we can disrupt syt1 function from the luminal domain using free radical modification, we infected dissociated hippocampal neurons with lentivirus expressing an enhanced HRP variant tagged to the luminal domain of syt1 (syt1-eHRP). To confirm proper trafficking of syt1-eHRP to the synapse, we fixed and labeled all synapses using a

synapsin antibody then labeled HRP containing synapses by developing HRP using a tyramide based fluorescent substrate to quantify the percent of synapses with HRP. We determined that syt1-eHRP was expressed in up to 79% of synapses (Fig. 2.1.A). To assess increase in evoked asynchronous neurotransmitter release, we looked at inhibitory transmission to avoid reverberatory activity after field stimulation (Maximov and Sudhof, 2005). We treated neurons expressing syt1-eHRP with H_2O_2 for 5 minutes and after washout, we observed a 40 percent decrease in eIPSC amplitude after treatment with H_2O_2 (Fig. 2.1 C-H: Ctrl n=7; p=0.7; Syt1-eHRP n=13; p=0.0472). Also, we observed an increase in asynchronous release as measured by the cumulative charge transfer within a second after stimulation after H_2O_2 treatment in neurons expressing syt1-eHRP (Fig. 2.1 E, H). We also observed a 4.9-fold increase in mIPSC frequency in syt1-eHRP expressing neurons after H_2O_2 treatment (Fig. 2.1 I-N: Ctrl n=12; p=0.1617; Syt1-eHRP n=10; p=0.0136) without a substantial change in the distribution of mIPSC amplitudes. Taken together, these results suggest that free radical generation within synaptic vesicles can acutely disrupt syt1 function from the luminal domain.

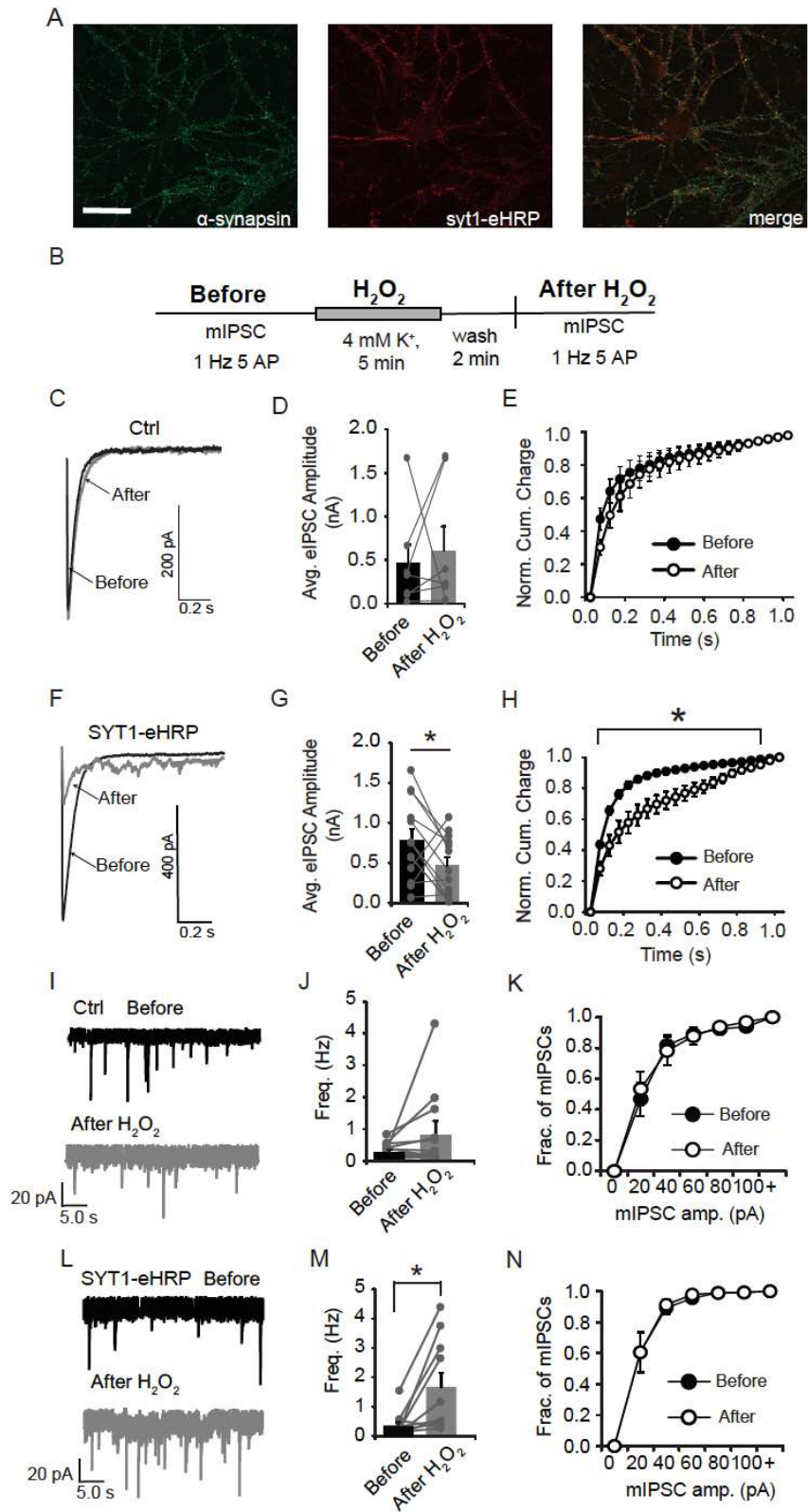


Figure 2.1 Acute chemo-genetic impairment of synaptotagmin-1. (A) Immunostaining of endogenous synapsin (green) and visualizing syt1-eHRP (red) using a TSA kit in neurons

infected with lentivirus expressing the syt1-eHRP plasmid. Right, merge of both images. (B) Diagram of experiment: A hippocampal neuron was patched and either mIPSC or eIPSC (evoked by 5 pulses at a 1 Hz frequency) recordings were taken before and after a 5 minute H_2O_2 treatment with a 2 minute washout period. (C) Representative traces of the 1st AP before (black) and after (gray) H_2O_2 treatment in control neurons. (D) Summary graph of the average IPSC amplitude in control neurons before (black) and after (gray) H_2O_2 treatment. (paired t-test ; $t_{(6)}=0.3966$; $n=7$; $p=0.7053$). (E) Normalized charge transfer plot for the average IPSC over a second in control neurons before (black) and after (white) H_2O_2 treatment (two-way RM ANOVA; $F_{(1,6)}=0.3415$; $p=0.5803$). (F) Representative traces of the 1st AP before (black) and after (gray) H_2O_2 treatment in syt1-eHRP neurons. (G) Summary graph of the average IPSC amplitude in syt1-eHRP neurons before (black) and after (gray) H_2O_2 treatment. (paired t-test ; $t_{(12)}=2.210$; $n=13$; $p=0.0472$). (H) Normalized charge transfer plot for the average IPSC over a second in syt1-eHRP neurons before (black) and after (white) H_2O_2 treatment (two-way RM ANOVA; $F_{(1,12)}=11.70$; $p=0.0051$). (I) Representative mIPSC recordings from control neurons before (black) and after (gray) H_2O_2 treatment. (J) Summary graph of the average mIPSC frequency in control neurons before (black) and after (gray) H_2O_2 treatment (values from the same neurons are connected). (paired t-test; $t_{(11)}=1.500$; $n=12$; $p=0.1617$). (K) Distribution of mIPSC amplitudes from control neurons before and after H_2O_2 treatment (two-way RM ANOVA; $F_{(1,11)}=0.4623$; $p=0.5106$). (L) Representative mIPSC recordings from syt1-eHRP neurons before (black) and after (gray) H_2O_2 treatment. (M) Summary graph of the average mIPSC frequency in syt1-eHRP neurons before (black) and after (gray) H_2O_2 treatment (values from the same neurons are connected). (paired t-test; $t_{(9)}=3.060$; $n=10$; $p=0.0136$). (N) Distribution of mIPSC amplitudes from syt1-eHRP neurons before and after H_2O_2 treatment. (two-way RM ANOVA; $F_{(1,9)}=0.1717$; $p=0.6883$). Scale bar, 30 μm .

Functional impact of synaptotagmin-1 luminal domain antibody on evoked and spontaneous release.

Our results demonstrate that free radical generation within synaptic vesicles can alter synaptic transmission. Dissection of functional alterations in spontaneous versus evoked neurotransmitter release suggest that synaptic vesicle populations giving rise to these two forms of neurotransmission are largely segregated. Although after strong stimulation, both synaptic vesicle populations can be recruited for exocytosis. Also, we have shown that free radical generation can be targeted to acutely disrupt a specific protein through the luminal domain, in this case, synaptotagmin-1. Synaptotagmin-1 functions dually as a clamp on spontaneous vesicle fusion and promoter for vesicle fusion after stimulation (Maximov and Sudhof, 2005; Liu et al., 2014). However, these observations raise the question how syt1— a synaptic vesicle specific protein with ubiquitous distribution among synaptic vesicle

populations — may underlie preferential regulation of spontaneous versus evoked release? To address this issue, we incubated dissociated hippocampal neurons in either a syt1 lumen polyclonal antibody solution or BSA in the presence of TTX or 47mM K⁺ to stimulate antibody uptake (Fig. 2.2.A, H). After treatment with 47 mM K⁺ and syt1 lumen antibody, we observed a decrease in eIPSC amplitude in comparison to the BSA treated cells (Fig. 2.2.B, C: BSA n=16; SYT1 Ab n=14; p=0.0038). There also was a significant increase in asynchronous release after stimulation in the syt1 lumen antibody treated neurons in comparison to the BSA treated neurons (Fig. 2.2.D: BSA n=16; SYT1 Ab n=14; p<0.0001). When we probed for changes in spontaneous transmission after 47 mM K⁺ and syt1 lumen antibody treatment, we found a 2-fold increase in mIPSC frequency and no change in mIPSC amplitude distribution in comparison to the BSA treated cells (Fig. 2.2. E-G: BSA n=6; SYT1 Ab n=8; p=0.0086). These findings suggest that syt1 function is acutely disrupted and corroborates our earlier results that show that after strong stimulation, we can manipulate both synaptic vesicles pools recycling spontaneously and in response to stimulation. Next, we treated neurons with syt1 lumen antibody in the presence of TTX to allow spontaneously recycling vesicles to take up syt1 lumen antibody. We did not observe a significant difference in eIPSC amplitude or increase in asynchrony after stimulation in comparison to the BSA treated group (Fig. 2.2. I-J)). However, we did observe a 4.5-fold increase in mIPSC frequency after syt1 lumen antibody treatment in TTX in comparison to the BSA treated group (Fig. 2.2. L, M: BSA n=10; Syt1 Ab n=9; p=0.0186). These findings corroborate our earlier results that free radical generation within spontaneously recycling vesicles alters spontaneous but not evoked transmission. Taken together, these results imply that syt1 molecules residing on spontaneously recycling vesicles may not mix with their counterparts residing on vesicles that recycle in response to stimulation.

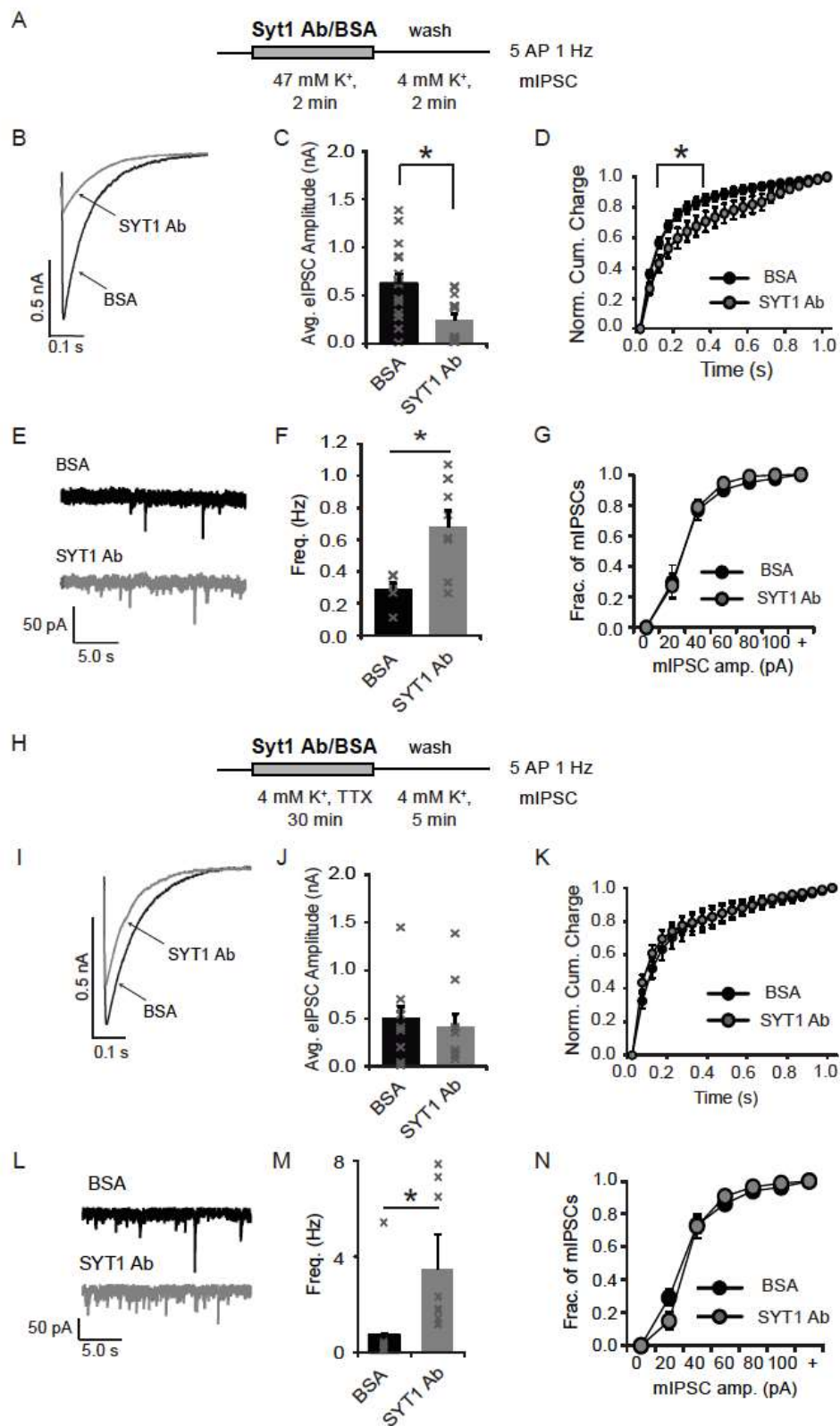


Figure 2.2 Synaptotagmin-1 luminal domain antibody acutely disrupts synaptotagmin-1 function. (A) Diagram of experiment: Neurons were incubated in either 1% syt1 lumen

antibody or 3% BSA 47mM modified tyrode's solution for 2 minutes and then washed out for two minutes before mIPSC or eIPSC (evoked by 5 pulses at a 1 Hz frequency) recordings were taken. (B) Representative traces of the 1st AP after treatment with either BSA (black) or syt1 lumen antibody (gray). (C) Summary graph of the average IPSC amplitude after treatment with either BSA (black) or syt1 lumen antibody (gray). (BSA, n=16; syt1 lumen antibody, n=14; $t_{(28)}=3.158$; $p=0.0038$; t-test). (D) Normalized charge transfer plot for the average IPSC over a second in neurons treated with BSA (black) and syt1 lumen antibody (gray; ordinary two-way ANOVA; $F_{(1,588)}=59.49$; $p<0.0001$). (E) Representative mIPSC traces from neurons treated with BSA (black) and syt1 lumen antibody (gray). (F) Summary graph of the average mIPSC frequency in neurons treated with BSA (black) and syt1 lumen antibody (gray). (BSA, n=6; syt1 lumen antibody, n=7; $t_{(12)}=3.138$; $p=0.0086$; t-test). (G) Distribution of mIPSC amplitude from neurons treated with BSA (black) and syt1 lumen antibody (gray). (ordinary two-way ANOVA; $F_{(1,84)}=0.3033$; $p=0.5833$). (H) Diagram of experiment: Neurons were incubated in either 1% syt1 lumen antibody or 3% BSA tyrode's solution for 30 minutes in the presence of tetrodotoxin (TTX) and then washed out for five minutes before mIPSC or eIPSC (evoked by 5 pulses at a 1 Hz frequency) recordings were taken. (I) Representative traces of the 1st AP after treatment with either BSA (black) or syt1 lumen antibody (gray). (J) Summary graph of the average IPSC amplitude after treatment with either BSA (black) or syt1 lumen antibody (gray). (BSA, n=11; syt1 lumen antibody, n=10; $t_{(19)}=0.5023$; $p=0.6212$; t-test). (K). Normalized charge transfer plot for the average IPSC over a second in neurons treated with BSA (black) and syt1 lumen antibody (gray). (ordinary two-way ANOVA; $F_{(1,399)}=2.394$; $p=0.1226$). (L) Representative mIPSC traces from neurons treated with BSA (black) and syt1 lumen antibody (gray). (M) Summary graph of the average mIPSC frequency in neurons treated with BSA (black) and syt1 lumen antibody (gray). (BSA, n=10; syt1 lumen antibody, n=9; $t_{(17)}=2.601$; $p=0.0186$; t-test). (N) Distribution of mIPSC amplitude from neurons treated with BSA (black) and syt1 lumen antibody (gray; ordinary two-way ANOVA; $F_{(1,119)}=0.1594$; $p=0.3069$).

DISCUSSION

To probe if syt1 is a target of free radical modification, we expressed an enhanced HRP variant tagged to the luminal domain of syt1 in cells, which, after H₂O₂ treatment, resulted in recapitulation of the syt1 loss-of-function phenotype. These results suggest that syt1 function can be disrupted acutely through free radical modification within the vesicle lumen indicating a role for the syt1 luminal region in vesicle trafficking (Han et al., 2004; Kwon and Chapman, 2012). This observation is consistent with the abundance of key cysteine residues in syt1 that may be specifically targeted by reactive oxygens (Fukuda et al., 2001). It is important to note that the expression of syt1-eHRP, by itself, did not significantly alter synaptic transmission and the effects seen here were observed only after

peroxide treatment. We further assessed the functional significance of the luminal domain of syt1 by taking advantage of a polyclonal antibody targeting the luminal domain. For this antibody to bind its antigen, synaptic vesicles need to undergo exocytosis making the lumen accessible from the synaptic cleft and thus the extracellular space (Sara et al., 2005). Uptake of the antibody upon mobilization of the recycling pool with elevated K^+ solution elicited asynchronous-evoked release upon stimulation and an increase in spontaneous events. This result is consistent with our HRP loading and free radical generation experiments during strong stimulation as discussed above. In contrast, labeling synaptic vesicles recycling spontaneously with antibody against syt1 led to an increase in frequency of spontaneous transmission with no observed defect in evoked transmission. These observations suggest that although syt1 is widely distributed across synaptic vesicle pools and regulates both spontaneous and evoked neurotransmission, its action on the two forms of release — i.e. suppression of spontaneous release and synchronization of evoked release — are due to distinct functions that do not necessarily co-exist on the same vesicle. This premise is consistent with the recent evidence that syt1 exists in two configurations at the synapse: one form promotes vesicle fusion upon stimulation, the other serves to clamp down on spontaneous transmission (Bai et al., 2016).

The exact mechanism by which tagging the luminal domain of syt1 disrupts its function in exocytosis is unclear at this point. Prior work has demonstrated that antibody bound to the syt1 luminal domain can still traffic to and out of vesicles and is not trapped on the plasma membrane (Hua et al., 2010; Wilhelm et al., 2010). The combination of multiple antibodies bound to different regions of the luminal domain of syt1 could potentially serve as a steric hindrance to syt1 function in synaptic vesicle exocytosis. However, this disruption in function seems to be reversed with strong stimulation (Hua et al., 2010; Wilhelm et al., 2010) possibly through the binding of Ca^{2+} to other non-bound syt1 molecules. In agreement with this premise, when we used a cypHer-tagged version of the syt1 luminal domain antibody, we could also show that N-terminal tagged syt1 could still go through exo-endocytotic recycling during strong (20Hz) stimulation suggesting that the tag does not cause syt1 to be trapped on the plasma membrane (data not shown).

Nevertheless, the functional impact of syt1 luminal domain antibodies we demonstrated here complicates straight forward interpretation of experiments using these antibodies with respect to putative segregation of action potential evoked and spontaneous synaptic vesicle recycling pathways (Hua et al., 2010; Wilhelm et al., 2010). Moreover, these results indicate that 20 Hz stimulation or elevated K^+ stimulation are too strong to reveal the differences between synaptic vesicle fusion propensities (Kavalali, 2015). In addition, results obtained using probes that tag synaptotagmin at its N-terminus (such as synaptotagmin-pHluorin) should also be interpreted with caution. However, given the minimal effects of eHRP on syt1 function, we do not anticipate smaller tags like myc or FLAG to affect syt1 function.

CHAPTER THREE

DYNAMIN 2 IS NOT REQUIRED FOR SYNAPTIC VESICLE RECYCLING AND NEUROTRANSMISSION

BACKGROUND

Dynamin 2 is the least expressed dynamin isoform in neurons as quantified by RT-PCR from rat sensory neurons (Cao, 1998). However, in the absence of the neuronal dynamins, dynamin 1 and 3, synaptic vesicle endocytosis persists. This residual retrieval of synaptic vesicles was reported to be partly due to dynamin 2 (S. M. Ferguson et al., 2007). In superior cervical ganglion neurons, knock down of dynamin 2 revealed defects in rapid recovery of the readily releasable pool of synaptic vesicles after high frequency stimulation (Tanifuji et al., 2013). A similar finding was reported in chromaffin cells where after prolonged stimulation, a dynamin 2 dependent endocytosis mechanism was activated to retrieve vesicles (Artalejo PNAS 2002). A function for dynamin 2 at the synapse is also supported by the finding that Ca^{2+} influx in neurons inhibits dynamin mediated endocytosis at the active zone and has been shown to reduce specifically, dynamin 2 GTPase activity in HeLa cells (Cousins MA 2000 j Neurosci).

Dynamin 2 is also implicated in exocytosis of vesicles in non-neuronal cell lines. In natural killer cells, dynamin 2 is required for the exocytosis of lytic granules required to dispatch pathogens (Arneson et al., 2008). Also, dynamin 2 has been shown to block focal

exocytosis in macrophages (Di et al., 2003). In chromaffin cells, dynamin activity regulates vesicle fusion pore expansion thereby modulating transmitter release (Jackson et al., 2015). In this section, we investigate the potential of dynamin 2 in synaptic vesicle endocytosis and neurotransmission in a small central synapse.

METHODS

Lentiviral Infection

HEK293 cells (ATCC) were transfected with 3 packaging plasmids (pMDLg/pRRE, pRSV-Rev, and pCMV-VSV-G) and a pFUGW transfer vector containing a Cre-recombinase construct using the Fugene 6 transfection reagent (Promega). Cell culture supernatants containing the virus were collected 72 hours later and spun down to participate out cellular debris and other contaminants. Neurons were infected at 4 days *in vitro* (DIV) by adding 300 μ l of virus containing supernatant to the neuronal culture media.

Cell Culture

Dissociated hippocampal cultures from postnatal day 0-3 *dnm2^{ff}* were prepared as previously described (Kavalali et al., 1999). Neurons were infected at 4 DIV with lentivirus expressing Cre recombinase or an empty L307 vector for control and experiments were performed at 17-21 DIV. All experiments were performed following protocols approved by the University of Texas Southwestern Institutional Animal Care and Use Committee.

Imaging

17-21 DIV neuronal cultures infected with lentivirus expressing either vGlut-pHluorin or vGlut-pHluorin and Cre recombinase were used for imaging experiments. Images were taken with an Andor iXon Ultra 897 High Speed Camera (Andor Technology LTd) through a Nikon Eclipse TE2000-U Microscope (Nikon) using a 100X Plan Fluor objective (Nikon). Images were illuminated with a Lambda-DG4 (Sutter instruments) and acquired at \sim 7 Hz with a 120 ms exposure time and binned at 4 by 4 to increase the SNR. Images were collected and processed using Nikon Elements Ar software prior to export to Microsoft excel for analysis. ROIs were randomly selected based on a threshold after

treatment with NH_4Cl .

Imaging Analysis

Individual synaptic puncta were selected randomly after NH_4Cl perfusion and all quenched pHluorin probes were unmasked. Single vesicle events were analyzed as reported in Leitz *et. al.* (2011). Dwell times were calculated as the time between the initial fluorescence step and the start of fluorescence decay predicted by the best fit decay (using a goodness of fit parameter). Decay time constants were determined by fitting data with single exponential decay curves using Levenberg-Marquardt least sum of squares minimizations (a minimum of 10 points, $\sim 1.7\text{s}$, was required for the fitting after calculating dwell times). Single vesicle events were analyzed offline with MatLab. For 20 Hz stimulation, amplitude measurement and single exponential decay fitting (using Levenberg-Marquardt least sum of squares minimizations) were performed offline in Clampfit.

Western Blot

Neuronal cultures were homogenized processed for western blot as described in Nosyreva and Kavalali (2010). Dynamin 2 antibody was used at a 1:800 dilution (Abcam) and protein bands were developed using enhanced chemiluminescence (ECL). Bands were analyzed using ImageJ software and dynamin 2 level was normalized to GDI loading control.

Electrophysiology

A modified Tyrode's solution was used for all experiments (except where noted otherwise) that contained (in mM): 145 NaCl, 4 KCl, 2 $\text{MgCl}_2 \cdot (6\text{H}_2\text{O})$, 10 glucose, 10 HEPES, 2 CaCl_2 (pH 7.4, osmolarity 300 mOsM). Pyramidal neurons were whole-cell voltage clamped at -70 mV with borosilicate glass electrodes (3-5 $\text{M}\Omega$) filled with a solution containing (in mM): 105 Cs-methanesulphonate, 10 CsCl, 5 NaCl, 10 HEPES, 20 TEA.Cl hydrate, 4 Mg-ATP, 0.3 GTP, 0.6 EGTA, 10 QX-314 (pH 7.3, osmolarity 290 mOsM). Excitatory-postsynaptic currents (EPSCs) were evoked with 0.1-ms, 10mA pulses delivered via a bipolar platinum electrode in a modified Tyrode's solution containing Picrotoxin (PTX, 50 μM) and DL-2-Amino-5-phosphonovaleric acid (APV, 50 μM , NMDA receptor blocker).

Spontaneous miniature EPSCs (mEPSCs) were recorded in a modified Tyrode's solution containing TTX (1 μ M), PTX (50 μ M) and APV (50 μ M). Data was analyzed offline with Clampfit 9 software.

Statistical Analysis

Statistical analyses were performed with Graphpad Prism 6.07 software using one of the following tests: Student's ordinary t-test, Two RM ANOVA, Kolmogorov-Smirnov test. Error bars represent SEM.

RESULTS

Dynamin 2 is effectively knocked out and cleared out from the synapse by as early as 17 DIV

Dynamin 2 is ubiquitously expressed across all mammalian tissues. It is functionally implicated in CME, other non-clathrin dependent forms of endocytosis, cellular migration, actin remodeling and reported to be necessary for mitosis (Durieux, Prudhon, Guicheney, & Bitoun, 2010). Complete loss of dynamin 2 has proven to be too strenuous on developing tissue and such a complete dynamin 2 KO mouse is non viable in utero (S. M. Ferguson & De Camilli, 2012). Here, we successfully knock out dynamin 2 in dissociated hippocampal neuronal cultures from *dnm2^{fl/fl}* mice by infecting them with lentivirus expressing Cre recombinase at 4 DIV (Figure 3.1). We confirmed dynamin 2 knock out by western blot analysis. The earliest we detected complete dynamin 2 KO is 17 DIV.

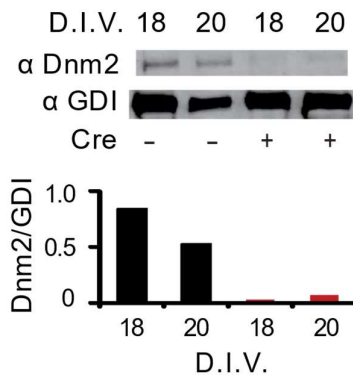


Figure 3.1. Western blot analysis of dynamin 2 KO. (Top) Western blot against dynamin

2 using a polyclonal dynamin 2 antibody in dynamin 2 KO neurons and littermate control. (Bottom) Quantification of the western blot.

Dynamin 2 is not required for synaptic transmission

The most direct evidence functionally implicating dynamin 2 in synaptic transmission was shown by Tanifuji et al. (2013). They reportedly knocked down dynamin 2 using siRNA in superior cervical ganglion neurons and demonstrated slight defects in neurotransmission during high and low frequency stimulation. Other reports have inferred dynamin 2 function(s) by probing synaptic transmission in the absence of neuronal dynamins, dynamins 1 and 3 (S. M. Ferguson et al., 2007; Raimondi et al., 2011). We investigated dynamin 2's role in synaptic transmission by voltage patch clamping pyramidal neurons in dissociated culture after dynamin 2 KO. We observed no changes in average eEPSC amplitude and synaptic facilitation after 1 Hz and 10 Hz stimuli (Figure 3.2 A, D, E). These findings suggest dynamin 2 is not necessary for evoked synaptic transmission. We also recorded spontaneous neurotransmission in the presence of tetrodotoxin to assess dynamin 2's function in spontaneously released vesicle recycling. We observed no changes in miniature excitatory postsynaptic currents (mEPSC) frequency and amplitude suggesting that dynamin 2 is not necessary for the recycling of spontaneously released vesicles (Figure 3.2 B, C). Dynamin 2 is the least expressed dynamin isoform in mammalian neural tissue (Cao et al., 1998). A possible role for dynamin 2 in synaptic vesicle recycling during high frequency activity can potentially be masked by the other highly expressed dynamin isoforms as dynamin 3 KO neurons reveal no overt neurotransmission defects while dynamin 1 and 3 double knockout neurons reveal an exacerbated dynamin 1 KO defect in neurotransmission (Raimondi et al., 2011).

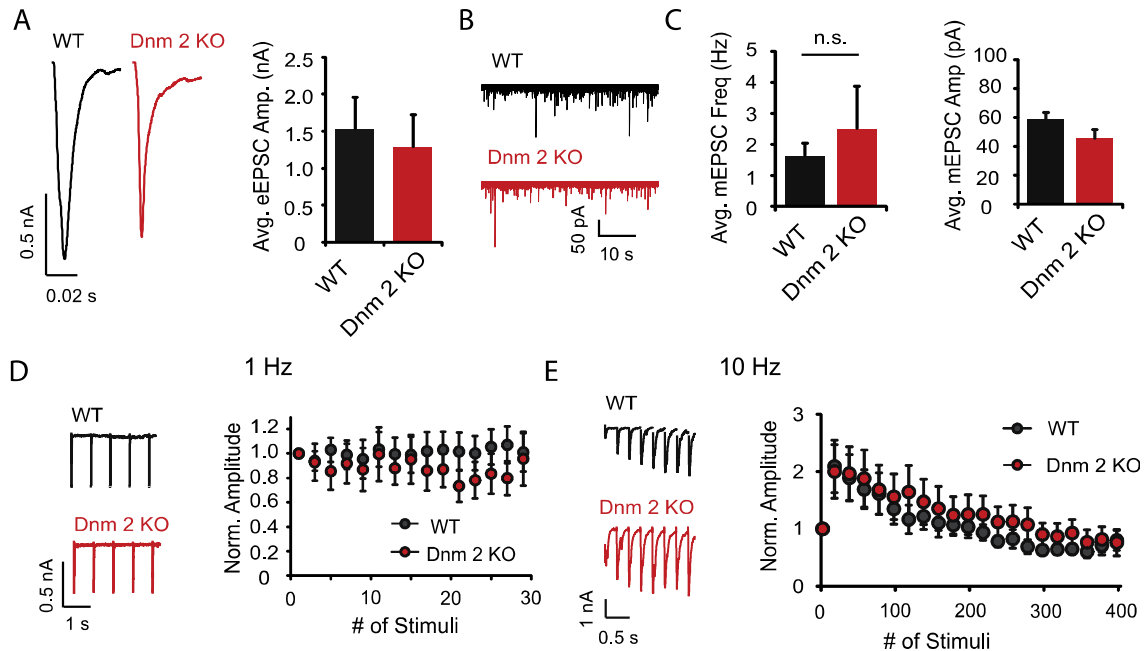


Figure 3.2. Excitatory neurotransmission in dynamin 2 KO neurons. (A) Left: sample eEPSC recording from WT littermate controls (black) and Dnm 2 KO (red). Right: average eEPSC amplitudes from WT (n=10) and Dnm 2 KO (n=9) neuronal cultures ($p=0.6596$, Student's ordinary t-test). (B) Sample mEPSC traces for WT (black) and Dnm 2 KO (red) neuronal cultures. (C) Left: average mEPSC frequency for WT (n=6) and Dnm 2 KO (n=8; $p=0.1816$, Student's ordinary t-test). Right: average mEPSC amplitude for WT and Dnm 2 KO neuronal cultures ($p=0.6282$, Student's ordinary t-test). (D) Left: sample eEPSC traces of the first 5 responses from WT (black) and Dnm 2 KO (red) neurons to 30 stimuli applied at a 1 Hz frequency. Right: normalized responses from WT (black) and Dnm 2 KO (red) neurons after 30 pulses 1 Hz stimuli (WT, n=10; Dnm 2 KO, n=9; $p=0.4385$, Two-way RM Anova). (E) Left: sample eEPSC traces of the first 13 responses from WT (black) and Dnm 2 KO (red) neurons to 400 stimuli applied at a 10 Hz frequency. Right: Normalized responses from WT (black) and Dnm 2 KO (red) neurons after 400 pulses 10 Hz stimuli (WT, n=10; Dnm 2 KO, n=9; $p=0.4903$, Two-way RM Anova).

Dynamin 2 is not required for the recycling of synaptic vesicles after high frequency activity

Reliable neurotransmission is dependent on tight coupling of synaptic vesicle exocytosis with endocytosis. Dynamin 2 was reported to play a role in the exocytosis-endocytosis coupling of vesicles in mouse pancreatic β -cells by Min *et al* (2007). . Also, dynamin 2 is implicated as a catalyst of scission of budding endosomes in other forms of endocytosis apart from CME in different cell types (Cao *et al.*, 2007; Y. W. Liu *et al.*, 2008;

Schlunck et al., 2004). Taken together, these findings purport a potential role for dynamin 2 in synaptic vesicle recycling. To test if dynamin 2 is required for synaptic vesicle recycling, we infected *dnm2^{f/f}* hippocampal neurons with lentivirus expressing vGlut-pHluorin and Cre recombinase and assessed synaptic vesicle recycling after a 20 Hz 100 pulse stimulus. We observed a slight decrease in the measured decay τ in *dnm2* KO synapses in comparison to WT littermate control synapses (Figure 3.3 A, B). To determine if acceleration in synaptic vesicle retrieval was due to a decrease in synaptic vesicle exocytic load, we measured the ratio of the amplitude of the ΔF after the stimulus and the maximal possible response $F_{\text{NH}_4\text{Cl}}$. We observed a decrease in exocytic load in dynamin 2 KO synapses suggesting that the decrease in decay τ is reflective of changes in exocytosis in dynamin 2 KO synapses (Figure 3.3 C). We repeated these experiments at 32 °C to assess synaptic vesicle recycling in the absence of dynamin 2 at a more physiological temperature (data not shown). Again, we observed a decrease in the measured decay τ in dynamin 2 KO neurons in comparison to control. However, we also observed a significant decrease in exocytic load in the dynamin 2 KO synapses after 20 Hz 100 pulse stimuli in comparison to the control recapitulating our earlier results. These findings suggest that dynamin 2 is not required for synaptic vesicle recycling after high frequency activity. However, this data also seems to allude to a role for dynamin 2 in synaptic vesicle exocytosis during high frequency stimulation.

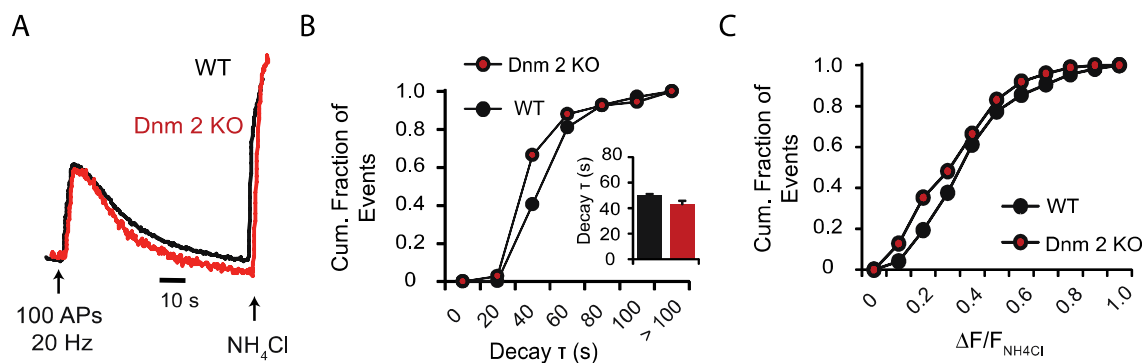


Figure 3.3. Synaptic vesicle retrieval in the absence of dynamin 2. (A) Sample pHluorin response to a 20 Hz 100 pulse stimuli for WT (black) and Dnm 2 KO (red) neuronal cultures. (B) Cumulative distribution of the calculated decay τ after decay in fluorescence is fit with a single exponential decay function for WT (black) and Dnm 2 KO (red) neuronal cultures (WT, $n=399$ puncta; Dnm 2 KO, $n=340$ puncta; $p<0.0001$, Kolmogorov-Smirnov test). Inset: Average calculated decay τ for WT (black) and Dnm 2 KO (red). (C) Cumulative distribution

of the ratio of ΔF in response to the 20 Hz 100 AP stimuli to the maximal possible response, $F_{\text{NH}_4\text{Cl}}$ for WT (black) and Dnm 2 KO (red) neurons ($p < 0.0001$, Kolmogorov-Smirnov test).

Dynamin 2 is not necessary for single synaptic vesicle retrieval.

Clathrin mediated endocytosis is generally thought to be the primary method of the retrieval of a single synaptic vesicle from the presynaptic terminal (Granseth et al., 2006). However recent studies suggest that synaptic vesicles can be retrieved by a much faster mechanism that is both dynamin and temperature dependent (Watanabe et al., 2013). Currently, dynamin 2 function in CME is not limited to catalyzing scission of the budding endosome but also plays a role in the early phases of CME (Grassart et al., 2014; Mettlen, Pucadyil, Ramachandran, & Schmid, 2009). Taking these into consideration, it is possible that dynamin 2 is essential for single vesicle recycling at the synapse. To test if dynamin 2 is required for single vesicle synaptic vesicle recycling, we infected $dnm2^{ff}$ with lentivirus expressing vGlut-pHluorin and Cre recombinase and stimulated single vesicle release with a sparse 30 pulses at 0.1 Hz stimulation paradigm (Figure 3.4 A). We observed no change in the amplitude of single vesicle events in dynamin 2 KO synapses in comparison to wildtype littermate controls suggesting no change in the level of vGlut-pHluorin expression (Figure 3.4 B). We also observed no change in the dwell time, the time a vGlut-pHluorin probe resided on the cellular surface prior to retrieval, of the single vesicle event suggesting that dynamin 2 KO neurons are endocytosed at a similar rate to the wildtype control (Figure 3.4 F-H). However, we did observe a slight left shift in the distribution of decay τ of the single vesicle events in dynamin 2 KO synapses (Figure 3.4 C-E) suggesting dynamin 2 functions to retard synaptic vesicle acidification. These experiments were repeated at 32 °C and similar observations were also made. There were no changes in single vesicle amplitude and dwell time between dynamin 2 KO and wildtype control synapses (Figure 3.5 A-E). However, again, there was a decrease in single vesicle decay τ (Figure 3.5 F-H). Interestingly, there was no observed difference in the dwell time for single events taken at room temperature and those observed at 32 °C for either wildtype or dynamin 2 KO (Figure 3.5 E). This would suggest that the mechanisms of single synaptic vesicle retrieval at room temperature are also prevalent and dominant at the more physiological relevant temperature of 32 °C.

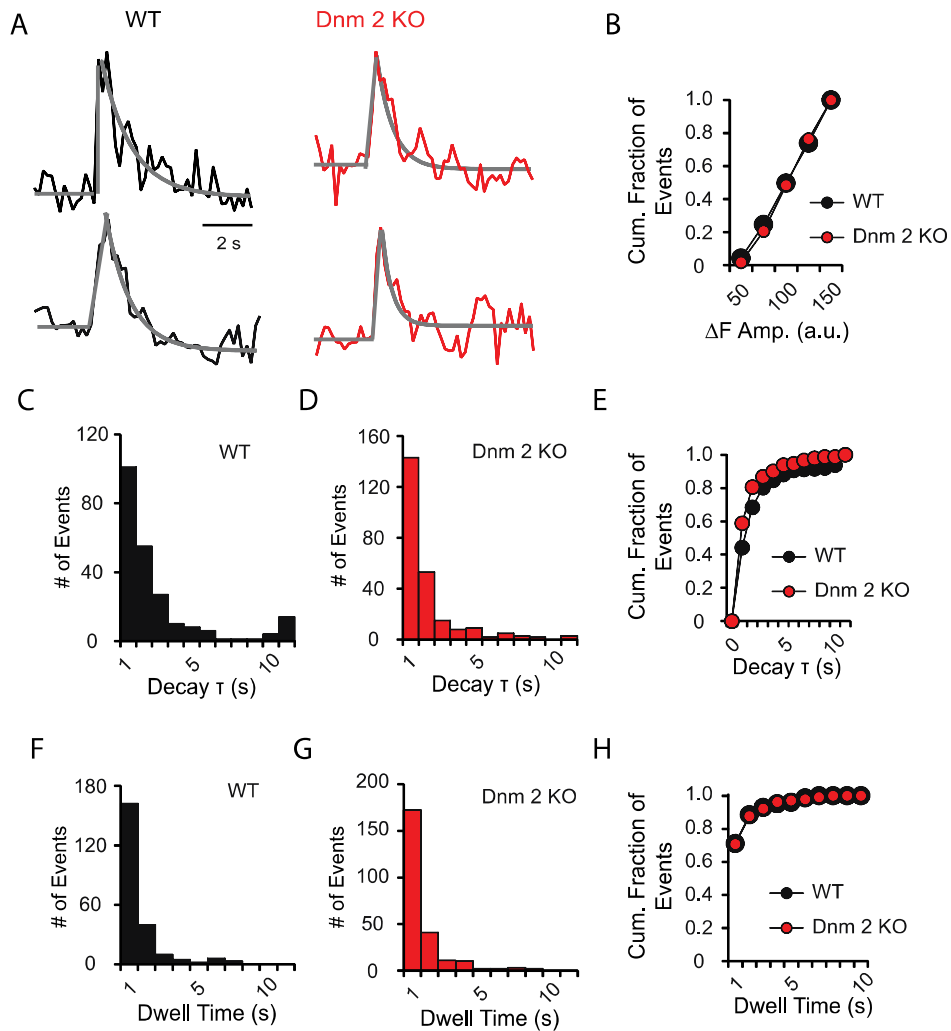


Figure 3.4. Recycling of single synaptic vesicle in the absence of dynamin 2 at room temperature. (A) Sample traces of single vesicle events for WT (black) and Dnm 2 KO (red). Gray line represents model single exponential decay fit to signal. (B) Cumulative fraction of events of the amplitude of single vesicle events for Dnm 3 KO (black, $n = 281$) and Dnm 2 KO (red, $n = 307$; $p = 0.0233$; Kolmogorov-Smirnov test). (C) Distribution of observed decay τ of single vesicle events from WT cultures (black, $n = 229$). (D) Distribution of observed decay τ for single vesicle fusion events from Dnm 2 KO cultures (red, $n = 244$). (E) Cumulative fraction of decay τ of single vesicle events in WT (black) and Dnm 2 KO (red; $p = 0.0017$; Kolmogorov-Smirnov test). (F) Distribution of observed dwell times of single vesicle events from WT cultures (black, $n = 229$). (G) Distribution of observed dwell times for single vesicle fusion events from Dnm 2 KO cultures (red, $n = 244$). (H) Cumulative fraction of dwell times of single vesicle events in WT (black) and Dnm 2 KO (red; $p = 0.0005$; Kolmogorov-Smirnov test).

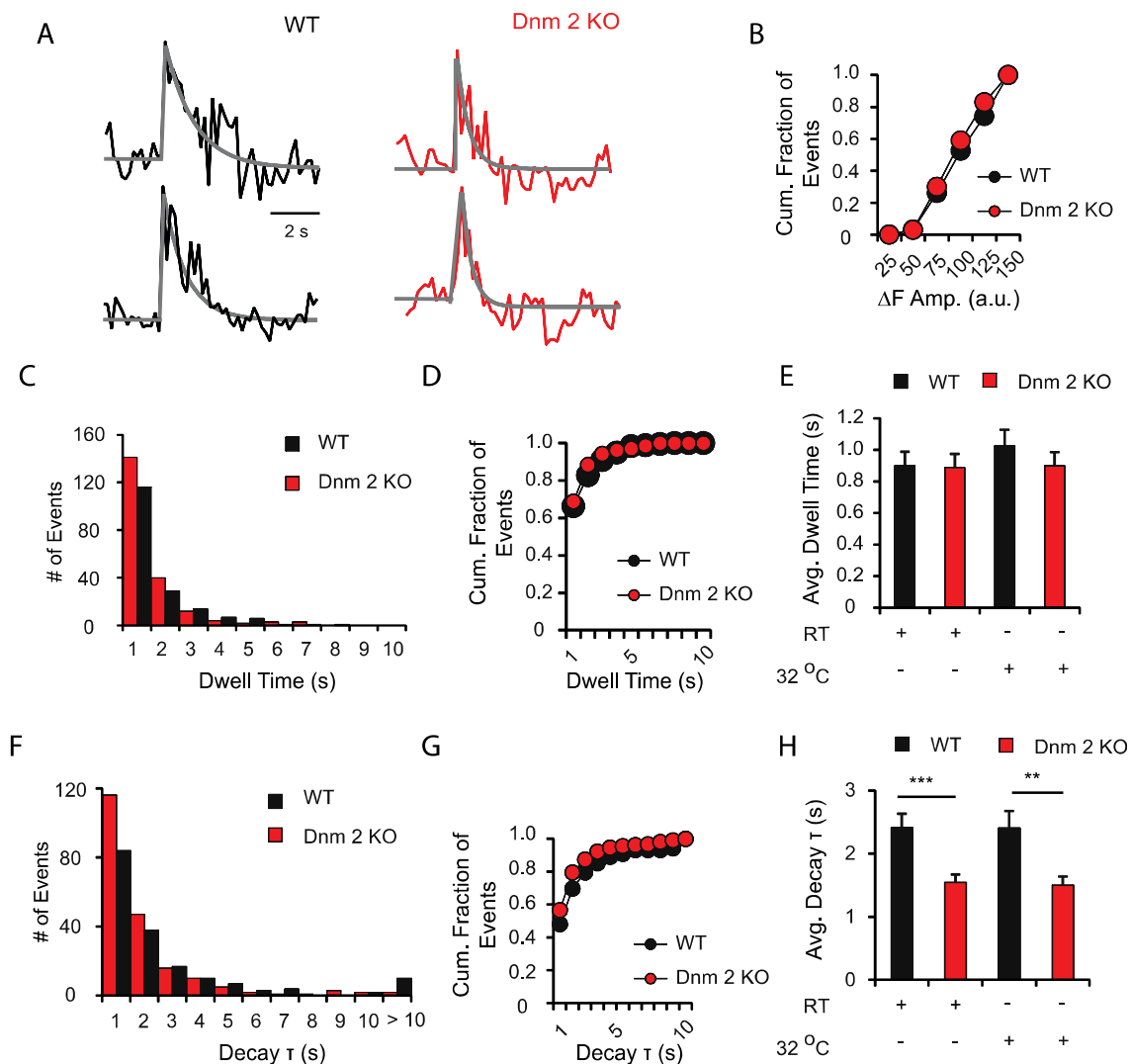


Figure 3.5. Kinetics of single vesicle recycling in the absence of dynamin 2 at 32 °C. (A) Sample traces of single vesicle events for WT (black) and Dnm 2 KO (red). Gray line represents model single exponential decay fit to signal. (B) Cumulative fraction of events of the amplitude of single vesicle events for Dnm 3 KO (black, $n = 246$) and Dnm 2 KO (red, $n = 264$; $p = 0.4771$; Kolmogorov-Smirnov test) at 32 °C. (C) Distribution of observed dwell times for WT (black, $n = 175$) and dynamin 2 KO (red, $n = 205$) neurons at 32 °C. (D) Cumulative fraction of the observed dwell times of single vesicle events from WT cultures (black) and dynamin 2 KO (red; $p = 0.3130$; Kolmogorov-Smirnov test). (E) Average dwell time from WT (black) and dynamin 2 KO (red) neurons at room temperature and 32 °C ($p = 0.9173$; Student's ordinary t-test; $p = 0.3385$; Student's ordinary t-test). (F) Distribution of observed decay τ of single vesicle events from WT cultures (black, $n = 175$) and dynamin 2 KO (red, $n = 205$) at 32 °C. (G) Cumulative fraction of decay τ of single vesicle events in WT (black) and Dnm 2 KO (red; $p = 0.0153$; Kolmogorov-Smirnov test). (H) Average decay τ of single vesicle events in WT (black) and Dnm 2 KO (red) at room temperature and 32 °C ($p = 0.0005$; Student's ordinary t-test; $p = 0.0023$; Student's ordinary t-test).

DISCUSSION

In this study we directly assess dynamin 2 function in synaptic vesicle recycling and neurotransmission in small central synapses. In the absence of dynamin 2, synaptic vesicle recycling and neurotransmission largely remain unperturbed in hippocampal neurons. This highlights the synapses' independence of dynamin 2 for synaptic vesicle recycling. It is also possible that this is reflective of the overlap of dynamin isoform function at the synapse. To parse out these two will require the reexpression of dynamin 2 on a dynamin TKO background and assess the ability of dynamin 2 to rescue the phenotype. We did observe a decrease in the fraction of synaptic vesicles released after 20 Hz 100 AP stimulation in dynamin 2 KO neurons suggestive of a decrease in release probability however, this experiment is limited by our inability to access changes in synaptic vesicle endocytosis during stimulation. To assess if the observed decrease in the fraction of synaptic vesicles released is due to an increased synaptic vesicle retrieval during stimulation will require a repeat experiment in the presence of NH_4Cl to label all released vesicles released in response to stimulation. A decrease in synaptic vesicle release probability in dynamin 2 KO neurons was not observed in our electrophysiological experiments.

Despite dynamin 2's involvement in both the early phase and scission of clathrin mediated endocytosis, dynamin 2 proved to be dispensable for single synaptic vesicle endocytosis (Grassart et al., 2014; Mettlen et al., 2009). This effect was present at both room temperature and at 32 °C. A key observation presented here is the kinetics of single vesicle retrieval being similar at both room temperature and 32 °C even though CME is reported to be the predominant mode of single synaptic vesicles at room temperature and 34 °C, ultrafast endocytosis dominates as primary means of vesicle retrieval (Granseth et al., 2006; Watanabe et al., 2013). We surmise that a singular form of endocytosis must be dominant at both room temperature and at the elevated temperature of 32 °C. It is possible the difference in elevated temperature to that which is reported could be the determinant for which form of endocytosis dominates at any given moment. In ultrafast endocytosis, the size of the retrieved endosome is about three times larger than a single synaptic vesicle raising doubts that only one vesicle is released prior to compensatory endocytosis (Watanabe et al., 2013). On the other hand,

clathrin mediated endocytosis functions on a timescale about ten times slower than what we report here suggesting that what we see is a CME independent mechanism (Grassart et al., 2014). We postulate that the endocytosis mechanism at play is kiss-and-run. Dynamin's function in regulating kiss-and-run exo-endocytosis has been characterized in chromaffin cells. There, it was demonstrated that the activator of dynamin, Ryngo 1-23 can increase the amount of neurotransmitter released (Jackson et al., 2015). Considering synaptic vesicles are actively acidified to exchange protons for neurotransmitters, it is possible that in the absence of an activated dynamin to extend the release of neurotransmitters, less protons are needed to refill a retrieved synaptic vesicle and this is reflected as a decrease in decay τ by our vGlut-pHluorin reporter.

CHAPTER FOUR

LOSS OF DYNAMIN AFFECTS SYNAPTIC VESICLE EXOCYTOSIS-ENDOCYTOSIS COUPLING AFTER STRONG STIMULATION

BACKGROUND

In the shibire mutant fly, at the restrictive temperature, synaptic terminals were depleted of synaptic vesicles and arrested budding endosomes were observed (Koenig & Ikeda, 1989). This finding suggests that in the absence of functional dynamin, synaptic terminals are depleted of vesicles and compensatory endocytosis arrested. However, the *Drosophila* genome encodes a single gene for dynamin while the mammalian genome encodes for three isoforms of dynamin, all of which are expressed in the nervous system and at the synapse (S. M. Ferguson & De Camilli, 2012). Taken together, this data will argue that dynamin is essential for endocytosis. However, there is evidence for dynamin independent endocytosis at the synapse. In hippocampal neuronal cultures, the presence of the dynamin inhibitor, dynasore, leaves spontaneous neurotransmission unperturbed while evoked synchronous and asynchronous transmission showed synaptic depression (Chung, Barylko, Leitz, Liu, & Kavalali, 2010). Similarly, the injection of nonhydrolyzable GTP into the calyx of Held synapse, revealed an initial block of synaptic vesicle retrieval that was followed by a resumption of synaptic vesicle endocytosis (Xu et al., 2008). The authors surmised that

dynamin independent endocytosis is only triggered after repetitive stimulation and membrane expansion. Similarly, a study in salamander retinal cone cells, a continuously active synapse, revealed no change in endocytosis in the presence of dynamin inhibitors (Van Hook & Thoreson, 2012) but this result was later refuted (Fuchs, Brandstatter, & Regus-Leidig, 2014; Jockusch, Praefcke, McMahon, & Lagnado, 2005). Here, we assess synaptic vesicle recycling in the absence of dynamin in a small central synapse.

METHODS

Lentiviral Infection

HEK293 cells (ATCC) were transfected with 3 packaging plasmids (pMDLg/pRRE, pRSV-Rev, and pCMV-VSV-G) and a pFUGW transfer vector containing a Cre-recombinase construct using the Fugene 6 transfection reagent (Promega). Cell culture supernatants containing the virus were collected 72 hours later and spun down to participate out cellular debris and other contaminants. Neurons were infected at 4 days *in vitro* (DIV) by adding 300 μ l of virus containing supernatant to the neuronal culture media.

Cell Culture

Dissociated hippocampal cultures from postnatal day 0-3 $dnm1^{f/f}dnm2^{f/f}dnm3$ KO were prepared as previously described (Kavalali et al., 1999). Neurons were infected at 4 DIV with lentivirus expressing Cre recombinase or an empty L307 vector for control and experiments were performed at 17-21 DIV. All experiments were performed following protocols approved by the University of Texas Southwestern Institutional Animal Care and Use Committee.

Immunocytochemistry

Neuronal cultures were processed for immunocytochemistry as described in Ramirez *et. al.* (2008) at 17-19 DIV. Antibodies against dynamin (Synaptic Systems), dynamin 1 (Abcam), dynamin 2 (Abcam), synapsin, vGlut-1 (Synaptic Systems) and vGAT (Synaptic Systems) were used at concentrations of 1:500, 1:300, 1:300, 1:1000, 1:500 and 1:500 respectively. Images were taken on a confocal microscope with a 63X objective.

Electron Microscopy

Neuronal cultures were incubated in modified tyrode's solution (see below) for 2 minutes and then rinsed twice with PBS and then fixed and processed for electron microscopy by the UTSW Electron Microscopy Core.

Western Blot

Neuronal cultures were homogenized and processed for western blot as described in Nosyreva and Kavalali (2010). Antibodies against dynamin (Synaptic Systems), dynamin 1 and dynamin 2 were used at a 1:1000, 1:3000 and 1:800 dilution respectively (source) and protein bands were developed using enhanced chemiluminescence (ECL). Bands were analyzed using ImageJ software and protein levels were normalized to GDI loading control.

Electrophysiology

A modified Tyrode's solution was used for all experiments (except where noted otherwise) that contained (in mM): 145 NaCl, 4 KCl, 2 MgCl₂•(6H₂O), 10 glucose, 10 HEPES, 2 CaCl₂ (pH 7.4, osmolarity 300 mOsM). Pyramidal neurons were whole-cell voltage clamped at -70 mV with borosilicate glass electrodes (3-5 MΩ) filled with a solution containing (in mM): 105 Cs-methanesulphonate, 10 CsCl, 5 NaCl, 10 HEPES, 20 TEA.Cl hydrate, 4 Mg-ATP, 0.3 GTP, 0.6 EGTA, 10 QX-314 (pH 7.3, osmolarity 290 mOsM). Excitatory-postsynaptic currents (EPSCs) were evoked with 0.1-ms, 10mA pulses delivered via a bipolar platinum electrode in a modified Tyrode's solution containing Picrotoxin (PTX, 50 μM) and DL-2-Amino-5-phosphonovaleric acid (APV, 50 μM, NMDA receptor blocker). Spontaneous miniature EPSCs (mEPSCs) were recorded in a modified Tyrode's solution containing TTX (1 μM), PTX (50 μM) and APV (50 μM). Inhibitory-postsynaptic currents (IPSCs) were evoked with 0.1-ms, 10mA pulses delivered via a bipolar platinum electrode in a modified Tyrode's solution containing 6-Cyano-7-nitroquinoxaline-2-3-dione (CNQX, 10 μM) and DL-2-Amino-5-phosphonovaleric acid (APV, 50 μM, NMDA receptor blocker). Spontaneous miniature IPSCs (mIPSCs) were recorded in a modified Tyrode's solution

containing TTX (1 μ M), CNQX (10 μ M) and APV (50 μ M). Data was analyzed offline with Clampfit 9 software.

Imaging

17-21 DIV neuronal cultures infected with lentivirus expressing either vGlut-pHluorin or vGlut-pHluorin and Cre recombinase were used for imaging experiments. Images were taken with an Andor iXon Ultra 897 High Speed Camera (Andor Technology LTd) through a Nikon Eclipse TE2000-U Microscope (Nikon) using a 100X Plan Fluor objective (Nikon). Images were illuminated with a Lambda-DG4 (Sutter instruments) and acquired at \sim 7 Hz with a 120 ms exposure time and binned at 4 by 4 to increase the SNR. Images were collected and processed using Nikon Elements Ar software prior to export to Microsoft excel for analysis. ROIs were randomly selected based on a threshold after treatment with NH_4Cl .

Imaging Analysis

Individual synaptic puncta were selected randomly after NH_4Cl perfusion and all quenched pHluorin probes were unmasked. Single vesicle events were analyzed as reported in Leitz *et. al.* (2011). Dwell times were calculated as the time between the initial fluorescence step and the start of fluorescence decay predicted by the best fit decay (using a goodness of fit parameter). Decay time constants were determined by fitting data with single exponential decay curves using Levenberg-Marquardt least sum of squares minimizations (a minimum of 10 points, \sim 1.7s, was required for the fitting after calculating dwell times). Single vesicle events were analyzed offline with MatLab. For 20 Hz stimulation, amplitude measurement and single exponential decay fitting (using Levenberg-Marquardt least sum of squares minimizations) were performed offline in Clampfit.

Statistical Analysis

Statistical analyses were performed with Graphpad Prism 6.07 software using one of the following tests: Student's ordinary t-test, Two RM ANOVA, Kolmogorov-Smirnov test. Error bars represent SEM.

RESULTS

Dynamin TKO neurons are viable and form synapses

We created a dynamin TKO mouse line by crossing a $dnm1^{f/f}dnm2^{f/f}$ mouse with a $dnm1^{f/f}dnm3$ KO mouse and then crossed the litters to make a $dnm1^{f/f}dnm2^{f/f}dnm3$ KO mouse line. We dissected out the hippocampus of $dnm1^{f/f}dnm2^{f/f}dnm3$ KO p0-3 pups and created dissociated neuronal cultures that we infect with lentivirus expressing Cre recombinase. These samples were homogenized at multiple time points and collected for western blot analysis. We assessed dynamin levels using a pan-dynamin antibody and specific antibodies against dynamins 1 and 2 (Figure 4.1 A, B). Whereas dynamin 1 is completely knocked out by 15 DIV, dynamin 2 is not fully cleared until 17 DIV so all proceeding experiments were conducted at or after 17 DIV (data not shown). We also performed immunohistochemistry to confirm dynamin was being cleared from the synapse. Staining for either dynamin 1 and 2 with the synaptic marker, synapsin reveal dynamin is cleared from individual synapses (Figure 4.2 A, B).

We also directly observed synaptic structures in dynamin TKO neurons at rest through electron microscopy. We observed a slight decrease in synaptic vesicle number per synapse in dynamin TKO neurons in comparison to the dynamin 3 KO littermate control neurons (Figure 4.3 A-C). The decrease in synaptic vesicle number was accompanied by a decrease in docked vesicles; vesicles residing on the presynaptic membrane (Figure 4.3 E). Docked vesicles are thought to be a physical correlate to the probability of vesicle release upon stimulation. Taken together, this data suggests that dynamin TKO neurons have a decreased vesicle release probability. These results are similar to the reported dynamin 1, 3 DKO phenotype (S. M. Ferguson et al., 2007; Lu, He, Fan, Xu, & Chen, 2008). Finally, we measured the outer diameter of synaptic vesicles and observed a slight but significant decrease in average diameter in dynamin TKO neurons in comparison to the dynamin 3 KO littermate control (Figure 4.3 D).

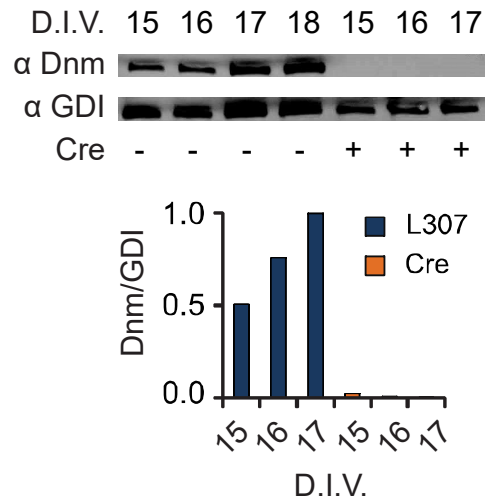


Figure 4.1. By 17 DIV, dynamin is effectively knocked out in dynamin TKO neuronal cultures. (Top) Western blot against dynamin using a pan-dynamin antibody in dynamin TKO and littermate dynamin 3 KO control neurons. (Bottom) Quantification of the western blot above.

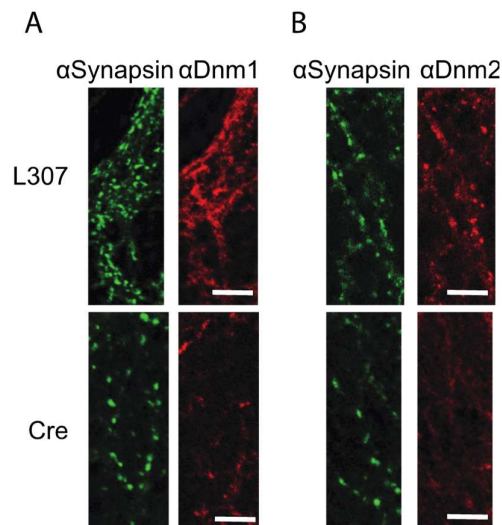


Figure 4.2. Both dynamins 1 and 2 are cleared from synapses by 17 DIV in dynamin TKO neurons. (A) Immunostaining against synapsin (green) and dynamin 1 (red) in dynamin 3 KO infected – *Top*: with L307 empty vector. *Bottom*: Cre recombinase (dynamin TKO). (B) Immunostaining against synapsin (green) and dynamin 2 (red) in dynamin 3 KO infected – *Top*: with L307 empty vector. *Bottom*: Cre recombinase (dynamin TKO). Scale bar = 5 μ m.

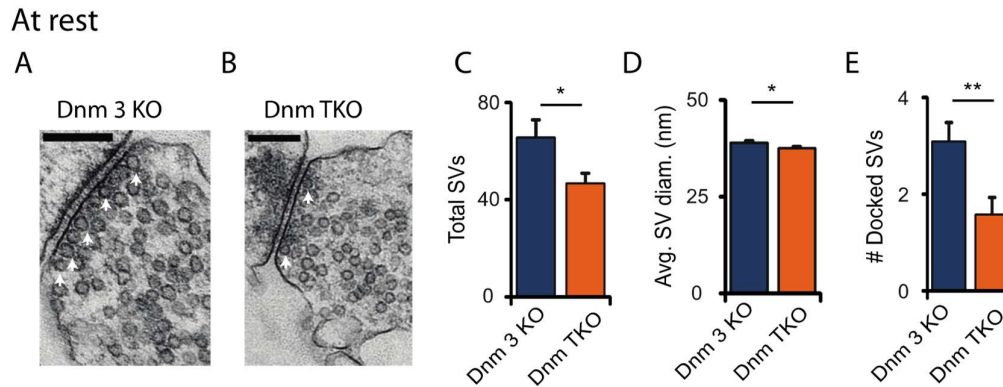


Figure 4.3. Synaptic structure of dynamin TKO neurons. (A) Electron micrograph image of a synapse taken from a Dnm 3 KO neuronal culture. (B) An electron micrograph image of a synapse taken from a Dnm TKO neuronal culture. (C) Average synaptic vesicle number per synapse in Dnm 3 KO (blue, $n = 41$) and Dnm TKO (orange, $n = 51$) neuronal cultures ($p = 0.0193$; Student's ordinary t-test) (D) Average synaptic vesicle diameter for Dnm 3 KO (blue, $n = 41$) and Dnm TKO (orange, $n = 51$) synapses ($p = 0.0023$, Student's ordinary t-test). (E) Average number of docked synaptic vesicles per synaptic area in Dnm 3 KO (blue, $n = 19$) and Dnm TKO (orange, $n = 22$) synapses ($p = 0.0039$; Student's ordinary t-test). Scale bar = 200 nm.

Loss of dynamins 1, 2 and 3 impairs excitatory neurotransmission

In the absence of the neuronal dynamins, dynamin 1 and 3, excitatory neurotransmission is characterized by a decrease in amplitude and release probability. However, these effects were shown to be reversible after chronic suppression of activity (Lou et al., 2012). To assess excitatory neurotransmission in the absence of dynamins, we voltage clamped $dnm1^{f/f}dnm2^{f/f}dnm3$ KO neurons infected with lentivirus expressing Cre recombinase in the presence of GABA receptor and NMDA blockers picrotoxin (PTX) and AP5 and measured evoked excitatory postsynaptic currents (EPSC). We observed a significant decrease in EPSC amplitude and facilitation to a train of 1 Hz and 10 Hz stimuli suggestive of a decrease in release probability (Figure 4.4 A, D-G). We also investigated changes in spontaneous neurotransmission in the absence of dynamin. We observed a decrease in mEPSC frequency and an increase in mEPSC amplitude (Figure 4.4 B, C). These findings are similar to the reported dynamin 1, 3 DKO phenotype (Lou et al., 2012). The decrease in mEPSC frequency can be attributed to a decrease in synaptic connections in dnm TKO cultures.

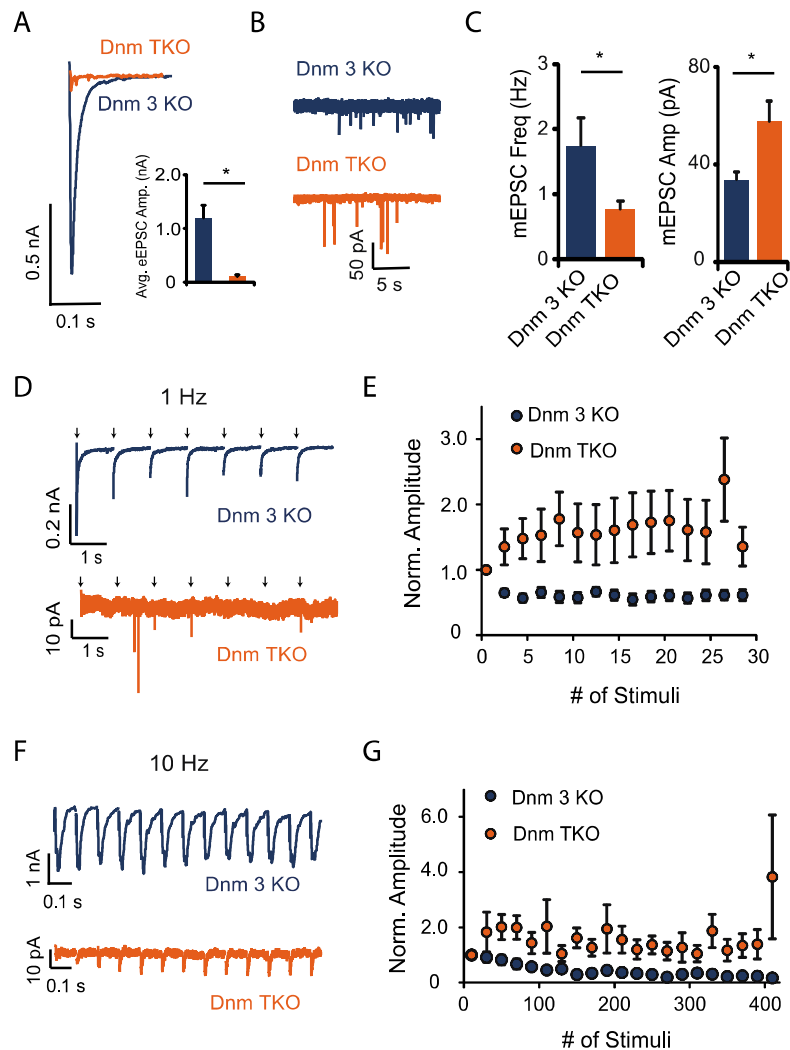


Figure 4.4. Decrease in release probability in excitatory neurotransmission in dynamin triple knockout neurons. (A) Sample eEPSC traces after a single stimulus from littermate control Dnm 3 KO (blue) and Dnm TKO (orange) neurons. Inset: Average eEPSC amplitudes of littermate control Dnm 3 KO (blue) and Dnm TKO (orange) neuronal cultures (Dnm 3 KO, n=10; Dnm TKO, n=10; p= 0.0003, Student's ordinary t-test). (B) Sample mEPSC recordings from Dnm 3 KO (blue) and Dnm TKO (orange) neurons. (C) Left: average mEPSC frequency for Dnm 3 KO (n=10) and Dnm TKO (n=11) neuronal cultures (p=0.0353, Student's ordinary t-test). Right: average mEPSC amplitudes for Dnm 3 KO and Dnm TKO (p=0.0202, Student's ordinary t-test). (D) Sample traces of the first 7 eEPSC responses to a 1 Hz 30 pulse stimulus for Dnm 3 KO (blue) and Dnm TKO (orange). Arrows indicate application of stimulus. (E) Normalized eEPSC amplitudes to the initial stimulus response after 1 Hz 30 pulse stimulus for Dnm 3 KO (blue, n = 10) and Dnm TKO (orange, n = 10; p = 0.0064, Two-way RM ANOVA). (F) Sample traces of the first 13 eEPSC responses to a 10 Hz 400 pulse stimulus for Dnm 3 KO (blue) and Dnm TKO (orange). (G) Normalized eEPSC amplitudes to the initial stimulus response after 10 Hz 400 pulse stimulus for Dnm 3 KO (blue, n = 7) and Dnm TKO (orange, n = 8; p = 0.0182, Two-way RM ANOVA).

Inhibitory neurotransmission in the absence of dynamins

The vesicular glutamate transporter-1 has been shown to play a central role in the recruitment and recycling of synaptic vesicle proteins from the presynaptic membrane (Pan, Marrs, & Ryan, 2015). In the absence of vGlut-1, the retrieval of key synaptic vesicle proteins was retarded. This raises the possibility that synaptic vesicle recycling in non glutamatergic synapses is different from glutamatergic synapses. To assess the dynamin dependence of inhibitory transmission, we whole cell clamped pyramidal dynamin TKO neurons and recorded inhibitory postsynaptic currents (IPSC). We observed no changes in evoked IPSC amplitude in dynamin TKO neurons in comparison to dynamin 3 KO neurons (Figure 4.5 A). There were no observable changes in synaptic depression between dynamin TKO and dynamin 3 KO neurons at either 1 Hz or 10 Hz (Figure 4.5 D-G). These results are in stark contrast to our dynamin TKO phenotype in excitatory neurotransmission. We also investigated spontaneous inhibitory neurotransmission and observed no changes in mIPSC frequency and amplitude (Figure 4.5 B, C).

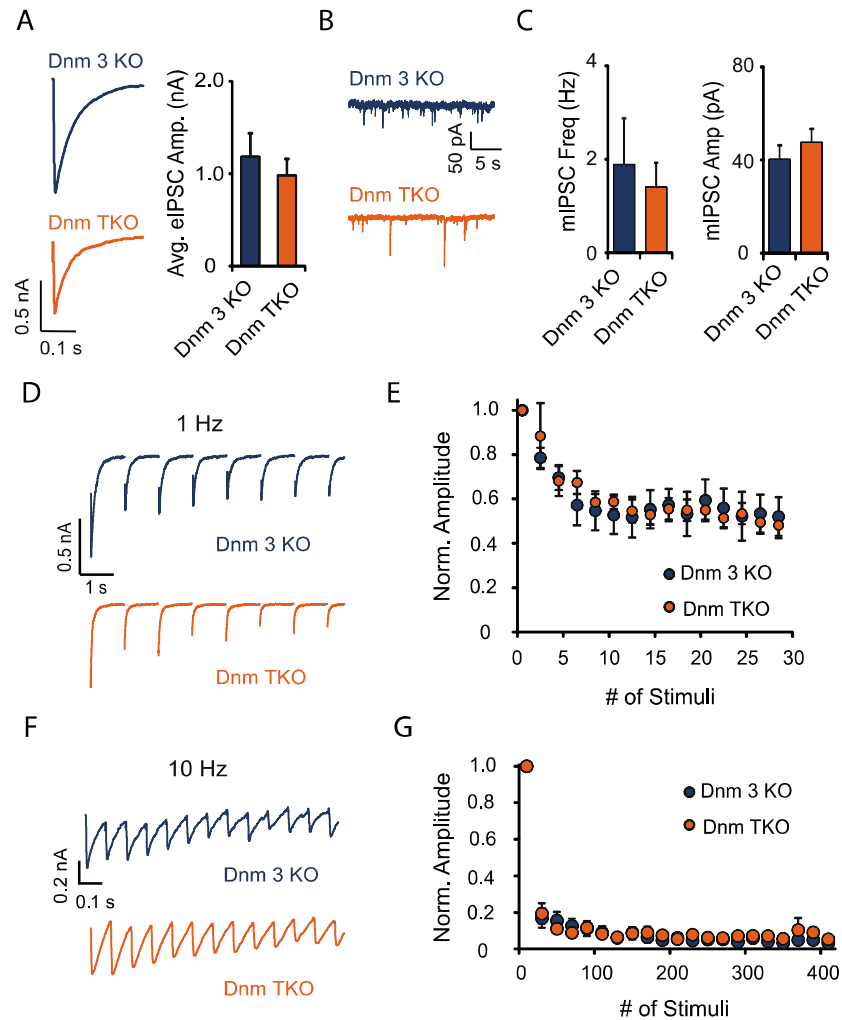


Figure 4.5. Inhibitory neurotransmission remains in-tact in the absence of dynamins.

(A) Left, sample eIPSC traces after a single stimulus from littermate control Dnm 3 KO (blue) and Dnm TKO (orange) neurons. Right, average eIPSC amplitudes of littermate control Dnm 3 KO (blue) and Dnm TKO (orange) neuronal cultures (Dnm 3 KO, $n = 11$; Dnm TKO, $n=12$; $p = 0.5124$, Student's ordinary t-test). (B) Sample mIPSC recordings from Dnm 3 KO (blue) and Dnm TKO (orange) neurons. (C) Left: average mIPSC frequency for Dnm 3 KO (blue, $n = 10$) and Dnm TKO (orange, $n = 11$) neuronal cultures ($p=0.6636$, Student's ordinary t-test). Right: average mIPSC amplitudes for Dnm 3 KO and Dnm TKO ($p=0.4047$, Student's ordinary t-test). (D) Sample traces of the first 7 eIPSC responses to a 1 Hz 30 pulse stimulus for Dnm 3 KO (blue) and Dnm TKO (orange). (E) Normalized eIPSC amplitudes to the initial stimulus response after 1 Hz 30 pulse stimulus for Dnm 3 KO (blue, $n = 9$) and Dnm TKO (orange, $n = 12$; $p = 0.9917$, Two-way RM ANOVA). (F) Sample traces of the first 13 eIPSC responses to a 10 Hz 400 pulse stimulus for Dnm 3 KO (blue) and Dnm TKO (orange). (G) Normalized eIPSC amplitudes to the initial stimulus response after 10 Hz 400 pulse stimulus for Dnm 3 KO (blue, $n = 8$) and Dnm TKO (orange, $n = 12$; $p = 0.7167$, Two-way RM ANOVA).

Dynamin is knocked out of both excitatory and inhibitory synapses

Our results have revealed a dichotomy pertaining to the dynamin dependence of synaptic neurotransmission. Dynamin is thought to be ubiquitously expressed in both excitatory and inhibitory synapses and has been shown to impair synaptic transmission in both excitatory and inhibitory synapses (S. M. Ferguson et al., 2007; Lou et al., 2012; Park et al., 2013; Tanifuji et al., 2013). One possible explanation for our reported dichotomy could be due to a potential incomplete turnover of dynamin in inhibitory synapses in comparison to excitatory synapses. To address this question, we performed immunocytochemistry to assess dynamin clearance in individual synapses in dynamin TKO neuronal cultures. We labeled excitatory synapses with antibodies against the vesicular glutamate transporter-1, vGlut-1 and inhibitory synapses with antibodies against the vesicular GABA transporter vGAT. We observed complete clearance of dynamin in both excitatory and inhibitory synapses suggesting that differences in synaptic transmission in dynamin TKO neurons are not due to lingering residual dynamin in GABAergic synapses (Figure 4.6 A, B).

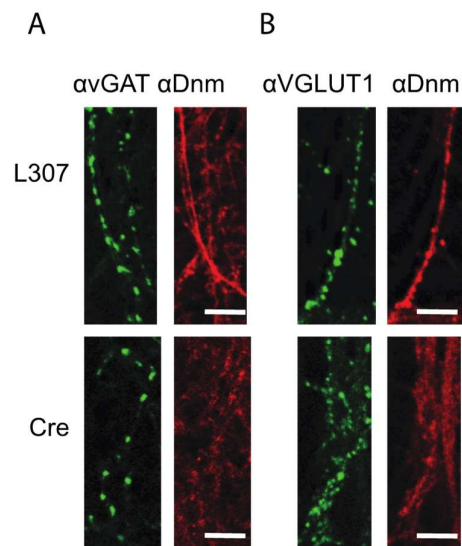


Figure 4.6. Dynamin is knocked out of both glutamatergic and GABAergic synapses in dynamin TKO neurons. (A) Immunostaining against VGAT (green) and dynamin (red) in dynamin 3 KO infected – *Top*: with L307 empty vector. *Bottom*: Cre recombinase (dynamin

TKO). (B) Immunostaining against VGLUT (green) and dynamin (red) in dynamin 3 KO infected with – *Top*: L307 empty vector. *Bottom*: Cre recombinase (dynamin TKO). Scale bar = 5 μm .

Multivesicular recycling in the absence of dynamins

The key phenotype of dynamin 1, 3 DKO is a drastic retardation in synaptic vesicle retrieval after strong stimulation (Raimondi et al., 2011). However, synaptic vesicle retrieval is not fully blocked and the residual synaptic vesicle retrieval was attributed to the presence of dynamin 2 (S. M. Ferguson et al., 2007). However, other reports have hinted at the presence of dynamin independent endocytic mechanisms at play in synaptic vesicle retrieval (Van Hook & Thoreson, 2012; Xu et al., 2008). To investigate multivesicular recycling in the absence of dynamin, we infected $\text{dnm1}^{\text{f/f}}\text{dnm2}^{\text{f/f}}\text{dnm3}^{\text{KO}}$ neurons with lentivirus expressing vGlut-pHluorin and Cre recombinase. We stimulated synaptic vesicle release with a 20 Hz 100 pulse stimulus and observed a phenotype ranging from full recovery after stimulation to no discernable synaptic vesicle retrieval at all (Figure 4.7 A, B). The subsequent fluorescence decay back to baseline was fit with a single exponential decay function and we used the decay τ as a measure of endocytosis (Figure 4.7 A). We observed an increase in decay τ in dynamin TKO neurons in comparison to dynamin 3 KO neurons (Figure 4.7 D). However a single exponential decay function cannot accurately model a step-like signal as reported by vGlut-pHluorin in dynamin TKO neurons after strong stimulation. So we calculated the ratio of the increase in fluorescence after stimulation, ΔF , to the level of fluorescence from baseline 150 seconds after stimulation, ΔF_{ret} (Figure 4.7 B). We termed this ratio the percent retrieval and observed that nearly 40% of dynamin TKO synapses recovered to less than 70% of the stimulation induced increase in fluorescence in comparison to less than 10% of dynamin 3 KO synapses (Figure 4.7 E). We also assessed synaptic vesicle release probability by dividing the ΔF in response to 20 Hz 100 AP stimulation by the maximum possible increase in fluorescence, $F_{\text{NH}_4\text{Cl}}$ and observed a decrease in vesicles released in dynamin TKO neurons in comparison to dynamin 3 KO control neurons (Figure 4.7 C). This finding corroborates our electron microscopy data showing a decreased number of docked vesicles in dynamin TKO synapses.

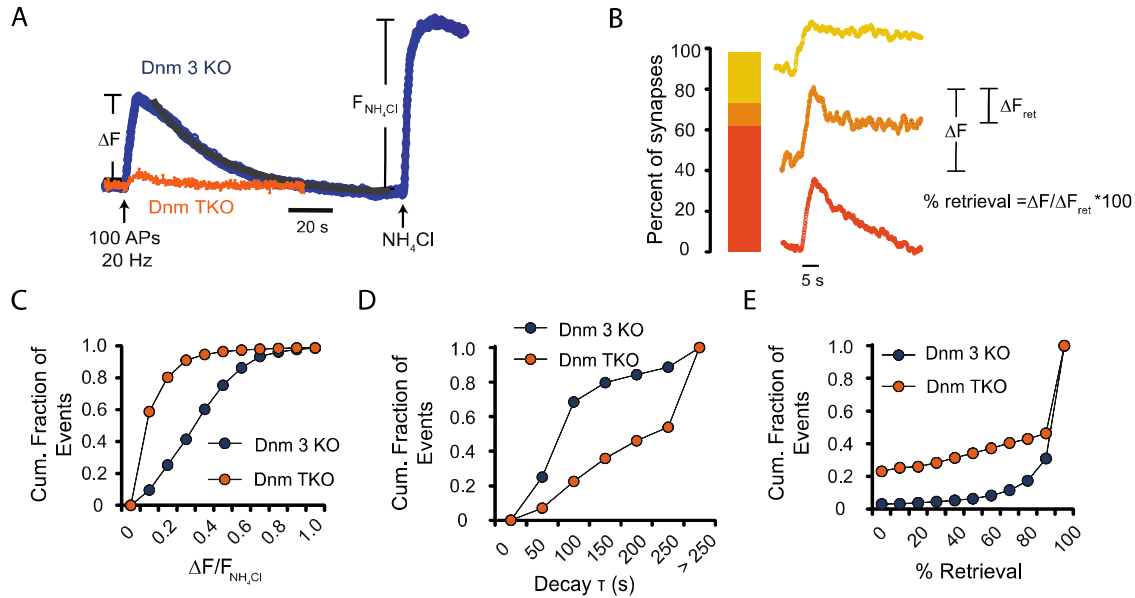


Figure 4.7. Synaptic vesicle recycling after high frequency stimulation in dynamin TKO neurons. (A) Sample pHLuorin response in Dnm 3 KO (blue) and Dnm TKO (orange) neuronal cultures after a 20 Hz 100 pulse stimuli, ΔF , and in response to NH_4Cl , F_{NH_4Cl} . (B) Percent distribution of the observed ΔF responses in Dnm TKO neurons and corresponding sample traces. ΔF in 63% of Dnm TKO synapses decayed close to baseline while 25% of Dnm TKO synapses showed minimal decay within to the measured timeframe of 150 s. ΔF in 12% of Dnm TKO synapses decayed to a baseline higher than prior to stimulation (C) Cumulative fraction of events of the ratio of the ΔF to the maximal response F_{NH_4Cl} of Dnm 3 KO (blue, $n=1885$ puncta) and Dnm TKO (orange, $n = 967$ puncta; $p<0.0001$, Kolmogorov-Smirnov test). (D) Cumulative fraction of calculated decay τ for Dnm 3 KO (blue) and Dnm TKO (orange; $p<0.0001$, Kolmogorov-Smirnov test). (E) Cumulative distribution of the percent fluorescence retrieved after 20 Hz 100 AP stimulation in Dnm 3 KO and Dnm TKO synapses (orange; $p<0.0001$, Kolmogorov-Smirnov test).

DISCUSSION

To investigate dynamin independent endocytosis at the synapses, we created a mouse floxed for dynamins 1 and 2 and constitutively knocked out dynamin 3. We dissected out the hippocampus and created dissociated cultures that were infected with lentivirus to knockout dynamins 1 and 2. Whereas dynamin 1 was effectively knocked out by as early as 15 DIV, dynamin 2 lingered a bit longer but was cleared by 17 DIV. This finding was corroborated with immunocytochemistry staining to confirm synaptic clearance of dynamin protein. So all experiments were conducted after 17 DIV. Overall, synapse morphology in dynamin TKO neurons revealed no gross defects outside of a decreased number of vesicles

and docked vesicles per synaptic area. This is in support of the reported dynamin 1, 3 DKO phenotype (Raimondi et al., 2011). However, our observed phenotype is milder than the *shibire* mutant at the restrictive temperature (Koenig & Ikeda, 1989). We also failed to observe any increase in arrested coated pits at the membrane in dynamin TKO neurons suggesting that synaptic vesicle recycling remains unperturbed. One question that remains is what exactly causes the decrease in synaptic vesicle number; defects in synaptic vesicle endocytosis or decrease in synaptic vesicle clearance from the active zone after exocytosis?

At the Calyx of Held, injection of nonhydrolyzable GTP resulted in an initial block in synaptic vesicle endocytosis that was mitigated with further stimulation (Xu et al., 2008). This suggests that dynamin independent endocytosis is triggered only as a counter to continuous membrane expansion. What we see here is full recovery after multivesicular exocytosis in a majority of our synapses. This is contrary to the reported dynamin 1, 3 DKO phenotype (Raimondi et al., 2011). One possible explanation is that a majority of our dynamin TKO synapses operate at maximum or near maximum membrane expansion such that dynamin independent endocytic mechanisms are regularly triggered. Hence, what we report here might not be reflective of a physiologically relevant phenomenon. One way to test this theory will involve silencing neuronal activity for an extended period and then reassessing synaptic vesicle endocytosis after multivesicular release. If we find more synapses display a defect in synaptic vesicle retrieval after multivesicular release, this will confirm that dynamin independent endocytosis is dominant after surplus membrane expansion.

Our data suggests that the mechanisms that underlie the recycling of synaptic vesicles releasing different neurotransmitters are not identical. Pan *et. al.* (2015) reported that impairing the retrieval of vGlut-1 from the presynaptic membrane retards retrieval of other necessary synaptic vesicle proteins. If the retrieval of synaptic vesicle proteins is predicated on the proper retrieval of vGlut-1, then synapses lacking vGlut-1 such as inhibitory synapses must rely on other mechanisms to ensure the timely and proper retrieval of crucial synaptic vesicle proteins. In excitatory transmission, we observed severe decrease in eEPSC amplitude and a decrease in release probability with increased failure rates in dynamin TKO neurons. We also observed an increase in mEPSC amplitude and decrease in mEPSC frequency.

However, we observe no significant changes in amplitude of eIPSCs and change in release probability. We also observe no change to the amplitude and frequency of mIPSC events. The effects observed is similar to prior reports of dynamin isoform knockout however the only report implicating dynamin function in inhibitory transmission demonstrates accelerated synaptic depression (S. M. Ferguson et al., 2007; Lou et al., 2012; Raimondi et al., 2011). Other reports have looked at dynamin function in inhibitory transmission using dynasore, a small molecule inhibitor of dynamin that also reveals an accelerated depression after continuous stimulation (Chung et al., 2010). However, dynasore has been discovered to have off target effects that also block endocytosis so its effects on neurotransmission possibly could be a dynamin independent effect (Park et al., 2013). The increase in mEPSC amplitude is thought to be due to the trapping of AMPA receptors on the postsynaptic surface. One question that arises from our data is if inhibitory synapses are uniquely developed to better deal with defects in synaptic vesicle endocytosis? This is plausible as inhibitory synapses are capable of tonic transmission and as such might have adapted a more robust compensatory mechanism to deal with defects that hamper neurotransmission (Evergren, Zotova, Brodin, & Shupliakov, 2006; Swadlow, 2003).

CHAPTER FIVE

THE RECYLCING OF A SINGLE SYNAPTIC VESICLE IS DYNAMIN INDEPENDENT

BACKGROUND

Physiologically, upon stimulation and depolarization of an axon, the influx of Ca^{2+} typically results in the release of a single synaptic vesicle. The release of a single synaptic vesicle is instantly followed by compensatory endocytosis. The exocytosis-endocytosis coupling of a single synaptic vesicle release can be slowed down by increasing extracellular Ca^{2+} and is dependent on synaptotagmin-1, the Ca^{2+} sensor for synchronized neurotransmission (Leitz & Kavalali, 2011; Y. C. Li, Chanaday, Xu, & Kavalali, 2017). In mouse pancreatic β -cells, the exocytosis-endocytosis coupling of insulin secretion was reported to be dynamin dependent (Jackson et al., 2015). Also, dynamin 1 function is

mediated through Ca^{2+} dependent dephosphorylation by the Ca^{2+} sensitive phosphatase, Calcineurin (Cousin & Robinson, 2001). Dynamin is also implicated in the different forms of single vesicle endocytosis (Graham et al., 2002; Granseth et al., 2006; Jackson et al., 2015; Watanabe et al., 2013). Clathrin mediated endocytosis is generally thought to be the major player in compensatory endocytosis of a single synaptic vesicle (Granseth et al., 2006). Dynamin functions in CME are well established (Grassart et al., 2014; Y. W. Liu et al., 2008; Vallis et al., 1999). Our earlier results revealed that dynamin 2 is not required for the retrieval of a single synaptic vesicle. However, dynamin 2's effect could be masked by the presence of dynamins 1 and 3. The other form of single vesicle retrieval is termed kiss-and-run. In kiss-and-run, a transient fusion pore is created between vesicle and membrane for release of vesicular contents before fusion pore closure and vesicle reformation. Dynamin GTPase activity is reported to regulate the development of the fusion pore in kiss-and-run endocytosis and regulates kiss-and-run dynamics through fusion pore expansion for neuropeptide release in chromaffin cells (Jackson et al., 2015). Finally, ultrafast endocytosis is reported to retrieve endosomes from the periaxial zone in response to the release of single synaptic vesicles. This form of endocytosis is active in small central synapses when neurons are held at a more physiological temperature of 34 °C. When at room temperature or 22 °C, CME is suggested to be the primary form of single synaptic vesicle retrieval (Watanabe et al., 2013; Watanabe et al., 2014). At either temperature, dynamin plays the crucial role of catalyzing scission of the budding endosome off the nascent membrane. Taken together, these reports suggest that in the absence of dynamin, synaptic vesicle retrieval should be arrested at the presynaptic membrane similar to the observed phenotype of the initial dynamin mutant, *shibire*, in *Drosophila* neuromuscular junctions (Koenig & Ikeda, 1989). Here, we investigate the potential role of dynamin independent endocytosis in the retrieval of a single synaptic vesicle.

METHODS

Lentiviral Infection

HEK293 cells (ATCC) were transfected with 3 packaging plasmids (pMDLg/pRRE, pRSV-Rev, and pCMV-VSV-G) and a pFUGW transfer vector containing a Cre-recombinase construct using the Fugene 6 transfection reagent (Promega). Cell culture supernatants

containing the virus were collected 72 hours later and spun down to participate out cellular debris and other contaminants. Neurons were infected at 4 days *in vitro* (DIV) by adding 300 μ l of virus containing supernatant to the neuronal culture media.

Cell Culture

Dissociated hippocampal cultures from postnatal day 0-3 *dnm1^{f/f}dnm2^{f/f}dnm3 KO* were prepared as previously described (Kavalali et al., 1999). Neurons were infected at 4 DIV with lentivirus expressing Cre recombinase or an empty L307 vector for control and experiments were performed at 17-21 DIV. All experiments were performed following protocols approved by the University of Texas Southwestern Institutional Animal Care and Use Committee.

Imaging

17-21 DIV neuronal cultures infected with lentivirus expressing either vGlut-pHluorin or vGlut-pHluorin and Cre recombinase were used for imaging experiments. Images were taken with an Andor iXon Ultra 897 High Speed Camera (Andor Technology LTd) through a Nikon Eclipse TE2000-U Microscope (Nikon) using a 100X Plan Fluor objective (Nikon). Images were illuminated with a Lambda-DG4 (Sutter instruments) and acquired at \sim 7 Hz with a 120 ms exposure time and binned at 4 by 4 to increase the SNR. Images were collected and processed using Nikon Elements Ar software prior to export to Microsoft excel for analysis. ROIs were randomly selected based on a threshold after treatment with NH_4Cl .

Imaging Analysis

Individual synaptic puncta were selected randomly after NH_4Cl perfusion and all quenched pHluorin probes were unmasked. Single vesicle events were analyzed as reported in Leitz *et. al.* (2011). Dwell times were calculated as the time between the initial fluorescence step and the start of fluorescence decay predicted by the best fit decay (using a goodness of fit parameter). Decay time constants were determined by fitting data with single exponential decay curves using Levenberg-Marquardt least sum of squares minimizations (a minimum of

10 points, ~ 1.7 s, was required for the fitting after calculating dwell times). Single vesicle events were analyzed offline with MatLab. For 20 Hz stimulation, amplitude measurement and single exponential decay fitting (using Levenberg-Marquardt least sum of squares minimizations) were performed offline in Clampfit.

Statistical Analysis

Statistical analyses were performed with Graphpad Prism 6.07 software using one of the following tests: Student's ordinary t-test, Two RM ANOVA, Kolmogorov-Smirnov test. Error bars represent SEM.

RESULTS

Single synaptic vesicle endocytosis is dynamin independent.

So far, dynamin function in synaptic vesicle recycling has been limited to synaptic vesicle recycling after high frequency stimulation. However, the more physiological relevant question is, is dynamin involved in the recycling of an individual synaptic vesicle? To address this, we knocked out dynamin in $dnm1^{f/f}dnm2^{f/f}dnm3$ KO neurons through lentiviral infection expressing Cre recombinase and vGlut-pHluorin and assessed single vesicle recycling using a sparse stimulation profile of 30 pulses at 0.1 Hz (Figure 5.1 A). We observed no change in amplitude of single vesicle events in dynamin TKO synapses in comparison to littermate control dynamin 3 KO synapses (Figure 5.1 B, C). This suggests there is no difference in vGlut-pHluorin expression in the different cultures. We also observed no difference in the measured decay τ of these events suggestive of no changes in vesicle reacidification in either group (Figure 5.1 F). Finally, we assessed dwell time and categorized events into 3 based on the event profile (Figure 5.1 D). Rapid decay were events that decayed instantaneously. Short dwell were events that resided on the membrane for more that 500ms and decayed to baseline before the end of the allotted timeframe. Long dwell were events that did not decay to baseline within the allotted time window. We assessed the fractional composition of the single vesicle events in these 3 categories and noted no changes in distribution between dynamin TKO and littermate control dynamin 3 KO synapses (Figure 5.1 E). We also looked at the fractional composition of single vesicle events from dynamin

TKO synapses with severe retardation of synaptic vesicle endocytosis after strong stimulation and observed no change to the distribution of the single vesicle events from these select synapses in comparison to distribution of control single vesicle events (Figure 5.1 D). We assessed the distribution of rapid decay and short dwell events and observed no differences between dynamin 3 KO and dynamin TKO single vesicle events (Figure 5.1 D). Taken together, our data suggest that the kinetics of single vesicle retrieval are dynamin independent.

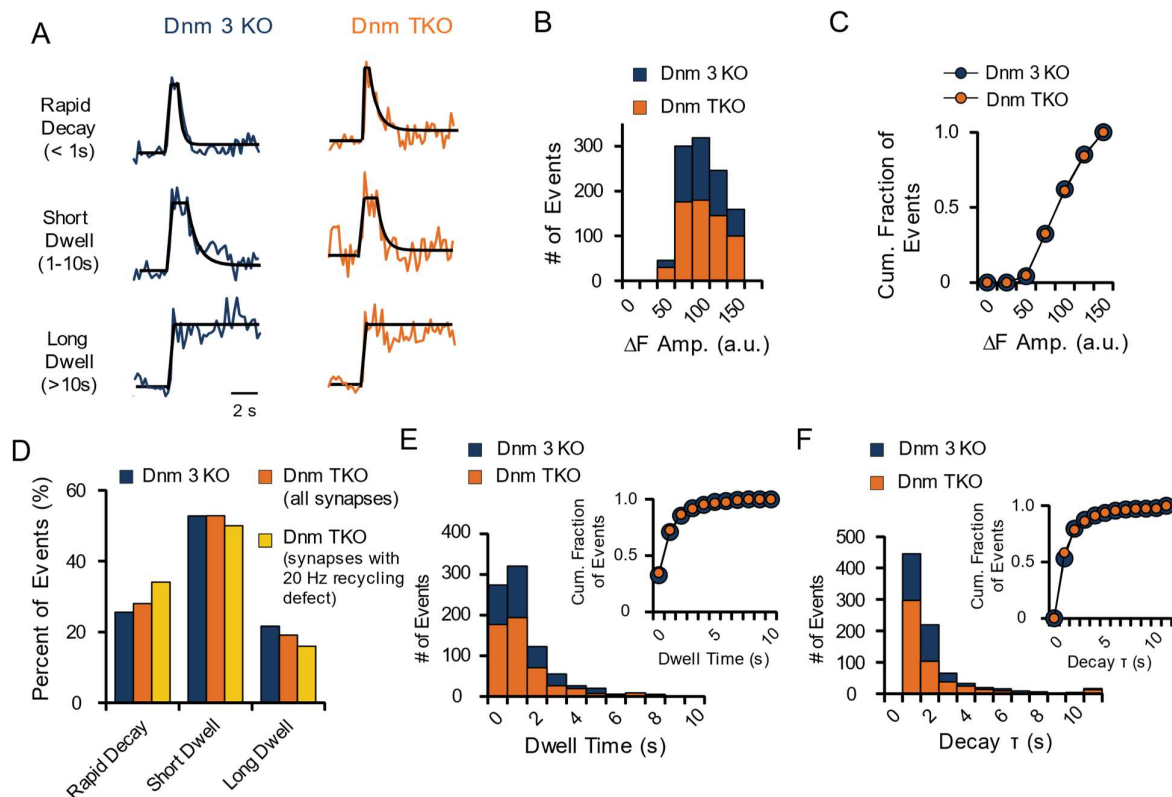


Figure 5.1. Single vesicle recycling is dynamin independent. (A) Sample traces of single vesicle events for Dnm 3 KO (blue) and Dnm TKO (orange). Events were categorized into 3 groups: Rapid decay, events with no detectable dwell time; Short dwell, events with a measurable dwell time and decays to baseline before subsequent stimulus; Long dwell, events with a measurable dwell time but do not decay before the next stimulus. (B) Amplitude distribution of single vesicle fusion events for Dnm 3 KO (blue, $n=1070$) and Dnm TKO cultures (orange, $n=631$; $p=0.9395$, Kolmogorov-Smirnov test). (C) Cumulative fraction of events of the amplitude of single vesicle events for Dnm 3 KO (blue) and Dnm TKO (orange). (D) Percentage of single vesicle events for the categories Rapid Decay, Short Dwell and Long Dwell from Dnm 3 KO (blue), Dnm TKO (orange, all events) and Dnm TKO (yellow, from

the 25% of synapses that recovered to less than 20% of ΔF after 20 Hz 100 AP stimulation). (E) Distribution of observed dwell times for single vesicle fusion events from Dnm 3 KO cultures (blue, $n = 838$) and Dnm TKO cultures (orange, $n = 510$; $p=0.4123$, Kolmogorov-Smirnov test). Inset: Cumulative distribution of dwell times for single vesicle events for Dnm 3 KO (blue) and Dnm TKO (orange). (F) Distribution of the calculated decay τ for single vesicle fusion events from Dnm 3 KO (blue, $n = 838$) and Dnm TKO (orange, $n = 510$; $p=0.1436$, Kolmogorov-Smirnov test). Inset: Cumulative distribution of decay τ for single vesicle events for Dnm 3 KO (blue) and Dnm TKO (orange).

Ca²⁺ dependent retardation of single vesicle retrieval is dynamin dependent

Prior work in our lab has demonstrated that increasing extracellular calcium can slowdown the retrieval of a single synaptic vesicle in small central synapses (Leitz & Kavalali, 2011). This retardation in synaptic vesicle retrieval is dependent on synaptotagmin-1, the Ca²⁺ sensor for synaptic vesicle exocytosis (Y. C. Li et al., 2017). In chromaffin cells, synaptotagmin-1 has been reported to interact directly with the PH domain of dynamin 1 to regulate fission pore expansion of single vesicles (McAdam et al., 2015). Taken together, we assessed if dynamin is involved in Ca²⁺ dependent retardation of single vesicle retrieval by repeating our single vesicle experiments in 8 mM extracellular Ca²⁺. We observed a trend towards increase in single vesicle dwell time in dynamin 3 KO synapses but not in dynamin TKO synapses (Figure 5.2 B, C). This was accompanied with a rightward shift in distribution of events towards long dwell events in dynamin 3 KO synapses but no shift in distribution for dynamin TKO single vesicle events (Figure 5.2A). Taken together, these results suggest that Ca²⁺ dependent retardation of single vesicle retrieval is dependent on dynamin. However, further experiments are needed given the current sample size.

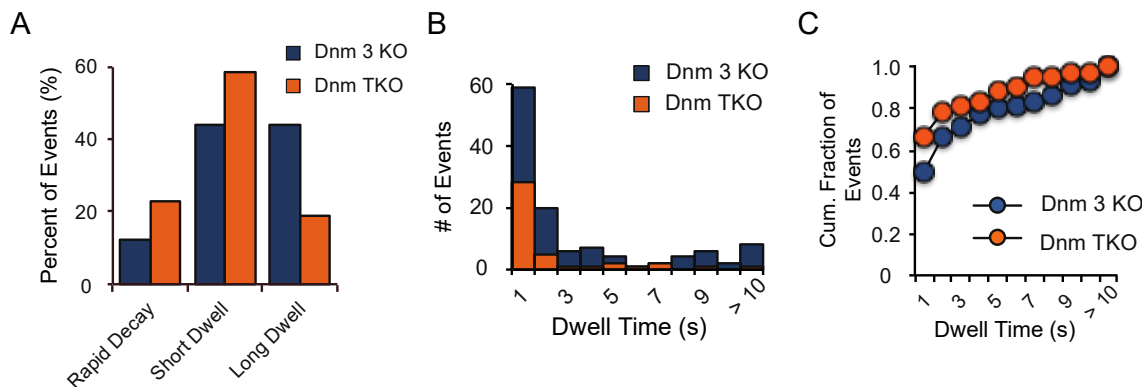


Figure 5.2. Single vesicle recycling in 8 mM extracellular Ca^{2+} in Dynamin TKO neurons. (A) Percentage of single vesicle events in 8 mM extracellular Ca^{2+} for the categories Rapid Decay, Short Dwell and Long Dwell from Dnm 3 KO (blue), Dnm TKO (orange). (B) Distribution of observed dwell times for single vesicle fusion events in 8 mM extracellular Ca^{2+} from Dnm 3 KO cultures (blue, $n = 119$) and Dnm TKO cultures (orange, $n = 42$; $p=0.4123$, Kolmogorov-Smirnov test). (C) Cumulative distribution of dwell times for single vesicle events in 8 mM extracellular Ca^{2+} for Dnm 3 KO (blue) and Dnm TKO (orange).

Spontaneous neurotransmission recycles independent of actin, DRP-1 and Arp2/3 complex

Our results so far have revealed dynamin is not required for the recycling of a single synaptic vesicle. We next attempted to identify crucial proteins for the recycling of a single synaptic vesicle in dynamin TKO neurons. In multiple cells lines, dynamin is localized in arp2/3 complex nucleated actin meshworks (Baldassarre et al., 2003; Gold et al., 1999; Lee & De Camilli, 2002; Orth et al., 2002; Schlunck et al., 2004). Similarly, during CME, both actin and dynamin are recruited to the site of retrieval in the early phase suggesting functional significance in initiation and maturation of CME (Grassart et al., 2014). In both the large calyx of Held and small central hippocampal synapses, knockout of actin isoforms revealed actin functions in all forms of synaptic vesicle endocytosis (X. S. Wu et al., 2016). Here, we assessed actin and arp2/3 complex function in the recycling of single synaptic vesicles by using the small molecule inhibitors of Latrunculin and CK-666 to inhibit actin and arp 2/3 complex, respectively. We also assessed DRP-1's function in synaptic vesicle recycling as mutations in DRP in drosophila leads to synaptic vesicle depletion (Rikhy, Kamat, Ramagiri, Sriram, & Krishnan, 2007). We knocked out all isoforms of dynamin by infecting dissociated $\text{dnm1}^{\text{f/f}}\text{dnm2}^{\text{f/f}}\text{dnm3}^{\text{KO}}$ neurons with lentivirus expressing cre recombinase and voltage clamped and recorded mEPSC events before and after 10 minutes treatment with a small molecule inhibitor. We observed no difference in mEPSC frequency and amplitude after treatment with either Latrunculin, CK-666 or Mdivi-1, inhibitors of actin, arp2/3 complex and DRP-1 (Figure 5.3 A, B). These findings suggest that in the absence of dynamin, actin, arp2/3 complex and DRP-1 do not play a role in the recycling of spontaneously released

synaptic vesicles.

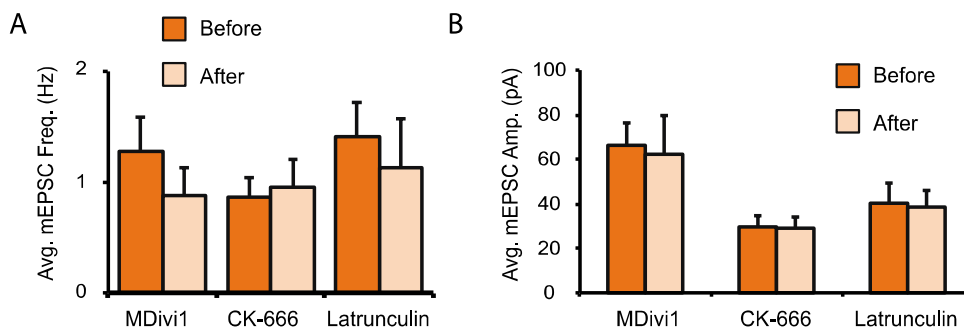


Figure 5.3. Spontaneous neurotransmission in dynamin TKO neurons after treatment with Mdivi1, CK-666 and Latrunculin (A) Average mEPSC frequency in Dnm TKO neurons before (orange) and after (beige) 10 minutes treatment with Mdivi1 ($n = 8$, $p = 0.3597$, Student's pairwise t-test), CK-666 ($n = 6$, $p = 0.7339$, Student's pairwise t-test) and Latrunculin ($n = 9$, $p = 0.4856$, Student's pairwise t-test). (B) Average mEPSC amplitude in Dnm TKO neurons before (orange) and after (beige) 10 minutes treatment with Mdivi1 ($n = 8$, $p = 0.7768$, Student's pairwise t-test), CK-666 ($n = 6$, $p = 0.9330$, Student's pairwise t-test) and Latrunculin ($n = 9$, $p = 0.5863$, Student's pairwise t-test).

DISCUSSION

So far, our data demonstrate that within the synapse, dynamin is functionally relevant after multivesicular release and subsequent endocytosis. However, the release of a single synaptic vesicle and compensatory retrieval of the released vesicle can be achieved without dynamin. This finding contradicts prior reports investigating the mechanics of the retrieval of single synaptic vesicles implicating dynamin as the catalyst of scission of the budding endosome (Granseth et al., 2006; Watanabe et al., 2013; Watanabe et al., 2014). One piece of reconciliatory evidence presented here is the finding that increased Ca^{2+} fails to slow down single vesicle endocytosis as seen in previous reports (Leitz & Kavalali, 2011; Y. C. Li et al., 2017). This finding suggests dynamin function is dependent on Ca^{2+} influx. However, it seems the threshold of local Ca^{2+} concentration needed to trigger dynamin dependent endocytosis at the synapse is higher than the local Ca^{2+} concentration needed to release a single vesicle. This is supported by reports that dynamin 1's function is dependent on calcineurin dependent dephosphorylation (Cousin & Robinson, 2001). Also, dynamin 2

GTPase activity is reported to be retarded in the presence of elevated Ca^{2+} (Cousin & Robinson, 2000). Synaptotagmin-1 is proposed to be the Ca^{2+} sensor that slows down the retrieval of single synaptic vesicles (Y. C. Li et al., 2017). Synaptotagmin-1 is also proposed to interact directly with dynamin-1 (McAdam et al., 2015). This raises the possibility that dynamin-1 is the effector for synaptotagmin-1 dependent retardation of single synaptic vesicle recycling. In that case, the absence of dynamin-1 will inhibit synaptotagmin-1's ability to slow down single vesicle endocytosis, which is what we report here.

Understanding actin's function in synaptic vesicle recycling is plagued by conflicting reports (Bleckert, Photowala, & Alford, 2012; Bourne, Morgan, & Pieribone, 2006; Sankaranarayanan, Atluri, & Ryan, 2003; Shupliakov et al., 2002). Latrunculin, a potent inhibitor of actin polymerization, was demonstrated to increase mEPSC frequency in cultured hippocampal neurons (Morales, Colicos, & Goda, 2000). This latrunculin induced inhibition of mEPSC frequency was blocked when neurons were simultaneously incubated in Jasplakinolide, an actin polymer stabilizer. Here, we report that, in treatment of dynamin TKO hippocampal neurons with latrunculin, CK-666 or Mdivi1 has no effect on mEPSC frequency and amplitude suggesting that actin, arp 2/3 complex and DRP-1 are not required for the recycling of spontaneously released synaptic vesicles in the absence of dynamin. This does not rule out a functional significance for these proteins in synaptic vesicle recycling in wildtype neurons. The loss of dynamins over time can induce compensatory mechanisms of synaptic vesicle recycling that is mechanistically independent of normal synaptic vesicle endocytic mechanisms.

CHAPTER SIX

CONCLUSIONS AND FUTURE DIRECTIONS

The data presented here provides further insight into the dynamics of synaptic vesicle endocytosis. By knocking out different dynamins and assessing endocytosis, I have demonstrated the robust nature of synaptic vesicle retrieval at the synapse. I have shown that dynamin primarily operates during activity but it is nonessential for the retrieval of an individual synaptic vesicle. In the presence of elevated Ca^{2+} or the induction of multivesicular release, dynamin mediated endocytosis is triggered and is the dominant form of endocytosis

at the synapse.

In addition to my work on dynamin function at the synapse, I have also provided novel insight into how synaptotagmin-1 regulates spontaneous and evoked neurotransmitter release. Synaptotagmin-1 has been proposed to function dually as the Ca^{2+} sensor for synchronized evoked release of synaptic vesicles and as a clamp on the release of spontaneously recycling synaptic vesicles (Geppert et al., 1994). These functions rely on distinct Ca^{2+} dependent interactions of synaptotagmin-1's as the Ca^{2+} dependence for the two forms of synaptic vesicle release are drastically different (Groffen et al., 2010; Xu, Pang, Shin, & Sudhof, 2009). A prior report had narrowed this dichotomy in synaptotagmin-1 function to the respective structural configuration of its C2 domains (Bai et al., 2016). Here, we report that synaptotagmin-1's ability to synchronize evoked release and clamp spontaneous release depends on the vesicle it resides on and these functions do not mix after a cycle of exo-endocytosis. Synaptotagmin-1 is also reported to function in synaptic vesicle endocytosis. Studies have shown that syt1 functions to accelerate endocytosis after multivesicular release and slow down endocytosis after the evoked release of a single vesicle (Y. C. Li et al., 2017). Furthermore, the endocytosis of a spontaneously released vesicle has been demonstrated to occur at a faster speed than a single vesicle that was released after stimulation (Leitz & Kavalali, 2011). Taken together with the recent work from our group, it is tempting to speculate that synaptotagmin-1 not only functions as a clamp but also hastens the retrieval of a spontaneously released vesicles. The persistence of spontaneous neurotransmission in the absence of dynamin as demonstrated by our data alludes to dynamin independent synaptotagmin-1 dependent process. If so, what is the mechanism and how is it regulated? These are questions to be addressed in the future.

The mechanism of the retrieval of a single synaptic vesicle is highly debated. Clathrin mediated endocytosis is the presumed mechanism behind single synaptic vesicle endocytosis (Granseth et al., 2006). Other reports have postulated the presence of kiss-and-run endocytosis at the synapse and an ultrafast form of endocytosis only observed at near physiological temperatures (Stevens & Williams, 2000; Watanabe et al., 2013; Zhang et al., 2009). Dynamin has been implicated in all three forms of endocytosis (Graham et al., 2002; Jackson et al., 2015; Watanabe et al., 2013). Dynamin is reported to be involved in the

initiation and maturation of a clathrin coat prior to its role in scission of the budding endosome (Grassart et al., 2014; Mettlen et al., 2009). Dynasore, an inhibitor of dynamin, albeit with off-target effects on endocytosis, has been shown to inhibit ultrafast endocytosis and the loss/mutation of dynamin is reported to affect fusion pore expansion during kiss-and-run (Jackson et al., 2015; Watanabe et al., 2013). We set out to address dynamin's role in single vesicle recycling by knocking out dynamins and assessing endocytosis at both room temperature and 32 °C. We report here that the loss of dynamin 2, the premier GTPase for scission of clathrin coated vesicles, does not affect how fast a vesicle is retrieved nor the time frame of vesicle reacidification. The kinetics of single vesicle retrieval were similar at both room temperature and 32 °C suggesting that a single form of endocytosis is responsible for the retrieval of a single synaptic vesicle. The timing of our observed single vesicle events are similar to those reported for kiss-and-run events (Alabi & Tsien, 2013). However, determining what endocytic pathway is employed for the retrieval of a single synaptic vesicle is beyond the limits of our current approach and would require a different technique.

Dynamin's functional requirement in synaptic vesicle recycling has been limited to retrieval during and after high frequency/strong stimulation. In the absence of dynamin 1 or dynamins 1 and 3, synaptic vesicle recycling is retarded after strong stimulation (S. M. Ferguson et al., 2007; Lou et al., 2012; Lou et al., 2008; Raimondi et al., 2011). Here, we report that synaptic vesicles can recycle in the absence of dynamins 1, 2 and 3 after high frequency stimulation. This study is consistent with Xu *et al.* (2008), where they demonstrated that synaptic vesicle recycling can occur after multiple rounds of stimulation in a synapse filled with non hydrolysable GTP. It is plausible that dynamin TKO neurons have undergone sufficient spontaneous network activity to trigger compensatory endocytic mechanisms in the absence of dynamins. Further work is required to decipher the components of compensatory dynamin independent endocytosis.

Synaptic transmission relies on the reliable retrieval of synaptic vesicles after exocytosis. The loss of dynamin, a key protein for synaptic vesicle scission from the nascent endosome or presynaptic membrane, would predict drastic defects in synaptic transmission. We observed such inconsistencies in evoked excitatory neurotransmission. The amplitude of evoked excitatory currents was drastically reduced and there was an increase in failed events

where stimulus was not followed by subsequent neurotransmission. However, we observed no defects in inhibitory neurotransmission, which is in contrast to prior reports (S. M. Ferguson et al., 2007). It is plausible that the ability of inhibitory synapses to maintain tonic neurotransmission, inhibitory synapses can better adapt to defects in synaptic vesicle endocytosis (Evergren et al., 2006; Swadlow, 2003). This would suggest differences in synaptic vesicle recycling dynamics at the level of the synapse. If true, future work can investigate how compensatory dynamin independent endocytosis is initiated in excitatory versus inhibitory synapses.

In the absence of dynamins, what could be mediating synaptic vesicle endocytosis? One plausible candidate is endophilin. Endophilin comprises a family of proteins characterized by possessing a Bin/Amphiphysin/Rvs (BAR) domain, a variable domain and a SH3 domain (Kjaerulff, Brodin, & Jung, 2011). These proteins are thought to sense membrane curvature during endocytosis and recruit other endocytic proteins to sites of endocytosis (Kjaerulff et al., 2011). At the synapse, endophilin has been implicated in clathrin-mediated endocytosis retrieval of synaptic vesicles (Fabian-Fine et al., 2003; Guichet et al., 2002; Schuske et al., 2003; Verstreken et al., 2002). However, recently, Bourcrot *et al.* (2015) discovered a fast endophilin dependent form of endocytosis that functions independent of clathrin. So far, fast endophilin mediated endocytosis (FEME) has been limited to receptor trafficking and requires ligand binding for initiation of endocytosis. Also, pre-enrichment of endophilin at the site of endocytosis is a requirement for FEME. In the presynaptic compartment, endophilin is enriched and upon synaptic stimulation, endophilin is recruited to the presynaptic membrane. Taken together, it is plausible that the accumulation of endophilin at the presynaptic membrane after synaptic stimulation induces FEME. Evidence for fast endophilin dependent endocytosis has been reported in ribbon synapses where dialysis of a small peptide inhibitor decreased the fast retrieval of synaptic vesicles while slow endocytosis of vesicles persists (Llobet et al., 2011). Currently, FEME is presumed to be dynamin dependent due to its susceptibility to dynamin inhibitors that have been shown to inhibit endocytosis in the absence of dynamin. Further work is required to fully understand endophilin's role in synaptic vesicle endocytosis.

REFERENCES

- Alabi, A. A., & Tsien, R. W. (2013). Perspectives on kiss-and-run: role in exocytosis, endocytosis, and neurotransmission. *Annu Rev Physiol*, *75*, 393-422.
doi:10.1146/annurev-physiol-020911-153305
- Alvarez de Toledo, G., Fernandez-Chacon, R., & Fernandez, J. M. (1993). Release of secretory products during transient vesicle fusion. *Nature*, *363*(6429), 554-558. doi:10.1038/363554a0
- Anggono, V., Smillie, K. J., Graham, M. E., Valova, V. A., Cousin, M. A., & Robinson, P. J. (2006). Syndapin I is the phosphorylation-regulated dynamin I partner in synaptic vesicle endocytosis. *Nat Neurosci*, *9*(6), 752-760. doi:10.1038/nn1695
- Armbruster, M., Messa, M., Ferguson, S. M., De Camilli, P., & Ryan, T. A. (2013). Dynamin phosphorylation controls optimization of endocytosis for brief action potential bursts. *Elife*, *2*, e00845. doi:10.7554/eLife.00845
- Arneson, L. N., Segovis, C. M., Gomez, T. S., Schoon, R. A., Dick, C. J., Lou, Z., . . . Leibson, P. J. (2008). Dynamin 2 regulates granule exocytosis during NK cell-mediated cytotoxicity. *J Immunol*, *181*(10), 6995-7001.
- Bai, H., Xue, R., Bao, H., Zhang, L., Yethiraj, A., Cui, Q., & Chapman, E. R. (2016). Different states of synaptotagmin regulate evoked versus spontaneous release. *Nat Commun*, *7*, 10971. doi:10.1038/ncomms10971
- Bal, M., Leitz, J., Reese, A. L., Ramirez, D. M., Durakoglugil, M., Herz, J., . . . Kavalali, E. T. (2013). Reelin mobilizes a VAMP7-dependent synaptic vesicle pool and selectively augments spontaneous neurotransmission. *Neuron*, *80*(4), 934-946. doi:10.1016/j.neuron.2013.08.024
- Baldassarre, M., Pompeo, A., Beznoussenko, G., Castaldi, C., Cortellino, S., McNiven, M. A., . . . Buccione, R. (2003). Dynamin participates in focal extracellular matrix degradation by invasive cells. *Mol Biol Cell*, *14*(3), 1074-1084. doi:10.1091/mbc.E02-05-0308
- Bethoney, K. A., King, M. C., Hinshaw, J. E., Ostap, E. M., & Lemmon, M. A. (2009). A possible effector role for the pleckstrin homology (PH) domain of dynamin. *Proc Natl Acad Sci U S A*, *106*(32), 13359-13364. doi:10.1073/pnas.0906945106
- Betz, W. J., & Bewick, G. S. (1992). Optical analysis of synaptic vesicle recycling at the frog neuromuscular junction. *Science*, *255*(5041), 200-203.
- Betz, W. J., Mao, F., & Bewick, G. S. (1992). Activity-dependent fluorescent staining and destaining of living vertebrate motor nerve terminals. *J Neurosci*, *12*(2), 363-375.
- Bleckert, A., Photowala, H., & Alford, S. (2012). Dual pools of actin at presynaptic terminals. *J Neurophysiol*, *107*(12), 3479-3492. doi:10.1152/jn.00789.2011
- Boulant, S., Kural, C., Zeeh, J. C., Ubelmann, F., & Kirchhausen, T. (2011). Actin dynamics counteract membrane tension during clathrin-mediated endocytosis. *Nat Cell Biol*, *13*(9), 1124-1131. doi:10.1038/ncb2307
- Bourne, J., Morgan, J. R., & Pieribone, V. A. (2006). Actin polymerization regulates clathrin coat maturation during early stages of synaptic vesicle recycling at lamprey synapses. *J Comp Neurol*, *497*(4), 600-609. doi:10.1002/cne.21006
- Calabrese, B., & Halpain, S. (2015). Differential targeting of dynamin-1 and dynamin-3 to nerve terminals during chronic suppression of neuronal activity. *Mol Cell Neurosci*, *68*, 36-45. doi:10.1016/j.mcn.2015.03.016
- Cao, H., Chen, J., Awoniyi, M., Henley, J. R., & McNiven, M. A. (2007). Dynamin 2 mediates

- fluid-phase micropinocytosis in epithelial cells. *J Cell Sci*, 120(Pt 23), 4167-4177.
doi:10.1242/jcs.010686
- Cao, H., Garcia, F., & McNiven, M. A. (1998). Differential distribution of dynamin isoforms in mammalian cells. *Mol Biol Cell*, 9(9), 2595-2609.
- Carroll, R. C., Beattie, E. C., Xia, H., Luscher, C., Altschuler, Y., Nicoll, R. A., . . . von Zastrow, M. (1999). Dynamin-dependent endocytosis of ionotropic glutamate receptors. *Proc Natl Acad Sci U S A*, 96(24), 14112-14117.
- Ceccarelli, B., Hurlbut, W. P., & Mauro, A. (1973). Turnover of transmitter and synaptic vesicles at the frog neuromuscular junction. *J Cell Biol*, 57(2), 499-524.
- Chamberland, S., & Toth, K. (2016). Functionally heterogeneous synaptic vesicle pools support diverse synaptic signalling. *J Physiol*, 594(4), 825-835. doi:10.1113/JP270194
- Chen, M. S., Obar, R. A., Schroeder, C. C., Austin, T. W., Poodry, C. A., Wadsworth, S. C., & Vallee, R. B. (1991). Multiple forms of dynamin are encoded by shibire, a Drosophila gene involved in endocytosis. *Nature*, 351(6327), 583-586. doi:10.1038/351583a0
- Chow, R. H., von Ruden, L., & Neher, E. (1992). Delay in vesicle fusion revealed by electrochemical monitoring of single secretory events in adrenal chromaffin cells. *Nature*, 356(6364), 60-63. doi:10.1038/356060a0
- Chung, C., Barylko, B., Leitz, J., Liu, X., & Kavalali, E. T. (2010). Acute dynamin inhibition dissects synaptic vesicle recycling pathways that drive spontaneous and evoked neurotransmission. *J Neurosci*, 30(4), 1363-1376. doi:10.1523/JNEUROSCI.3427-09.2010
- Collins, A., Warrington, A., Taylor, K. A., & Svitkina, T. (2011). Structural organization of the actin cytoskeleton at sites of clathrin-mediated endocytosis. *Curr Biol*, 21(14), 1167-1175. doi:10.1016/j.cub.2011.05.048
- Cousin, M. A., & Robinson, P. J. (2000). Ca²⁺ influx inhibits dynamin and arrests synaptic vesicle endocytosis at the active zone. *J Neurosci*, 20(3), 949-957.
- Cousin, M. A., & Robinson, P. J. (2001). The dephosphins: dephosphorylation by calcineurin triggers synaptic vesicle endocytosis. *Trends Neurosci*, 24(11), 659-665.
- de Lange, R. P., de Roos, A. D., & Borst, J. G. (2003). Two modes of vesicle recycling in the rat calyx of Held. *J Neurosci*, 23(31), 10164-10173.
- Deak, F., Schoch, S., Liu, X., Sudhof, T. C., & Kavalali, E. T. (2004). Synaptobrevin is essential for fast synaptic-vesicle endocytosis. *Nat Cell Biol*, 6(11), 1102-1108. doi:10.1038/ncb1185
- Di, A., Nelson, D. J., Bindokas, V., Brown, M. E., Libunao, F., & Palfrey, H. C. (2003). Dynamin regulates focal exocytosis in phagocytosing macrophages. *Mol Biol Cell*, 14(5), 2016-2028. doi:10.1091/mbc.E02-09-0626
- Durieux, A. C., Prudhon, B., Guichenev, P., & Bitoun, M. (2010). Dynamin 2 and human diseases. *J Mol Med (Berl)*, 88(4), 339-350. doi:10.1007/s00109-009-0587-4
- Eguchi, K., Taoufiq, Z., Thorn-Seshold, O., Trauner, D., Hasegawa, M., & Takahashi, T. (2017). Wild-Type Monomeric alpha-Synuclein Can Impair Vesicle Endocytosis and Synaptic Fidelity via Tubulin Polymerization at the Calyx of Held. *J Neurosci*, 37(25), 6043-6052. doi:10.1523/JNEUROSCI.0179-17.2017
- Evergren, E., Zotova, E., Brodin, L., & Shupliakov, O. (2006). Differential efficiency of the endocytic machinery in tonic and phasic synapses. *Neuroscience*, 141(1), 123-131. doi:10.1016/j.neuroscience.2006.03.038
- Fabian-Fine, R., Verstreken, P., Hiesinger, P. R., Horne, J. A., Kostyleva, R., Zhou, Y., . . .

- Meinertzhagen, I. A. (2003). Endophilin promotes a late step in endocytosis at glial invaginations in *Drosophila* photoreceptor terminals. *J Neurosci*, *23*(33), 10732-10744.
- Faelber, K., Posor, Y., Gao, S., Held, M., Roske, Y., Schulze, D., . . . Daumke, O. (2011). Crystal structure of nucleotide-free dynamin. *Nature*, *477*(7366), 556-560. doi:10.1038/nature10369
- Ferguson, K. M., Lemmon, M. A., Schlessinger, J., & Sigler, P. B. (1994). Crystal structure at 2.2 Å resolution of the pleckstrin homology domain from human dynamin. *Cell*, *79*(2), 199-209.
- Ferguson, S. M., Brasnjo, G., Hayashi, M., Wolfel, M., Collesi, C., Giovedi, S., . . . De Camilli, P. (2007). A selective activity-dependent requirement for dynamin 1 in synaptic vesicle endocytosis. *Science*, *316*(5824), 570-574. doi:10.1126/science.1140621
- Ferguson, S. M., & De Camilli, P. (2012). Dynamin, a membrane-remodelling GTPase. *Nat Rev Mol Cell Biol*, *13*(2), 75-88. doi:10.1038/nrm3266
- Ferguson, S. M., Raimondi, A., Paradise, S., Shen, H., Mesaki, K., Ferguson, A., . . . De Camilli, P. (2009). Coordinated actions of actin and BAR proteins upstream of dynamin at endocytic clathrin-coated pits. *Dev Cell*, *17*(6), 811-822. doi:10.1016/j.devcel.2009.11.005
- Fernandez-Chacon, R., Konigstorfer, A., Gerber, S. H., Garcia, J., Matos, M. F., Stevens, C. F., . . . Sudhof, T. C. (2001). Synaptotagmin I functions as a calcium regulator of release probability. *Nature*, *410*(6824), 41-49. doi:10.1038/35065004
- Fish, K. N., Schmid, S. L., & Damke, H. (2000). Evidence that dynamin-2 functions as a signal-transducing GTPase. *J Cell Biol*, *150*(1), 145-154.
- Ford, M. G., Jenni, S., & Nunnari, J. (2011). The crystal structure of dynamin. *Nature*, *477*(7366), 561-566. doi:10.1038/nature10441
- Fredj, N. B., & Burrone, J. (2009). A resting pool of vesicles is responsible for spontaneous vesicle fusion at the synapse. *Nat Neurosci*, *12*(6), 751-758. doi:10.1038/nn.2317
- Fuchs, M., Brandstatter, J. H., & Regus-Leidig, H. (2014). Evidence for a Clathrin-independent mode of endocytosis at a continuously active sensory synapse. *Front Cell Neurosci*, *8*, 60. doi:10.3389/fncel.2014.00060
- Fukuda, M., Kanno, E., Ogata, Y., & Mikoshiba, K. (2001). Mechanism of the SDS-resistant synaptotagmin clustering mediated by the cysteine cluster at the interface between the transmembrane and spacer domains. *J Biol Chem*, *276*(43), 40319-40325. doi:10.1074/jbc.M105356200
- Gaffield, M. A., & Betz, W. J. (2006). Imaging synaptic vesicle exocytosis and endocytosis with FM dyes. *Nat Protoc*, *1*(6), 2916-2921. doi:10.1038/nprot.2006.476
- Gandhi, S. P., & Stevens, C. F. (2003). Three modes of synaptic vesicular recycling revealed by single-vesicle imaging. *Nature*, *423*(6940), 607-613. doi:10.1038/nature01677
- Geppert, M., Goda, Y., Hammer, R. E., Li, C., Rosahl, T. W., Stevens, C. F., & Sudhof, T. C. (1994). Synaptotagmin I: a major Ca²⁺ sensor for transmitter release at a central synapse. *Cell*, *79*(4), 717-727.
- Gold, E. S., Underhill, D. M., Morrissette, N. S., Guo, J., McNiven, M. A., & Aderem, A. (1999). Dynamin 2 is required for phagocytosis in macrophages. *J Exp Med*, *190*(12), 1849-1856.
- Gonzalez-Jamett, A. M., Baez-Matus, X., Hevia, M. A., Guerra, M. J., Olivares, M. J., Martinez, A. D., . . . Cardenas, A. M. (2010). The association of dynamin with synaptophysin regulates quantal size and duration of exocytotic events in chromaffin cells. *J Neurosci*, *30*(32), 10683-10691. doi:10.1523/JNEUROSCI.5210-09.2010
- Gormal, R. S., Nguyen, T. H., Martin, S., Papadopulos, A., & Meunier, F. A. (2015). An acto-myosin

- II constricting ring initiates the fission of activity-dependent bulk endosomes in neurosecretory cells. *J Neurosci*, 35(4), 1380-1389. doi:10.1523/JNEUROSCI.3228-14.2015
- Grabs, D., Slepnev, V. I., Songyang, Z., David, C., Lynch, M., Cantley, L. C., & De Camilli, P. (1997). The SH3 domain of amphiphysin binds the proline-rich domain of dynamin at a single site that defines a new SH3 binding consensus sequence. *J Biol Chem*, 272(20), 13419-13425.
- Graham, M. E., O'Callaghan, D. W., McMahon, H. T., & Burgoyne, R. D. (2002). Dynamin-dependent and dynamin-independent processes contribute to the regulation of single vesicle release kinetics and quantal size. *Proc Natl Acad Sci U S A*, 99(10), 7124-7129. doi:10.1073/pnas.102645099
- Granseth, B., Odermatt, B., Royle, S. J., & Lagnado, L. (2006). Clathrin-mediated endocytosis is the dominant mechanism of vesicle retrieval at hippocampal synapses. *Neuron*, 51(6), 773-786. doi:10.1016/j.neuron.2006.08.029
- Grassart, A., Cheng, A. T., Hong, S. H., Zhang, F., Zenzer, N., Feng, Y., . . . Drubin, D. G. (2014). Actin and dynamin2 dynamics and interplay during clathrin-mediated endocytosis. *J Cell Biol*, 205(5), 721-735. doi:10.1083/jcb.201403041
- Gray, N. W., Fourgeaud, L., Huang, B., Chen, J., Cao, H., Oswald, B. J., . . . McNiven, M. A. (2003). Dynamin 3 is a component of the postsynapse, where it interacts with mGluR5 and Homer. *Curr Biol*, 13(6), 510-515.
- Gray, N. W., Kruchten, A. E., Chen, J., & McNiven, M. A. (2005). A dynamin-3 spliced variant modulates the actin/cortactin-dependent morphogenesis of dendritic spines. *J Cell Sci*, 118(Pt 6), 1279-1290. doi:10.1242/jcs.01711
- Groffen, A. J., Martens, S., Diez Arazola, R., Cornelisse, L. N., Lozovaya, N., de Jong, A. P., . . . Verhage, M. (2010). Doc2b is a high-affinity Ca²⁺ sensor for spontaneous neurotransmitter release. *Science*, 327(5973), 1614-1618. doi:10.1126/science.1183765
- Gu, C., Yaddanapudi, S., Weins, A., Osborn, T., Reiser, J., Pollak, M., . . . Sever, S. (2010). Direct dynamin-actin interactions regulate the actin cytoskeleton. *EMBO J*, 29(21), 3593-3606. doi:10.1038/emboj.2010.249
- Guichet, A., Wucherpfennig, T., Dudu, V., Etter, S., Wilsch-Brauniger, M., Hellwig, A., . . . Schmidt, A. A. (2002). Essential role of endophilin A in synaptic vesicle budding at the Drosophila neuromuscular junction. *EMBO J*, 21(7), 1661-1672. doi:10.1093/emboj/21.7.1661
- Guillaud, L., Dimitrov, D., & Takahashi, T. (2017). Presynaptic morphology and vesicular composition determine vesicle dynamics in mouse central synapses. *Elife*, 6. doi:10.7554/eLife.24845
- Hamao, K., Morita, M., & Hosoya, H. (2009). New function of the proline rich domain in dynamin-2 to negatively regulate its interaction with microtubules in mammalian cells. *Exp Cell Res*, 315(7), 1336-1345. doi:10.1016/j.yexcr.2009.01.025
- Han, W., Rhee, J. S., Maximov, A., Lao, Y., Mashimo, T., Rosenmund, C., & Sudhof, T. C. (2004). N-glycosylation is essential for vesicular targeting of synaptotagmin 1. *Neuron*, 41(1), 85-99.
- Harata, N., Ryan, T. A., Smith, S. J., Buchanan, J., & Tsien, R. W. (2001). Visualizing recycling synaptic vesicles in hippocampal neurons by FM 1-43 photoconversion. *Proc Natl Acad Sci U S A*, 98(22), 12748-12753. doi:10.1073/pnas.171442798
- Harris, K. M., & Sultan, P. (1995). Variation in the number, location and size of synaptic vesicles provides an anatomical basis for the nonuniform probability of release at hippocampal CA1 synapses. *Neuropharmacology*, 34(11), 1387-1395.

- Hayashida, M., Tanifuji, S., Ma, H., Murakami, N., & Mochida, S. (2015). Neural activity selects myosin IIB and VI with a specific time window in distinct dynamin isoform-mediated synaptic vesicle reuse pathways. *J Neurosci*, *35*(23), 8901-8913. doi:10.1523/JNEUROSCI.5028-14.2015
- Henkel, A. W., Lubke, J., & Betz, W. J. (1996). FM1-43 dye ultrastructural localization in and release from frog motor nerve terminals. *Proc Natl Acad Sci U S A*, *93*(5), 1918-1923.
- Henley, J. R., Krueger, E. W., Oswald, B. J., & McNiven, M. A. (1998). Dynamin-mediated internalization of caveolae. *J Cell Biol*, *141*(1), 85-99.
- Heuser, J. E., & Reese, T. S. (1973). Evidence for recycling of synaptic vesicle membrane during transmitter release at the frog neuromuscular junction. *J Cell Biol*, *57*(2), 315-344.
- Hua, Z., Leal-Ortiz, S., Foss, S. M., Waites, C. L., Garner, C. C., Voglmaier, S. M., & Edwards, R. H. (2011). v-SNARE composition distinguishes synaptic vesicle pools. *Neuron*, *71*(3), 474-487. doi:10.1016/j.neuron.2011.06.010
- Ivanov, V. N., Ronai, Z., & Hei, T. K. (2006). Opposite roles of FAP-1 and dynamin in the regulation of Fas (CD95) translocation to the cell surface and susceptibility to Fas ligand-mediated apoptosis. *J Biol Chem*, *281*(3), 1840-1852. doi:10.1074/jbc.M509866200
- Jackson, J., Papadopulos, A., Meunier, F. A., McCluskey, A., Robinson, P. J., & Keating, D. J. (2015). Small molecules demonstrate the role of dynamin as a bi-directional regulator of the exocytosis fusion pore and vesicle release. *Mol Psychiatry*, *20*(7), 810-819. doi:10.1038/mp.2015.56
- Jaiswal, J. K., Rivera, V. M., & Simon, S. M. (2009). Exocytosis of post-Golgi vesicles is regulated by components of the endocytic machinery. *Cell*, *137*(7), 1308-1319. doi:10.1016/j.cell.2009.04.064
- Jockusch, W. J., Praefcke, G. J., McMahon, H. T., & Lagnado, L. (2005). Clathrin-dependent and clathrin-independent retrieval of synaptic vesicles in retinal bipolar cells. *Neuron*, *46*(6), 869-878. doi:10.1016/j.neuron.2005.05.004
- Kabbani, N., Jeromin, A., & Levenson, R. (2004). Dynamin-2 associates with the dopamine receptor signalplex and regulates internalization of activated D2 receptors. *Cell Signal*, *16*(4), 497-503.
- Kasproicz, J., Kuenen, S., Swerts, J., Miskiewicz, K., & Verstreken, P. (2014). Dynamin photoinactivation blocks Clathrin and alpha-adaptin recruitment and induces bulk membrane retrieval. *J Cell Biol*, *204*(7), 1141-1156. doi:10.1083/jcb.201310090
- Kavalali, E. T. (2015). The mechanisms and functions of spontaneous neurotransmitter release. *Nat Rev Neurosci*, *16*(1), 5-16. doi:10.1038/nrn3875
- Kavalali, E. T., & Jorgensen, E. M. (2014). Visualizing presynaptic function. *Nat Neurosci*, *17*(1), 10-16. doi:10.1038/nn.3578
- Kavalali, E. T., Klingauf, J., & Tsien, R. W. (1999). Activity-dependent regulation of synaptic clustering in a hippocampal culture system. *Proc Natl Acad Sci U S A*, *96*(22), 12893-12900.
- Kjaerulf, O., Brodin, L., & Jung, A. (2011). The structure and function of endophilin proteins. *Cell Biochem Biophys*, *60*(3), 137-154. doi:10.1007/s12013-010-9137-5
- Klingauf, J., Kavalali, E. T., & Tsien, R. W. (1998). Kinetics and regulation of fast endocytosis at hippocampal synapses. *Nature*, *394*(6693), 581-585. doi:10.1038/29079
- Koenig, J. H., & Ikeda, K. (1989). Disappearance and reformation of synaptic vesicle membrane upon transmitter release observed under reversible blockage of membrane retrieval. *J Neurosci*, *9*(11), 3844-3860.

- Koenig, J. H., & Ikeda, K. (1996). Synaptic vesicles have two distinct recycling pathways. *J Cell Biol*, *135*(3), 797-808.
- Krueger, E. W., Orth, J. D., Cao, H., & McNiven, M. A. (2003). A dynamin-cortactin-Arp2/3 complex mediates actin reorganization in growth factor-stimulated cells. *Mol Biol Cell*, *14*(3), 1085-1096. doi:10.1091/mbc.E02-08-0466
- Kwon, S. E., & Chapman, E. R. (2012). Glycosylation is dispensable for sorting of synaptotagmin 1 but is critical for targeting of SV2 and synaptophysin to recycling synaptic vesicles. *J Biol Chem*, *287*(42), 35658-35668. doi:10.1074/jbc.M112.398883
- Lee, E., & De Camilli, P. (2002). Dynamin at actin tails. *Proc Natl Acad Sci U S A*, *99*(1), 161-166. doi:10.1073/pnas.012607799
- Leitz, J., & Kavalali, E. T. (2011). Ca²⁺(+) influx slows single synaptic vesicle endocytosis. *J Neurosci*, *31*(45), 16318-16326. doi:10.1523/JNEUROSCI.3358-11.2011
- Li, H., Foss, S. M., Dobryy, Y. L., Park, C. K., Hires, S. A., Shaner, N. C., . . . Voglmaier, S. M. (2011). Concurrent imaging of synaptic vesicle recycling and calcium dynamics. *Front Mol Neurosci*, *4*, 34. doi:10.3389/fnmol.2011.00034
- Li, Y., & Tsien, R. W. (2012). pHTomato, a red, genetically encoded indicator that enables multiplex interrogation of synaptic activity. *Nat Neurosci*, *15*(7), 1047-1053. doi:10.1038/nn.3126
- Li, Y. C., Chanaday, N. L., Xu, W., & Kavalali, E. T. (2017). Synaptotagmin-1- and Synaptotagmin-7-Dependent Fusion Mechanisms Target Synaptic Vesicles to Kinetically Distinct Endocytic Pathways. *Neuron*, *93*(3), 616-631 e613. doi:10.1016/j.neuron.2016.12.010
- Lin, H. C., Barylko, B., Achiriloaie, M., & Albanesi, J. P. (1997). Phosphatidylinositol (4,5)-bisphosphate-dependent activation of dynamin I and II lacking the proline/arginine-rich domains. *J Biol Chem*, *272*(41), 25999-26004.
- Liu, H., Bai, H., Xue, R., Takahashi, H., Edwardson, J. M., & Chapman, E. R. (2014). Linker mutations reveal the complexity of synaptotagmin 1 action during synaptic transmission. *Nat Neurosci*, *17*(5), 670-677. doi:10.1038/nn.3681
- Liu, Y. W., Surka, M. C., Schroeter, T., Lukiyanchuk, V., & Schmid, S. L. (2008). Isoform and splice-variant specific functions of dynamin-2 revealed by analysis of conditional knock-out cells. *Mol Biol Cell*, *19*(12), 5347-5359. doi:10.1091/mbc.E08-08-0890
- Llobet, A., Gallop, J. L., Burden, J. J., Camdere, G., Chandra, P., Vallis, Y., . . . McMahon, H. T. (2011). Endophilin drives the fast mode of vesicle retrieval in a ribbon synapse. *J Neurosci*, *31*(23), 8512-8519. doi:10.1523/JNEUROSCI.6223-09.2011
- Lou, X., Fan, F., Messa, M., Raimondi, A., Wu, Y., Looger, L. L., . . . De Camilli, P. (2012). Reduced release probability prevents vesicle depletion and transmission failure at dynamin mutant synapses. *Proc Natl Acad Sci U S A*, *109*(8), E515-523. doi:10.1073/pnas.1121626109
- Lou, X., Paradise, S., Ferguson, S. M., & De Camilli, P. (2008). Selective saturation of slow endocytosis at a giant glutamatergic central synapse lacking dynamin 1. *Proc Natl Acad Sci U S A*, *105*(45), 17555-17560. doi:10.1073/pnas.0809621105
- Lu, J., He, Z., Fan, J., Xu, P., & Chen, L. (2008). Overlapping functions of different dynamin isoforms in clathrin-dependent and -independent endocytosis in pancreatic beta cells. *Biochem Biophys Res Commun*, *371*(2), 315-319. doi:10.1016/j.bbrc.2008.04.077
- Lu, J., Helton, T. D., Blanpied, T. A., Racz, B., Newpher, T. M., Weinberg, R. J., & Ehlers, M. D. (2007). Postsynaptic positioning of endocytic zones and AMPA receptor cycling by physical

- coupling of dynamin-3 to Homer. *Neuron*, 55(6), 874-889. doi:10.1016/j.neuron.2007.06.041
- Lundmark, R., & Carlsson, S. R. (2004). Regulated membrane recruitment of dynamin-2 mediated by sorting nexin 9. *J Biol Chem*, 279(41), 42694-42702. doi:10.1074/jbc.M407430200
- Lundmark, R., & Carlsson, S. R. (2005). Expression and properties of sorting nexin 9 in dynamin-mediated endocytosis. *Methods Enzymol*, 404, 545-556. doi:10.1016/S0076-6879(05)04048-6
- Mahapatra, S., Fan, F., & Lou, X. (2016). Tissue-specific dynamin-1 deletion at the calyx of Held decreases short-term depression through a mechanism distinct from vesicle resupply. *Proc Natl Acad Sci U S A*, 113(22), E3150-3158. doi:10.1073/pnas.1520937113
- Mahapatra, S., & Lou, X. (2017). Dynamin-1 deletion enhances post-tetanic potentiation and quantal size after tetanic stimulation at the calyx of Held. *J Physiol*, 595(1), 193-206. doi:10.1113/JP271937
- Marra, V., Burden, J. J., Thorpe, J. R., Smith, I. T., Smith, S. L., Hausser, M., . . . Staras, K. (2012). A preferentially segregated recycling vesicle pool of limited size supports neurotransmission in native central synapses. *Neuron*, 76(3), 579-589. doi:10.1016/j.neuron.2012.08.042
- Maximov, A., & Sudhof, T. C. (2005). Autonomous function of synaptotagmin 1 in triggering synchronous release independent of asynchronous release. *Neuron*, 48(4), 547-554. doi:10.1016/j.neuron.2005.09.006
- McAdam, R. L., Varga, K. T., Jiang, Z., Young, F. B., Blandford, V., McPherson, P. S., . . . Sossin, W. S. (2015). The juxtamembrane region of synaptotagmin 1 interacts with dynamin 1 and regulates vesicle fission during compensatory endocytosis in endocrine cells. *J Cell Sci*, 128(12), 2229-2235. doi:10.1242/jcs.161505
- McMahon, H. T., & Boucrot, E. (2011). Molecular mechanism and physiological functions of clathrin-mediated endocytosis. *Nat Rev Mol Cell Biol*, 12(8), 517-533. doi:10.1038/nrm3151
- McNiven, M. A., Kim, L., Krueger, E. W., Orth, J. D., Cao, H., & Wong, T. W. (2000). Regulated interactions between dynamin and the actin-binding protein cortactin modulate cell shape. *J Cell Biol*, 151(1), 187-198.
- Mettlen, M., Pucadyil, T., Ramachandran, R., & Schmid, S. L. (2009). Dissecting dynamin's role in clathrin-mediated endocytosis. *Biochem Soc Trans*, 37(Pt 5), 1022-1026. doi:10.1042/BST0371022
- Miesenbock, G., De Angelis, D. A., & Rothman, J. E. (1998). Visualizing secretion and synaptic transmission with pH-sensitive green fluorescent proteins. *Nature*, 394(6689), 192-195. doi:10.1038/28190
- Min, L., Leung, Y. M., Tomas, A., Watson, R. T., Gaisano, H. Y., Halban, P. A., . . . Hou, J. C. (2007). Dynamin is functionally coupled to insulin granule exocytosis. *J Biol Chem*, 282(46), 33530-33536. doi:10.1074/jbc.M703402200
- Mooren, O. L., Kotova, T. I., Moore, A. J., & Schafer, D. A. (2009). Dynamin2 GTPase and cortactin remodel actin filaments. *J Biol Chem*, 284(36), 23995-24005. doi:10.1074/jbc.M109.024398
- Morales, M., Colicos, M. A., & Goda, Y. (2000). Actin-dependent regulation of neurotransmitter release at central synapses. *Neuron*, 27(3), 539-550.
- Morlot, S., & Roux, A. (2013). Mechanics of dynamin-mediated membrane fission. *Annu Rev Biophys*, 42, 629-649. doi:10.1146/annurev-biophys-050511-102247
- Morton, A., Marland, J. R., & Cousin, M. A. (2015). Synaptic vesicle exocytosis and increased cytosolic calcium are both necessary but not sufficient for activity-dependent bulk

- endocytosis. *J Neurochem*, 134(3), 405-415. doi:10.1111/jnc.13132
- Nicholson-Fish, J. C., Kokotos, A. C., Gillingwater, T. H., Smillie, K. J., & Cousin, M. A. (2015). VAMP4 Is an Essential Cargo Molecule for Activity-Dependent Bulk Endocytosis. *Neuron*, 88(5), 973-984. doi:10.1016/j.neuron.2015.10.043
- Nosyreva, E., & Kavalali, E. T. (2010). Activity-dependent augmentation of spontaneous neurotransmission during endoplasmic reticulum stress. *J Neurosci*, 30(21), 7358-7368. doi:10.1523/JNEUROSCI.5358-09.2010
- Obar, R. A., Collins, C. A., Hammarback, J. A., Shpetner, H. S., & Vallee, R. B. (1990). Molecular cloning of the microtubule-associated mechanochemical enzyme dynamin reveals homology with a new family of GTP-binding proteins. *Nature*, 347(6290), 256-261. doi:10.1038/347256a0
- Ochoa, G. C., Slepnev, V. I., Neff, L., Ringstad, N., Takei, K., Daniell, L., . . . De Camilli, P. (2000). A functional link between dynamin and the actin cytoskeleton at podosomes. *J Cell Biol*, 150(2), 377-389.
- Orth, J. D., Krueger, E. W., Cao, H., & McNiven, M. A. (2002). The large GTPase dynamin regulates actin comet formation and movement in living cells. *Proc Natl Acad Sci U S A*, 99(1), 167-172. doi:10.1073/pnas.012607899
- Pan, P. Y., Marrs, J., & Ryan, T. A. (2015). Vesicular glutamate transporter 1 orchestrates recruitment of other synaptic vesicle cargo proteins during synaptic vesicle recycling. *J Biol Chem*, 290(37), 22593-22601. doi:10.1074/jbc.M115.651711
- Park, R. J., Shen, H., Liu, L., Liu, X., Ferguson, S. M., & De Camilli, P. (2013). Dynamin triple knockout cells reveal off target effects of commonly used dynamin inhibitors. *J Cell Sci*, 126(Pt 22), 5305-5312. doi:10.1242/jcs.138578
- Piedras-Renteria, E. S., Pyle, J. L., Diehn, M., Glickfeld, L. L., Harata, N. C., Cao, Y., . . . Tsien, R. W. (2004). Presynaptic homeostasis at CNS nerve terminals compensates for lack of a key Ca²⁺ entry pathway. *Proc Natl Acad Sci U S A*, 101(10), 3609-3614. doi:10.1073/pnas.0308188100
- Poskanzer, K. E., Marek, K. W., Sweeney, S. T., & Davis, G. W. (2003). Synaptotagmin I is necessary for compensatory synaptic vesicle endocytosis in vivo. *Nature*, 426(6966), 559-563. doi:10.1038/nature02184
- Raimondi, A., Ferguson, S. M., Lou, X., Armbruster, M., Paradise, S., Giovedi, S., . . . De Camilli, P. (2011). Overlapping role of dynamin isoforms in synaptic vesicle endocytosis. *Neuron*, 70(6), 1100-1114. doi:10.1016/j.neuron.2011.04.031
- Raingo, J., Khvotchev, M., Liu, P., Darios, F., Li, Y. C., Ramirez, D. M., . . . Kavalali, E. T. (2012). VAMP4 directs synaptic vesicles to a pool that selectively maintains asynchronous neurotransmission. *Nat Neurosci*, 15(5), 738-745. doi:10.1038/nn.3067
- Ramirez, D. M., Andersson, S., & Russell, D. W. (2008). Neuronal expression and subcellular localization of cholesterol 24-hydroxylase in the mouse brain. *J Comp Neurol*, 507(5), 1676-1693. doi:10.1002/cne.21605
- Ramirez, D. M., & Kavalali, E. T. (2011). Differential regulation of spontaneous and evoked neurotransmitter release at central synapses. *Curr Opin Neurobiol*, 21(2), 275-282. doi:10.1016/j.conb.2011.01.007
- Ramirez, D. M., Khvotchev, M., Trauterman, B., & Kavalali, E. T. (2012). Vti1a identifies a vesicle pool that preferentially recycles at rest and maintains spontaneous neurotransmission. *Neuron*, 73(1), 121-134. doi:10.1016/j.neuron.2011.10.034

- Rikhy, R., Kamat, S., Ramagiri, S., Sriram, V., & Krishnan, K. S. (2007). Mutations in dynamin-related protein result in gross changes in mitochondrial morphology and affect synaptic vesicle recycling at the *Drosophila* neuromuscular junction. *Genes Brain Behav*, *6*(1), 42-53. doi:10.1111/j.1601-183X.2006.00218.x
- Sankaranarayanan, S., Atluri, P. P., & Ryan, T. A. (2003). Actin has a molecular scaffolding, not propulsive, role in presynaptic function. *Nat Neurosci*, *6*(2), 127-135. doi:10.1038/nn1002
- Sankaranarayanan, S., De Angelis, D., Rothman, J. E., & Ryan, T. A. (2000). The use of pHluorins for optical measurements of presynaptic activity. *Biophys J*, *79*(4), 2199-2208. doi:10.1016/S0006-3495(00)76468-X
- Sara, Y., Virmani, T., Deak, F., Liu, X., & Kavalali, E. T. (2005). An isolated pool of vesicles recycles at rest and drives spontaneous neurotransmission. *Neuron*, *45*(4), 563-573. doi:10.1016/j.neuron.2004.12.056
- Schlunck, G., Damke, H., Kiosses, W. B., Rusk, N., Symons, M. H., Waterman-Storer, C. M., . . . Schwartz, M. A. (2004). Modulation of Rac localization and function by dynamin. *Mol Biol Cell*, *15*(1), 256-267. doi:10.1091/mbc.E03-01-0019
- Schuske, K. R., Richmond, J. E., Matthies, D. S., Davis, W. S., Runz, S., Rube, D. A., . . . Jorgensen, E. M. (2003). Endophilin is required for synaptic vesicle endocytosis by localizing synaptojanin. *Neuron*, *40*(4), 749-762.
- Sever, S., Muhlberg, A. B., & Schmid, S. L. (1999). Impairment of dynamin's GAP domain stimulates receptor-mediated endocytosis. *Nature*, *398*(6727), 481-486. doi:10.1038/19024
- Shaner, N. C., Campbell, R. E., Steinbach, P. A., Giepmans, B. N., Palmer, A. E., & Tsien, R. Y. (2004). Improved monomeric red, orange and yellow fluorescent proteins derived from *Discosoma* sp. red fluorescent protein. *Nat Biotechnol*, *22*(12), 1567-1572. doi:10.1038/nbt1037
- Shen, Y., Rosendale, M., Campbell, R. E., & Perrais, D. (2014). pHuji, a pH-sensitive red fluorescent protein for imaging of exo- and endocytosis. *J Cell Biol*, *207*(3), 419-432. doi:10.1083/jcb.201404107
- Shpetner, H. S., Herskovits, J. S., & Vallee, R. B. (1996). A binding site for SH3 domains targets dynamin to coated pits. *J Biol Chem*, *271*(1), 13-16.
- Shpetner, H. S., & Vallee, R. B. (1989). Identification of dynamin, a novel mechanochemical enzyme that mediates interactions between microtubules. *Cell*, *59*(3), 421-432.
- Shupliakov, O., Bloom, O., Gustafsson, J. S., Kjaerulff, O., Low, P., Tomilin, N., . . . Brodin, L. (2002). Impaired recycling of synaptic vesicles after acute perturbation of the presynaptic actin cytoskeleton. *Proc Natl Acad Sci U S A*, *99*(22), 14476-14481. doi:10.1073/pnas.212381799
- Snellman, J., Mehta, B., Babai, N., Bartoletti, T. M., Akmentin, W., Francis, A., . . . Zenisek, D. (2011). Acute destruction of the synaptic ribbon reveals a role for the ribbon in vesicle priming. *Nat Neurosci*, *14*(9), 1135-1141. doi:10.1038/nn.2870
- Soulet, F., Schmid, S. L., & Damke, H. (2006). Domain requirements for an endocytosis-independent, isoform-specific function of dynamin-2. *Exp Cell Res*, *312*(18), 3539-3545. doi:10.1016/j.yexcr.2006.07.018
- Stevens, C. F., & Williams, J. H. (2000). "Kiss and run" exocytosis at hippocampal synapses. *Proc Natl Acad Sci U S A*, *97*(23), 12828-12833. doi:10.1073/pnas.230438697
- Sudhof, T. C. (2000). The synaptic vesicle cycle revisited. *Neuron*, *28*(2), 317-320.

- Sudhof, T. C. (2004). The synaptic vesicle cycle. *Annu Rev Neurosci*, 27, 509-547.
doi:10.1146/annurev.neuro.26.041002.131412
- Swadlow, H. A. (2003). Fast-spike interneurons and feedforward inhibition in awake sensory neocortex. *Cereb Cortex*, 13(1), 25-32.
- Takamori, S., Holt, M., Stenius, K., Lemke, E. A., Gronborg, M., Riedel, D., . . . Jahn, R. (2006). Molecular anatomy of a trafficking organelle. *Cell*, 127(4), 831-846.
doi:10.1016/j.cell.2006.10.030
- Takei, K., McPherson, P. S., Schmid, S. L., & De Camilli, P. (1995). Tubular membrane invaginations coated by dynamin rings are induced by GTP-gamma S in nerve terminals. *Nature*, 374(6518), 186-190. doi:10.1038/374186a0
- Tan, T. C., Valova, V. A., Malladi, C. S., Graham, M. E., Berven, L. A., Jupp, O. J., . . . Robinson, P. J. (2003). Cdk5 is essential for synaptic vesicle endocytosis. *Nat Cell Biol*, 5(8), 701-710.
doi:10.1038/ncb1020
- Tanabe, K., & Takei, K. (2009). Dynamic instability of microtubules requires dynamin 2 and is impaired in a Charcot-Marie-Tooth mutant. *J Cell Biol*, 185(6), 939-948.
doi:10.1083/jcb.200803153
- Tanifuji, S., Funakoshi-Tago, M., Ueda, F., Kasahara, T., & Mochida, S. (2013). Dynamin isoforms decode action potential firing for synaptic vesicle recycling. *J Biol Chem*, 288(26), 19050-19059. doi:10.1074/jbc.M112.445874
- Taylor, M. J., Perrais, D., & Merrifield, C. J. (2011). A high precision survey of the molecular dynamics of mammalian clathrin-mediated endocytosis. *PLoS Biol*, 9(3), e1000604.
doi:10.1371/journal.pbio.1000604
- Thompson, H. M., Cao, H., Chen, J., Euteneuer, U., & McNiven, M. A. (2004). Dynamin 2 binds gamma-tubulin and participates in centrosome cohesion. *Nat Cell Biol*, 6(4), 335-342.
doi:10.1038/ncb1112
- Thompson, H. M., Skop, A. R., Euteneuer, U., Meyer, B. J., & McNiven, M. A. (2002). The large GTPase dynamin associates with the spindle midzone and is required for cytokinesis. *Curr Biol*, 12(24), 2111-2117.
- Torre, E., McNiven, M. A., & Urrutia, R. (1994). Dynamin 1 antisense oligonucleotide treatment prevents neurite formation in cultured hippocampal neurons. *J Biol Chem*, 269(51), 32411-32417.
- Vallis, Y., Wigge, P., Marks, B., Evans, P. R., & McMahon, H. T. (1999). Importance of the pleckstrin homology domain of dynamin in clathrin-mediated endocytosis. *Curr Biol*, 9(5), 257-260.
- van der Blik, A. M., & Meyerowitz, E. M. (1991). Dynamin-like protein encoded by the *Drosophila* shibire gene associated with vesicular traffic. *Nature*, 351(6325), 411-414.
doi:10.1038/351411a0
- Van Hook, M. J., & Thoreson, W. B. (2012). Rapid synaptic vesicle endocytosis in cone photoreceptors of salamander retina. *J Neurosci*, 32(50), 18112-18123.
doi:10.1523/JNEUROSCI.1764-12.2012
- Veitch, N. C. (2004). Horseradish peroxidase: a modern view of a classic enzyme. *Phytochemistry*, 65(3), 249-259.
- Verstreken, P., Kjaerulff, O., Lloyd, T. E., Atkinson, R., Zhou, Y., Meinertzhagen, I. A., & Bellen, H. J. (2002). Endophilin mutations block clathrin-mediated endocytosis but not neurotransmitter release. *Cell*, 109(1), 101-112.

- Voglmaier, S. M., Kam, K., Yang, H., Fortin, D. L., Hua, Z., Nicoll, R. A., & Edwards, R. H. (2006). Distinct endocytic pathways control the rate and extent of synaptic vesicle protein recycling. *Neuron*, *51*(1), 71-84. doi:10.1016/j.neuron.2006.05.027
- Warnock, D. E., Baba, T., & Schmid, S. L. (1997). Ubiquitously expressed dynamin-II has a higher intrinsic GTPase activity and a greater propensity for self-assembly than neuronal dynamin-I. *Mol Biol Cell*, *8*(12), 2553-2562.
- Watanabe, S., Rost, B. R., Camacho-Perez, M., Davis, M. W., Sohl-Kielczynski, B., Rosenmund, C., & Jorgensen, E. M. (2013). Ultrafast endocytosis at mouse hippocampal synapses. *Nature*, *504*(7479), 242-247. doi:10.1038/nature12809
- Watanabe, S., Trimbuch, T., Camacho-Perez, M., Rost, B. R., Brokowski, B., Sohl-Kielczynski, B., . . . Jorgensen, E. M. (2014). Clathrin regenerates synaptic vesicles from endosomes. *Nature*, *515*(7526), 228-233. doi:10.1038/nature13846
- Wilhelm, B. G., Groemer, T. W., & Rizzoli, S. O. (2010). The same synaptic vesicles drive active and spontaneous release. *Nat Neurosci*, *13*(12), 1454-1456. doi:10.1038/nn.2690
- Wu, X. S., Lee, S. H., Sheng, J., Zhang, Z., Zhao, W. D., Wang, D., . . . Wu, L. G. (2016). Actin Is Crucial for All Kinetically Distinguishable Forms of Endocytosis at Synapses. *Neuron*, *92*(5), 1020-1035. doi:10.1016/j.neuron.2016.10.014
- Wu, Y., O'Toole, E. T., Girard, M., Ritter, B., Messa, M., Liu, X., . . . De Camilli, P. (2014). A dynamin 1-, dynamin 3- and clathrin-independent pathway of synaptic vesicle recycling mediated by bulk endocytosis. *Elife*, *3*, e01621. doi:10.7554/eLife.01621
- Xu, J., McNeil, B., Wu, W., Nees, D., Bai, L., & Wu, L. G. (2008). GTP-independent rapid and slow endocytosis at a central synapse. *Nat Neurosci*, *11*(1), 45-53. doi:10.1038/nn2021
- Xu, J., Pang, Z. P., Shin, O. H., & Sudhof, T. C. (2009). Synaptotagmin-1 functions as a Ca²⁺ sensor for spontaneous release. *Nat Neurosci*, *12*(6), 759-766. doi:10.1038/nn.2320
- Xue, J., Graham, M. E., Novelle, A. E., Sue, N., Gray, N., McNiven, M. A., . . . Robinson, P. J. (2011). Calcineurin selectively docks with the dynamin Ixb splice variant to regulate activity-dependent bulk endocytosis. *J Biol Chem*, *286*(35), 30295-30303. doi:10.1074/jbc.M111.273110
- Xue, L., Sheng, J., Wu, X. S., Wu, W., Luo, F., Shin, W., . . . Wu, L. G. (2013). Most vesicles in a central nerve terminal participate in recycling. *J Neurosci*, *33*(20), 8820-8826. doi:10.1523/JNEUROSCI.4029-12.2013
- Yamada, H., Abe, T., Satoh, A., Okazaki, N., Tago, S., Kobayashi, K., . . . Takei, K. (2013). Stabilization of actin bundles by a dynamin 1/cortactin ring complex is necessary for growth cone filopodia. *J Neurosci*, *33*(10), 4514-4526. doi:10.1523/JNEUROSCI.2762-12.2013
- Yarar, D., Waterman-Storer, C. M., & Schmid, S. L. (2005). A dynamic actin cytoskeleton functions at multiple stages of clathrin-mediated endocytosis. *Mol Biol Cell*, *16*(2), 964-975. doi:10.1091/mbc.E04-09-0774
- Zhang, Q., Li, Y., & Tsien, R. W. (2009). The dynamic control of kiss-and-run and vesicular reuse probed with single nanoparticles. *Science*, *323*(5920), 1448-1453. doi:10.1126/science.1167373
- Zhu, Y., Xu, J., & Heinemann, S. F. (2009). Two pathways of synaptic vesicle retrieval revealed by single-vesicle imaging. *Neuron*, *61*(3), 397-411. doi:10.1016/j.neuron.2008.12.024
- Zoncu, R., Perera, R. M., Sebastian, R., Nakatsu, F., Chen, H., Balla, T., . . . De Camilli, P. V. (2007). Loss of endocytic clathrin-coated pits upon acute depletion of phosphatidylinositol

4,5-bisphosphate. *Proc Natl Acad Sci U S A*, 104(10), 3793-3798.
doi:10.1073/pnas.0611733104